



**RAFAEL MARQUES
PATRÍCIO**

**DESENHO DE POLÍMEROS SUSTENTÁVEIS A
PARTIR DO ÁCIDO 2,5-FURANODICARBOXÍLICO E
AVALIAÇÃO DA SUA (BIO)DEGRADABILIDADE**

**DESIGN OF SUSTAINABLE POLYMERS BASED ON
2,5-FURANODICARBOXYLIC ACID AND
EVALUATION OF THEIR (BIO)DEGRADABILITY**



**RAFAEL MARQUES
PATRÍCIO**

**DESENHO DE POLÍMEROS SUSTENTÁVEIS A
PARTIR DO ÁCIDO 2,5-FURANODICARBOXÍLICO E
AVALIAÇÃO DA SUA (BIO)DEGRADABILIDADE**

**DESIGN OF SUSTAINABLE POLYMERS BASED ON
2,5-FURANODICARBOXYLIC ACID AND
EVALUATION OF THEIR (BIO)DEGRADABILITY**

Tese apresentada à Universidade de Aveiro para cumprimento dos requisitos necessários à obtenção do grau de Mestre em Bioquímica, realizada sob a orientação científica da Doutora Andreia Fernandes de Sousa, Investigadora do Departamento de Química & CICECO da Universidade de Aveiro e Doutora Teresa Rocha Santos, Investigadora Principal com Agregação do Departamento de Química & CESAM da Universidade de Aveiro.

Dedico este trabalho à minha família, pelo incansável apoio.

o júri

Presidente

Professor Doutor Mário Manuel Quialheiro Simões
Professor Auxiliar do Departamento de Química da Universidade de Aveiro

Arguente

Doutora Ana Luísa Patrício da Silva
Investigadora Júnior do Departamento de Biologia da Universidade de Aveiro

Orientadora

Doutora Paula Andreia Fernandes de Sousa
Investigadora Doutorada do Departamento de Química da Universidade de Aveiro

Agradecimentos

A realização da presente dissertação de mestrado neste contexto atípico de pandemia global só foi possível devido a todo o apoio e incentivo que recebi, aos quais estarei eternamente grato.

Em primeiro lugar, um agradecimento especial à Doutora Andreia Sousa, pela orientação científica, disponibilidade, críticas e correções, pelo saber que transmitiu e toda a dedicação que teve comigo.

À Doutora Teresa Rocha Santos, pela orientação científica, críticas e correções, e disponibilidade durante todo o percurso.

À Ana Paço, por toda a disponibilidade, apoio no laboratório, partilha de conhecimentos e por todas as palavras de tranquilidade quando as coisas correram menos bem.

À Chaima Bouyahya, por ter partilhado o trabalho de laboratório comigo e ter sido uma excelente parceira.

A todos os colegas de ambos os laboratórios. Em particular quero agradecer o apoio no laboratório ao Sami Zaidi, à Beatriz Agostinho, à Fuzia Sebti e à Doutora Patrícia Ramos.

A todas as pessoas responsáveis pelas técnicas de caracterização usadas neste trabalho.

A toda a minha família e amigos por estarem sempre presentes. Em especial aos meus pais, por todo o apoio, carinho, educação e por tornarem tudo isto possível.

À minha irmã, companheira para a vida, e claro também ao Steve, por ambos serem um grande apoio.

À Francisca, por caminhar sempre ao meu lado, por todo o carinho, amizade, apoio e incentivo.

A todas as pessoas que não mencionei, mas que de alguma forma fizeram parte desta experiência.

A todos o meu **Muito Obrigado!**

palavras-chave

Poli(2,5-furanodicarboxilato de etileno), copoliésteres, poli(2,5-furandicarboxilato de isosorbido)-co-poli(1,12-dodecanodioato de isosorbido), (bio)degradação, *Penicillium brevicompactum*

resumo

A produção massiva de polímeros convencionais (comumente designados por plásticos) com base em recursos fósseis e a poluição do meio ambiente têm fomentado a investigação em polímeros de origem renovável como alternativas mais sustentáveis. Neste sentido, o ácido 2,5-furandicarboxílico (FDCA) é um destacado monômero de origem renovável para a síntese de polímeros, nomeadamente o poli(2,5-furanodicarboxilato de etileno) (PEF). O PEF tem uma série de propriedades térmicas, mecânicas e de barreira bastante promissoras, o que o torna uma alternativa renovável ao polímero de origem fóssil poli(tereftalato de etileno) (PET), para a produção de embalagens plásticas, entre outras aplicações. Para diminuir possíveis impactos ambientais é importante que, para além da sua origem renovável, o fim-de-vida do PEF (assim como de qualquer *plástico*) seja devidamente acautelado, nomeadamente via (bio)degradação. Contudo, há uma falha na literatura no que toca ao estudo do fim-de-vida, nomeadamente via (bio)degradação dos polímeros baseados no FDCA, tais como o PEF. Nesse sentido, no presente trabalho pretendemos estudar a biodegradação do PEF (Cap.II) utilizando o fungo *Penicillium brevicompactum*. Neste estudo, foi avaliado a biodegradação do PEF pelo fungo *P. brevicompactum* por análise gravimétrica e por espectroscopia de infravermelho. O *P. brevicompactum* não demonstrou capacidade de degradar o PEF. Pelo contrário, foi observado um efeito negativo no crescimento do fungo. Estes resultados intensificam a hipótese de que o PEF é pouco biodegradável e evidenciam a necessidade de desenhar outros polímeros cuja biodegradabilidade possa ser mais efetiva e modelada.

Por conseguinte, num segundo estudo, sintetizou-se com sucesso uma nova série de (co)poliésteres de origem renovável, os poli(2,5-furandicarboxilato de isosorbido)-co-poli(1,12-dodecanodioato de isosorbido)s (PIsFDDs) e avaliou-se a sua (bio)degradação (Cap.III). A estrutura dos PIsFDDs foi confirmada detalhadamente por caracterização via espectroscopias de infravermelho, ressonância magnética de ^1H e ^{13}C e difração de raios-X; e as suas propriedades térmicas avaliadas por TGA, DSC e DMTA. Estes novos polímeros, dependendo das quantidades relativas de FDCA e ácido dodecanodioico, exibiram carácter amorfo ou semi-cristalino e estabilidade térmica até cerca de 290 °C. Adicionalmente, realizou-se a (bio)degradação hidrolítica/enzimática dos PIsFDDs, onde se observou valores promissores, nomeadamente para o PIsFDD 10/90 a perda de peso atingiu os 10.5% após 35 dias de incubação, apresentando, em geral, potencial para serem aplicados em produtos (bio)degradáveis.

keywords

Poly(ethylene 2,5-furandicarboxylate), copolyesters, poly(isosorbide 2,5-furandicarboxylate)-co-poly(isosorbide 1,12-dodecanedioate), (bio)degradation, *Penicillium brevicompactum*

abstract

The excessive production of conventional polymers (routinely called *plastics*), and the related depletion of fossil sources, as well as the environmental pollution, has prompted massive research on sustainable polymers alternatives to current fossil-based homologs. 2,5-Furandicarboxylic acid (FDCA) has been highlighted as a promising bio-based key chemical for polyesters production, mainly due to the similarity of this renewable monomer with the well-known terephthalic acid (TPA). One of the most promising FDCA-based polyesters developed so far is, undoubtedly, poly(ethylene 2,5-furandicarboxylate) (PEF). PEF is considered the renewable alternative to the fossil-based poly(ethylene terephthalate) (PET), suitable for packaging applications, among others. PEF has a very interesting set of properties, including, for example, high thermal properties and superior barrier behavior. Despite the enormous efforts put in studying PEF properties and applications, PEF end-life has been barely addressed.

In this vein, in this work, we aim to study the biodegradation of PEF using the *Penicillium brevicompactum* fungus (Chapter. II). The biodegradation of PEF by the fungus was evaluated through gravimetric and ATR-FTIR analyses. *P. brevicompactum* did not demonstrate the ability to degrade PEF. On the contrary, a negative effect was observed on the growth of the fungus. These results intensify the hypothesis that PEF is poorly biodegradable and highlight the need to better study alternative more biodegradable polymers.

Therefore a series of copolyesters from the FDCA and other renewable-based aliphatic compounds the poly(isosorbide 2,5-furandicarboxylate)-co-poly(isosorbide 1,12-dodecanedioate) (PIsFDD) were successfully synthesized. Their structure was checked by ATR-FTIR, ¹H and ¹³C NMR, and X-ray diffraction, and their thermal properties were evaluated by TGA, DSC, and DMTA. The PIsFDD copolyesters depending on the monomeric quantities exhibited amorphous or semi-crystalline character and thermal stability up to 290 °C. Additionally, hydrolytic/enzymatic degradation of PIsFDDs showed promising results namely for PIsFDD 10/90 a 10.5% weight loss was reached. These copolyesters showed the potential to be applied as (bio)degradable products.

Table of contents

Table of contents	i
List of Figures	iii
List of Tables	v
List of Abbreviations, symbols, and acronyms	vi
I. Introduction	1
i. Aims and scope	3
1. Furanic polyesters	4
1.1. 2,5-furandicarboxylic acid monomers	4
1.2. Poly(ethylene 2,5-furandicarboxylate) (PEF).....	5
1.3. Furanic – aliphatic polyesters	8
2. Polymer Degradation.....	13
2.1. What is polymer degradation?	13
2.2. Abiotic degradation	14
2.3. Biodegradation of polymers	15
2.4. Polymer degrading microorganisms – <i>Penicillium brevicompactum</i>	20
II. Synthesis of Poly(ethylene 2,5-furandicarboxylate) (PEF) and evaluation of biodegradation by the fungus <i>Penicillium brevicompactum</i>	23
1. Background	23
2. Material and Methods.....	23
2.1. Materials	23
2.2. Synthesis of dimethyl 2,5-furandicarboxylate (DMFDC):.....	24
2.3. Synthesis of poly(ethylene 2,5-furandicarboxylate) and film preparation:	24
2.4. <i>Microorganism - Penicillium brevicompactum</i>	25
2.5. PEF biodegradation test by the fungus <i>Penicillium brevicompactum</i>	25
2.6. Analysis	27
3. Results and Discussion	28
3.1. Synthesis of DMFDC and PEF and characterization	28
3.2. PEF biodegradation by the fungus <i>Penicillium brevicompactum</i>	30
3.2.1. Weight and ATR-FTIR analysis of <i>Penicillium brevicompactum</i>	31
3.2.2. Weight and ATR-FTIR analysis of the PEF microparticles	35
4. Conclusion.....	38

III. Synthesis, characterization and degradation of poly(isosorbide 2,5-furandicarboxylate)-co-poly(isosorbide 1,12-dodecanedioate) copolyesters (PIsFDDs).....	39
1. Background	39
2. Material and Methods.....	40
2.1. Materials	40
2.2. Synthesis of dimethyl 2,5-furandicarboxylate (DMFDC).....	40
2.3. Synthesis of copolyesters poly(isosorbide 2,5-furandicarboxylate)-co-(isosorbide 1,12-dodecanedioate)s (PIsFxDDy)	40
2.4. Film preparation.....	41
2.5. Hydrolytic and enzymatic degradation tests	42
2.5.1. Solutions preparation.....	43
2.6. Characterization techniques	43
3. Results and discussion.....	44
3.1. Structural characterization of the PIsFDD copolyesters	44
3.2. X-ray diffraction analysis (XRD).....	48
3.3. Thermal behavior.....	48
3.4. Degradation studies of PIsFDDs and their homopolymers counterparts	52
4. Conclusion.....	54
IV. Conclusion and future perspectives	55
V. References.....	57
VI. Supplementary data.....	67
1. Supplementary data A- Preliminary test to evaluate the growth and consumption of culture medium by the fungus <i>Penicillium brevicompactum</i> during the biodegradation of PEF.	67
2. Supplementary data B- Chapter II.....	71
3. Supplementary data C- Chapter III.....	73

List of Figures

Figure 1- Global production of bioplastics in 2018.....	2
Figure 2- Similar chemical structures of TPA and FDCA.....	4
Figure 3- General route to obtain HMF and FDCA from hexoses and C6 based polysaccharides.....	4
Figure 4- Chemical structure of fossil-based PET (left) and renewable-based PEF (right).5	
Figure 5- Derivatives of the FDCA: dimethyl 2,5-furandicarboxylate (DMFDC); Bis(hydroxyethyl)-2,5-furandicarboxylate (BHEFDC); 2,5-furandicarbonyl dichloride (FDCDCI).....	7
Figure 6- Scheme of PEF synthesis by the two-stage melt approach.	7
Figure 7- Molecular structures of isoidide, isosorbide, and isomannide.	9
Figure 8- Polycondensation reaction of FDCDCI with isosorbide or isoidide.....	10
Figure 9- Scheme of PEF-co-PLA synthesis through polycondensation of BHEFDC and PLA.....	11
Figure 10- Scheme of synthesis route of copolyesters PDIsFs from Isosorbide, 1,10-Decanodiol, and DMFDC. Adapted from Chebbi et al. ⁶⁷	12
Figure 11- Scheme of co-polyesters PEDFs synthesis from DMFDC (DMFD in the figure), DMDC, and EG.....	13
Figure 12- Schematic representation of the different steps involved in biodegradation. Adapted from Haider et al. ¹¹	16
Figure 13- Parameters that affect the biodegradation of polymers.....	20
Figure 14- DMFDC synthesis scheme.....	24
Figure 15- PEF synthesis scheme.....	24
Figure 16- Composition of the Erlenmeyer used in biodegradation test.....	26
Figure 17- Schematic summary of the PEF biodegradation test by the fungus <i>Penicillium brevicompactum</i>	27
Figure 18- ATR-FTIR spectrums of FDCA, DMFDC, and PEF.....	29
Figure 19- ¹ H NMR spectra of PEF [300 MHz, TCE+ 3 drops TFA, reference (TCE) = 6.00 ppm.....	30
Figure 20- Variation of <i>Penicillium brevicompactum</i> biomass throughout the experiment.	31
Figure 21- Differences between Erlenmeyer flasks at 42 days of incubation. A) GC flasks (live fungus) B) PEF+P.b flasks (dead fungus).....	32

Figure 22- Infrared spectra in the region 400-4000 cm^{-1} from <i>Penicillium brevicompactum</i> throughout the experiment.	34
Figure 23- Variation of PEF microparticles before and after their exposure to <i>Penicillium brevicompactum</i>	35
Figure 24- Infrared spectra in the region 500-4000 cm^{-1} from the PEF microparticles throughout the experiment.	37
Figure 25- Synthesis of poly(isosorbide 2,5-furandicarboxylate)-co-(isosorbide 1,12-dodecanedioate) copolyesters.	41
Figure 26- PIsDD, PIsF, and PIsFDD copolymer specimens produced by melting.	42
Figure 27- ATR-FTIR spectra of prepared PIsFDD copolyesters, PIsF, and PIsDD homopolyesters.	45
Figure 28- (A) Chemical structure of F-Is-F, DD-Is-DD, and F-Is-DD triads (B) ^1H NMR spectra of PIsF, PIsDD, and PIsFDDs copolyesters in CDCl_3	46
Figure 29- XRD patterns of PIsFDD copolyesters, PIsF, and PIsDD homopolyesters.	48
Figure 30- DSC 1 st /2 nd scan curves of copolyesters, and 1st scan curve of PIsDD homopolyester.	49
Figure 31- $\tan \delta$ of PIsDD, PIsF, and PIsFDD copolyesters, at 1 and 10 Hz.	50
Figure 32- TGA and DTG thermograms of PIsFDD and corresponding homopolyesters.	51
Figure 33- a) hydrolytic degradation in PBS (37°C); b) enzymatic degradation in PBS using lipase from porcine pancreas (37°C) c) hydrolytic degradation under marine conditions.	53
Supplementary data-figure 1- Infrared spectra in the region 500-4000 cm^{-1} from the PEF microparticles throughout the experiment.	70
Supplementary data-figure 2- Infrared spectra in the region 500-4000 cm^{-1} from the culture medium.	71
Supplementary data-figure 3- ^{13}C ssNMR of culture medium from 56 days of incubation and PEF (film).	72
Supplementary data-figure 4- ATR-FTIR spectra of all prepared PIsFDD copolyesters, PIsF, and PIsDD homopolyesters.	73
Supplementary data-figure 5- ^1H NMR spectra of PIsF, PIsDD, and all PIsFDDs copolyesters in CDCl_3	73

List of Tables

Table 1- Comparison of properties between PEF and PET.	6
Table 2 - ATR-FTIR Data of FDCA, DMFDC, and PEF	29
Table 3 - ¹ H NMR resonances of PEF [300 MHz, TCE-d ₂ + 3 drops TFA-d, reference (TCE) = 6.00 ppm].....	30
Table 4- Variation of <i>Penicillium brevicompactum</i> biomass throughout the experiment ...	32
Table 5 - Variation of PEF microparticles before and after their exposure to <i>Penicillium brevicompactum</i>	36
Table 6 - Molar composition obtained by ¹ H NMR, yields and intrinsic viscosities of purified PIsFDD samples.....	47
Table 7- Thermal Properties of copolyesters PIsFDD with Different Compositions	51
Supplementary data table 1 - Variation of <i>Penicillium brevicompactum</i> biomass throughout the experiment.....	68
Supplementary data table 2- Culture medium loss during the test	69
Supplementary data table 3- Variation of PEF microplastics before and after their exposure to <i>Penicillium brevicompactum</i>	70
Supplementary data table 4- ¹ H NMR resonances [300 MHz, CDCl ₃ , reference (CDCl ₃) = 7.26 ppm] of PIsFDD copolyesters, PIsF, and PIsDD homopolyesters.....	74

List of Abbreviations, symbols, and acronyms

ATR-FTIR	Attenuated total reflection Fourier transform infrared spectroscopy
BHEFDC	Bis(hydroxyethyl-2,5-furandicarboxylate)
BioPE	Bio-based poly(ethylene)
bioPET	Bio-based poly(ethylene terephthalate)
DAHs	1,4:3,6-dianhydrohexitols
DDA	Dodecanedioic acid
DMDC	Dimethyl dodecanedioate
DMFDC	Dimethyl 2,5-furandicarboxylate
DMTA	Dynamic mechanical thermal analyses
DSC	Differential scanning calorimetry
EG	Ethylene glycol
EPS	Poly(styrene), expandable
FDCA	2,5-Furandicarboxylic acid
FDCDCI	2,5-Furandicarbonyl dichloride
HiC	Cutinase from the fungus <i>Humicola insolens</i>
HMF	5-hydroxymethylfurfural
Is	Isosorbide
M_n	Number-average molecular weight
PPL	lipase from porcine pancreas
NMR	¹ H, ¹³ C Nuclear magnetic resonance
PBF	Poly(butylene 2,5-furandicarboxylate)
PBT	Poly(butylene terephthalate)
PCDMF	Poly(1,4-cyclohexane-dimethylene 2,5-furandicarboxylate)
PDDF	Poly(1,12-dodecylene 2,5-furandicarboxylate)
PDF	Poly(1,10-decylene 2,5-furandicarboxylate)
PDIsF	Poly(decamethylene-co-isosorbide 2,5-furandicarboxylate)
PE	Poly(ethylene)
PEDF	Poly(ethylene dodecanedioate 2,5-furandicarboxylate)
PEF	Poly(ethylene 2,5-furandicarboxylate)
PEF-co-PLA	Poly(ethylene 2,5-furandicarboxylate)-co-poly(lactic acid)
PET	Poly(ethylene terephthalate)
PHA	Poly(hydroxyalkanoates)

PHF	Poly(1,6-hexylene 2,5-furandicarboxylate)
PIsFDD	poly(isosorbide 2,5-furandicarboxylate)-co-poly(isosorbide 1,12-dodecanedioate)
PLA	Poly(lactic acid)
PNF	Poly(1,9-nonylene 2,5-furandicarboxylate)
POF	Poly(1,8-octylene 2,5-furandicarboxylate)
PP	Poly(propylene)
PPT	Poly(propylene terephthalate)
PS	Poly(styrene)
PUR	Poly(urethane)
PVC	Poly(vinyl chloride)
T_c	Crystallization temperature
T_{cc}	Cold-crystallization temperature
T_{d,max}	Maximum degradation temperature
T_{d,5%}	Decomposition temperature at 5% weight loss
T_g	Glass transition
TGA	Thermogravimetric analysis
Thc_cut1	Cutinase 1 from the bacterium <i>Thermobifida cellulosilytica</i>
T_m	Melting temperature
TPA	Terephthalic acid
XRD	X-ray diffraction analysis

I. Introduction

The human population has been increasing at explosive rates to the actual exorbitant number of 7.7 billion and it is expected to reach 9.7 billion by 2050¹. With this explosive increase, we are confronting serious challenges, such as resources and energy scarcity, and global environmental pollution^{2,3}. The development of a sustainable world is one of the most demanding challenges for our society, as it is viewed as the **“development that meets the needs of the present without compromising the ability of future generations to meet their own needs”**⁴. In this regard, to make sustainable development a worldwide reality, in 2016, the United Nations (UN) resolution entitled *“Transforming our World: The 2030 Agenda for Sustainable Development”* came into force⁵. One of the main focuses of this agenda is **“to protect the planet from degradation, including through sustainable consumption and production, sustainable managing its natural resources and taking urgent action on climate change, so that it can support the need of the present and future generations”**⁵. This agenda has as **Goal 12. “Ensure sustainable consumption and production patterns”**⁵. Hence, entirely aligned with the meaning of sustainability. The contemporary world relies on polymers (routinely called ‘*plastics*’). The success of plastics as a material has been substantial due to their properties and versatility. Their proprieties include high durability, lightweight, chemical- and light-resistant, and toughness^{6,7}. These properties together with their low cost have driven the annual worldwide demand for plastics to reach 359 million tonnes in 2018⁸. However, this demand is largely supported by fossil-based polymers, such as: poly(propylene) (PP), poly(ethylene) (PE) with different densities, poly(vinyl chloride) (PVC), poly(urethane) (PUR), poly(ethylene terephthalate) (PET), poly(styrene) (PS)/ poly(styrene), expandable (EPS)⁸. This excessive production of polymers from finite fossil resources requires the search for alternative ones from renewable resources⁹.

In addition, conventional polymers have typically low biodegradability in the environment, which is a property appreciated in some applications (such as tubes, aircraft), but in what concerns massive-use packaging (“convenience packaging”) and other “short-term” applications, polymers waste and management is particularly warring due to plastic accumulation in the environment^{10,11}. It is estimated that over 5800 million tons (Mt) of plastic waste is currently in the environment, and is expected to reach 12000 Mt by 2050¹². Plastics entering the marine environment have received particular concern¹³ because their amount increase in the ocean at a shocking rate of 4.8-12.7 Mt per year¹⁴ and also due to their ability to reach microplastics (particles <5 mm in diameter) and nano-plastics (particles

<1 µm in diameter) size¹⁵. This debris is spread globally across the oceans, having consequences on all ecological systems¹⁶. For example, microplastics are a concern especially because they can be transferred along the food chain, causing toxicity due to the additives and monomers that constitute them, and due to their ability to absorb water contaminants^{17,18}. Nanoplastics have shown similar behavior to microplastics, but with the additional problem of being more likely to cross biological membranes affecting the normal functioning of cells^{18,19}. These problems have been forcing a change in our society, making scientists and industrials search for renewable-based, biodegradable, and more harmless polymers¹⁰.

The emergence of the biorefinery concept in the early 2000s²⁰ brought with it the opportunity to replace the non-sustainable fossil-based model of development with a more sustainable one based on renewable resources. Biorefinery refers to **“the sustainable processing of biomass into a spectrum of marketable products (food, feed, materials, chemicals) and energy (fuels, power, heat)”**²¹. In 2004, the US National Renewable Energy Laboratory highlighted 12 promising building block chemicals produced from biomass, all of them with the ability to be converted into several high-value bio-based chemicals or materials²². 2,5-Furandicarboxylic acid (FDCA) was one of those highlighted building blocks, as this diacid can be used for the development of promising bio-based polymers.²³. The term “bio-based” refers to polymers derived from biomass²⁴.

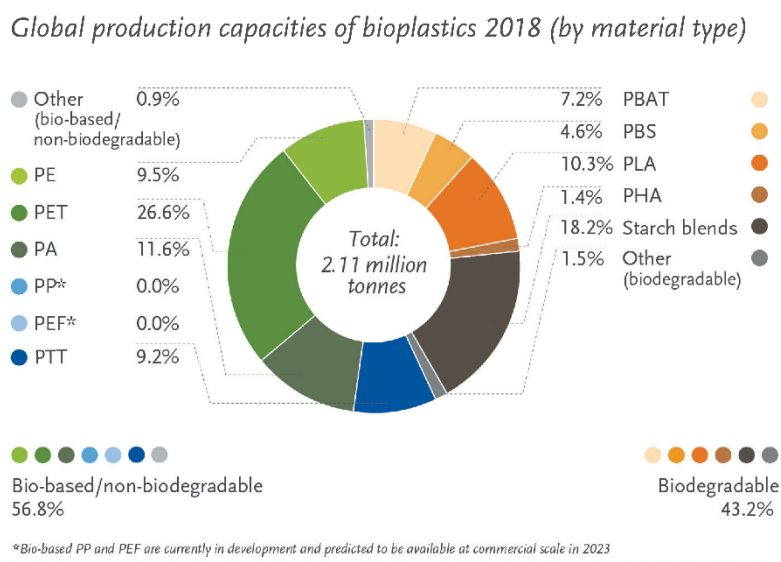


Figure 1-Global production of bioplastics in 2018. Adapted from reference²⁵

In 2018, the bioplastics market represented 1% (2.11Mt) of world plastic production. However, it is a growing market, not only due to its increasing demand but also due to the

emergence of new bio-based polymers. Now, the bioplastics market (**Figure 1**) consists of bio-based biodegradable polymers such as poly(lactic acid) (PLA) and poly(hydroxyalkanoates) (PHA)), but also non-biodegradable bio-based polymers (such as bio-based polyethylene (bioPE), bio-based poly(ethylene terephthalate) (bioPET). Poly(ethylene 2,5-furandicarboxylate) (PEF), a bio-based polymer derived from FDCA, is expected to hit the market in 2023²⁵.

i. Aims and scope

Due to this need of replacing non-renewable polymers with more sustainable and (bio)degradable alternatives, the present thesis had two main goals.

We first aim to evaluate the biodegradation of PEF by the fungus *Penicillium brevicompactum* and secondly, we aim to synthesize a series of new bio-based copolyesters based on the FDCA and other aliphatic compounds and to evaluate their degradation under different conditions. In this way, the present thesis is divided into four main chapters. In **Chapter I**, we address all the theoretical concepts needed to understand and develop the works underlying the dissertation. **Chapter II** presents the work on PEF synthesis and biodegradation by the fungus *P. brevicompactum*. In **Chapter III**, we present the work developed in the synthesis, characterization, and degradation of poly(isosorbide 2,5-furandicarboxylate)-co-poly(isosorbide 1,12-dodecanedioate) (PIsFDD) copolyesters. Finally, in **Chapter IV**, we summarize the main general conclusions and the future perspectives.

1. Furanic polyesters

1.1. 2,5-furandicarboxylic acid monomers

2,5-Furandicarboxylic acid (FDCA) is one of the 12 highlighted chemicals, it is a bio-based rigid aromatic monomer and both industry and academy had increased the interest to explore it²³. The chemical structure of FDCA is similar to terephthalic acid (TPA) (**Figure 2**). Due to this similarity, the FDCA has been recognized as a promising bio-based substitute for TPA, which is a petroleum-based monomer widely used for the synthesis of high-performance polymers²⁶, such as PET (used e.g. for the production of plastic bottles), but also poly(butylene terephthalate) (PBT) and poly(propylene terephthalate) (PPT)^{27,28}.

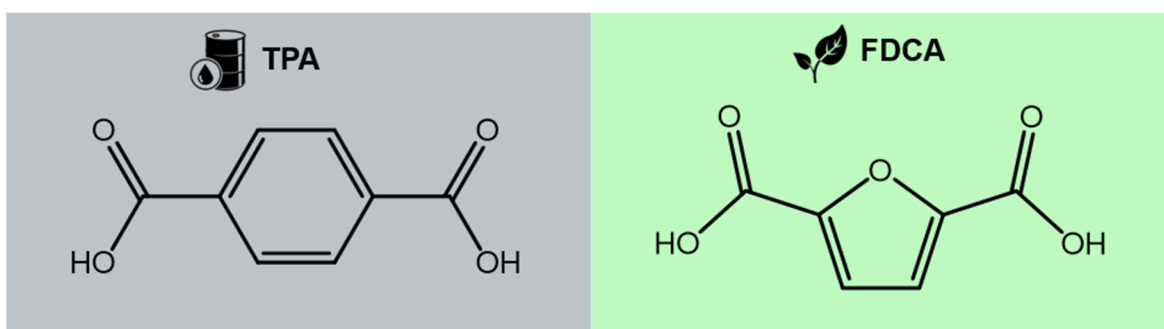


Figure 2- Similar chemical structures of TPA and FDCA

Generally, the FDCA is obtained via catalytic oxidation of 5-hydroxymethylfurfural (HMF) from hexoses²⁹: first, the production of 5-hydroxymethylfurfural by dehydration of hexoses, and secondly, its oxidative conversion into FDCA (**Figure 3**).

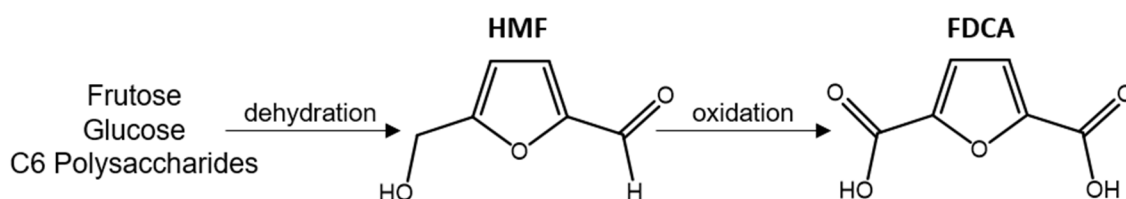


Figure 3- General route to obtain HMF and FDCA from hexoses and C6 based polysaccharides. Adapted from Sousa *et al.*²³.

The HMF oxidation into FDCA has been the focus of many studies, resulting in a wide variety of procedures. Then, FDCA was successfully prepared by oxidation of HMF using distinct types of oxidation conditions and catalysts (homogeneous and heterogeneous

metal catalysts as well bio- or electrocatalysts)^{23,30}. Some interesting examples of this oxidation procedures, with high yield (>90%), was FDCA prepared under mild conditions, by oxidation of aqueous HMF with O₂, using several types of catalysts, namely Pt, Pt/Bi, Pd, and Au modified with Pd or Pt and supported in different carbon forms (carbon nanotubes and graphene)²³. However, FDCA synthesis is out of the scope of this appraisal.

A wide variety of polymeric materials have been obtained from FDCA²³, including polyesters, polyamides, polyurethanes, and epoxy resins. Most of the studies have been related to FDCA-based polyesters, which is also one of the main focus of this study.

There are several types of polyesters derived from FDCA, which are divided into two main groups, depending on the chemical unit to which FDCA is attached: (i) furanic–aliphatic polyesters, derived from FDCA and an aliphatic unity, including those with a linear carbon chain (that can span from C2 to C18, or even further), or instead, those with a more rigid cyclic structure and (ii) furanic-aromatic polyesters, derived from FDCA and an aromatic unity, such as benzenic or furanic based²³. Among FDCA-based polyesters, PEF is the most studied because of its similarities to the engineering plastic PET (**Figure 4**). Poly(propylene 2,5-furandicarboxylate) (PPF), poly(butylene 2,5-furandicarboxylate) (PBF) and poly(1,4-cyclohexane-dimethylene 2,5-furandicarboxylate) (PCDMF) are also very promising materials³¹.

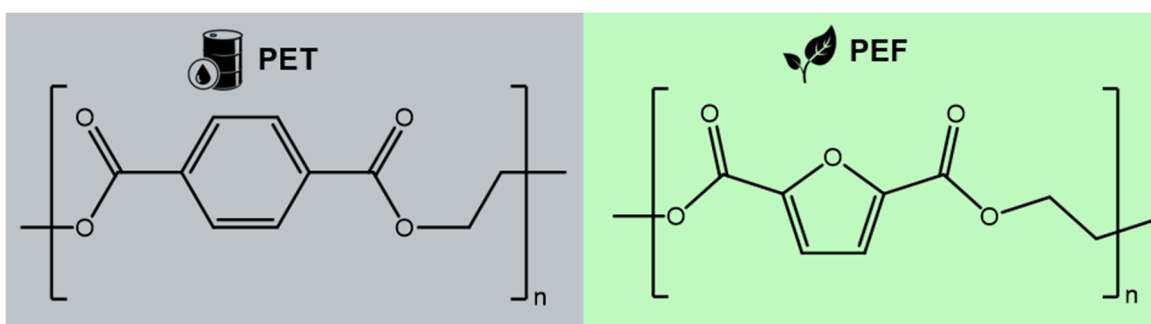


Figure 4- Chemical structure of fossil-based PET (left) and renewable-based PEF (right).

1.2. Poly(ethylene 2,5-furandicarboxylate) (PEF)

As previously mentioned, 100% renewable-based PEF has been proposed as an important alternative to its fossil-based counterpart PET³². PET is one of the dominant polymers in the global market with an annual output of over 50 Mt³³. Compared with PET, PEF is considered to have a lower carbon footprint, equivalent thermal and mechanical properties, and importantly superior barrier properties. Moreover, the production of PEF has been

claimed to decrease the non-renewable energy use by about 40-50% and greenhouse gas emissions by 45-55% what makes PEF an excellent sustainable alternative to PET³⁴.

The large-scale production of PEF is being fostered by companies such as Avantium BV., but it is still not a commercial reality, yet. In 2015, Avantium company using YXY technology opened an operational pilot plant for PEF production³⁵. This pilot project achieved promising results, which led the company Avantium to announce that PEF will reach the market by 2023, for high-value applications such as high-barrier films and specialty bottles³⁶.

Regarding the properties of PEF, it is a semicrystalline homopolyester, showing accordingly both a glass transition (T_g) around 75–80 °C and a melting temperature (T_m) at 210–215 °C. Also, PEF is thermally stable up to approximately 300 °C. Several studies demonstrated PET and PEF have similar properties (**Table 1**), but PEF has a higher T_g and a lower T_m ³². For example, in the work conducted by Burgess *et al.*³⁷ PEF films had $T_g = 85$ °C; $T_m = 211$ °C; and thermal decomposition (T_d) = 389°C, while PET presented $T_g = 76$ °C; $T_m = 247$ °C; and $T_d = 413$ °C³⁷. The Young's modulus and the maximum stress of PEF are 2070–2450 MPa and 35–67 MPa, respectively, which are comparable to those of PET (2000 MPa and 45 MPa, respectively), Young's modulus of PEF is slightly higher³⁸. The elongation at break was about 4%, and much lower than the observed in PET (90–250%)³⁹. PEF has increased barrier properties: about 11 times less permeable to oxygen⁴⁰, 19 times less to carbon dioxide⁴¹ and, 3 times less to water⁴² when compared to PET.

Table 1- Comparison of properties between PEF and PET ^{37–39}.

Properties	PEF	PET
T_g	85 °C	76 °C
T_m	211 °C	247 °C
T_d	389 °C	413 °C
Young's modulus	2070–2450 MPa	2000 MPa
Maximum stress	35–67 MPa	45 MPa
Elongation at break	4%	90–250%

PEF synthesis. Studies concerning PEF synthetic conditions have been performed: different approaches (polycondensation and/or polyesterification); using FDCA or its derivatives (**Figure 5**); varying temperatures pressures, catalysts; or time²³.

The most used approach is based on a 2-stage melt polymerization (**Figure 6**). Briefly, this approach consists of (i) first-stage esterification or transesterification reaction of FDCA or dimethyl 2,5-furandicarboxylate (DMFDC) with ethylene glycol (EG) respectively, carried

out under nitrogen and heating up to 215 °C, followed by, in a second-stage (ii), a slow evacuation of the excess of diol and a polytransesterification reaction with increasing temperature (up to 215–245 °C) under reduced pressure²³.

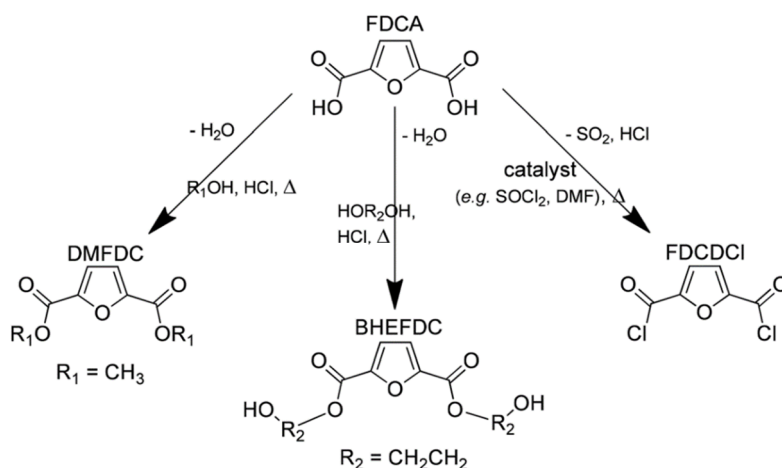


Figure 5- Derivatives of the FDCA: dimethyl 2,5-furandicarboxylate (DMFDC); Bis(hydroxyethyl)-2,5-furandicarboxylate (BHEFDC); 2,5-furandicarbonyl dichloride (FDCDCI). Adapted from Sousa *et al.*²³.

Additionally, some studies implemented a third-stage (iii) of solid-state polycondensation during several days and using temperatures between PEF glass transition and melting point, aiming at increasing the polyester degree of polymerization obtaining a higher molecular weight PEF^{33,43}. To prevent the decarboxylation of FDCA it is preferable to use the derivative DMFDC instead of the FDCA as starting monomer⁴⁴.

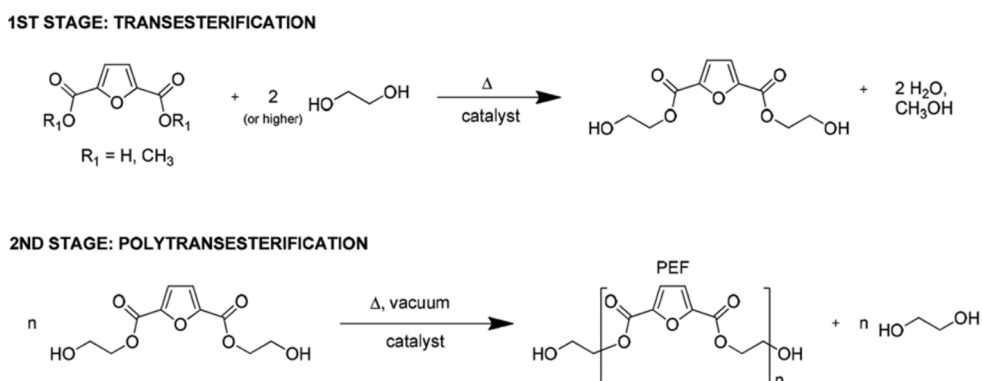


Figure 6-Scheme of PEF synthesis by the two-stage melt approach. Adapted from Sousa *et al.*²³.

Weinberger *et al.*⁴⁵ have studied the potential of amorphous PEF films to be degraded by two different enzymes, cutinase 1 from the bacterium *Thermobifida cellulosilytica* (Thc_cut1) and cutinase from the fungus *Humicola insolens* (HiC). The authors concluded that PEF is highly degraded by the fungal enzyme HiC, leading to a 100% degradation of the polymer to soluble molecules (FDCA and oligomers) after only 72 h of reaction, being a promising enzyme to be used in PEF recycling, but also showing that PEF may be sensitive to fungal biodegradation⁴⁵. Austin *et al.*⁴⁶ used the enzyme PETase extracted from the bacteria *Ideonella sakaiensis* 201-F6, which has the rare ability to biodegrade PET, to study the degradation of PEF. They showed that PETase is able to degrade PEF and is potentially more active for PEF than for PET⁴⁶. So far, studies on standard biodegradation of PEF are almost non-existent. To the best of our knowledge, the only study is a test carried out by Organic Waste Systems (Gent, Belgium) which showed that PEF degrades much faster than PET under industrial composting conditions (250-400 days with air/oxygen and at 58 °C, in soil)^{47,48}. At this time, Avantium has a 10-year field study underway to assess the biodegradation of this polymer⁴⁸. However, more studies are required to assess the biodegradation of PEF, either under control laboratory conditions to find the best options to carry out PEF (bio)degradation, but especially under environmentally relevant conditions.

1.3. Furanic – aliphatic polyesters

Furanic–aliphatic polyesters are one of the most studied families of furan polymers. The research about this family is mainly due to the wide range of aliphatic molecules that can form monomers with the FDCA, allowing the synthesis of various polyesters with a wide variety of end-properties. Some of the aliphatic molecules used may be of linear chain or cyclic structure, and studies tend to have these molecules also obtained from renewable sources, a factor that contributes to the development of more sustainable polymers²³. Polyesters obtained from these furan-aliphatic moieties have been shown to have a wide range of thermo-mechanical properties^{39,49} and some also promising ability to be (bio)degradable^{50,51}. For now, the PEF (discussed in the previous topic) is the most relevant member. But in addition to PEF, many other furanic – linear aliphatic and furanic-cycloaliphatic copolyesters are part of this interesting family²³.

Some examples of homopolyesters are PPF, PBF, poly(1,6-hexylene 2,5-furandicarboxylate) (PHF), poly(1,8-octylene 2,5-furandicarboxylate) (POF), poly(1,9-nonylene 2,5-furandicarboxylate) (PNF), poly(1,10-decylene 2,5-furandicarboxylate) (PDF), poly-(1,12-dodecylene 2,5-furandicarboxylate) (PDDF)^{38,52}, among many others. PBF is also an important polymer because it is the renewable counterpart of the fossil-based plastic PBT

(this latter quite used in electronics). The thermal and mechanical properties of PBF are very similar to those of PBT^{49,53}.

Scientific knowledge regarding furan-cycloaliphatic homopolyesters, which are normally formed by reacting FDCA with cycloaliphatic diols, is not yet abundant and is mostly focused on the use of 1,4:3,6-dianhydrohexitols (DAHs)²³. DAHs are bicyclic dihydroxyethers derived from C6-sugar alcohols that have two hydroxyl groups located at the C2 and C5 positions that may have different spatial arrangements, leading to three possible stereoisomers, namely from the most reactive to the least reactive: isoidide > isosorbide > isomannide (**Figure 7**).

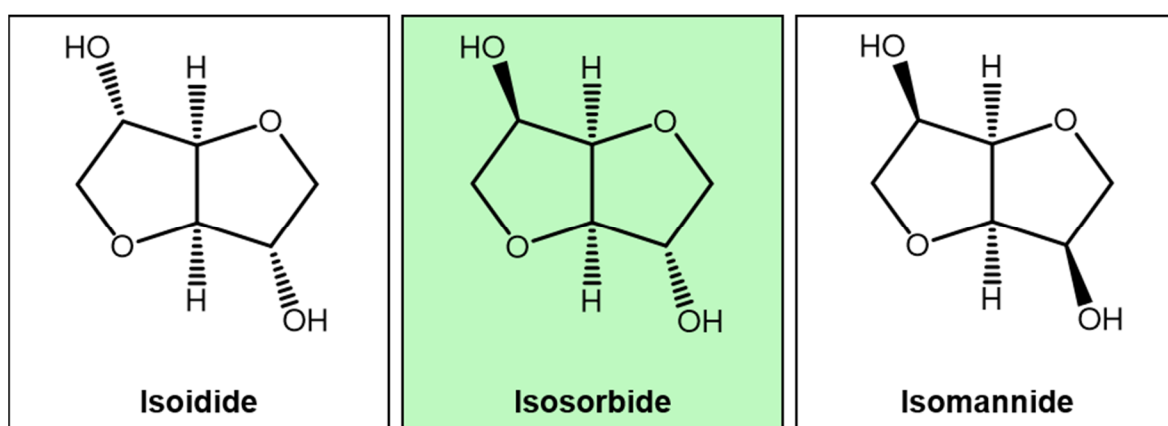


Figure 7- Molecular structures of isoidide, isosorbide, and isomannide.

Isoidide, despite being the most reactive, is not the most used since its precursor is scarce in nature. Isosorbide is the only DAH that is manufactured on an industrial scale and has been the most used in the development of these polyesters²³. These DAHs may impart attractive characteristics to polymers such as stiffness, chirality, and non-toxicity, contributing to the synthesis of polyesters with high glass transition temperature, and/or special optical properties⁵⁴. Due to the low reactive character of DAHs, low molecular weight polyesters are usually formed⁵⁴. Poly(isosorbide 2,5-furandicarboxylate) and poly(isoidide 2,5-furandicarboxylate) were produced by Gomes *et al.*⁵⁵ (**Figure 8**) using 2,5-furandicarbonyl dichloride (FDCDCI) and isosorbide or isoidide *via* a solution polycondensation at low temperatures. Both polymers showed high glass transition temperatures, the first with a $T_g = 180\text{ }^\circ\text{C}$ ($M_n \approx 13\ 750\text{ g mol}^{-1}$), and the second with a $T_g = 140\text{ }^\circ\text{C}$ ($M_n \approx 5670\text{ g mol}^{-1}$). These two polyesters showed amorphous structures⁵⁵.

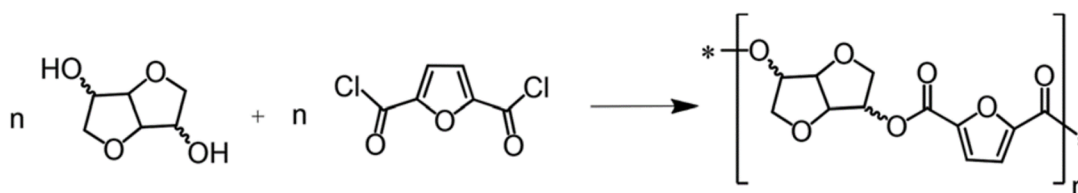


Figure 8- Polycondensation reaction of FDCDCI with isosorbide or isoidide. Adapted from Sousa *et al.*²³.

More recently, Terzopoulou *et al.*⁵⁶ also synthesized poly(isosorbide 2,5-furandicarboxylate) but in this study, the authors prepared this polyester *via* a more eco-friendly melt polycondensation process using DMFDC and isosorbide. The differential scanning calorimetry (DSC) thermogram showed a $T_g = 157\text{ }^\circ\text{C}$, which is lower than that reported in the previous work. It exhibited high thermal stability since it only degraded at temperatures above $300\text{ }^\circ\text{C}$. The authors confirmed by Wide-angle X-ray diffraction that this homopolyester was amorphous, prompted by the asymmetric nature of isosorbide with *exo* and *endo* isosorbide hydroxyl groups⁵⁶.

Ways for increasing (bio)degradation. There is a lack of (bio)degradation knowledge of the furanic – aliphatic homopolyesters mentioned above, with very few studies assessing their potential (bio)degradability^{47,57–60}. One exception is the work carried out by Karolina Haernvall *et al.*⁶⁰ evaluating the susceptibility to enzymatic hydrolysis of various furanic – linear aliphatic polyesters formed with linear diols with 3, 5, 6, 8, 9, or 12 carbons, or diethylene glycol. They used enzyme cutinase 1 of the bacteria *T. cellulosilytica* (Thc_Cut1) at $50\text{ }^\circ\text{C}$ and pH 7.0. After a 72h incubation period, the authors concluded that all tested homopolyesters suffered some enzymatic damage⁶⁰. Unfortunately, it is expected that their (bio)degradation will be difficult to occur, since, as already observed with the petrochemical counterparts, they also have a strong potential to resist hydrolysis, as well as fungal and bacterial attack⁵¹. Thus, the use of these homopolyesters can lead to serious environmental problems due to the accumulation of plastic waste.

A simple way to overcome this problem is to increase the (bio)degradability of these polyesters right from the start through adequate polymer design achieved through copolymerization of FDCA and aliphatic comonomers – furanic-aliphatic copolyesters⁵¹.

Copolymerization is a well-known technique, which allows the modification and improvement of the polymer properties to target properties, not being used exclusively to improve (bio)degradability. A wide range of furanic-aliphatic copolyesters can be synthesized, either by using different combinations of diols or simply by using additional

acids or hydroxyacids²³. Some studies had reported these copolyesters which improved (bio)degradability^{51,61–68}. Others only synthesize them and characterize their properties, but do not evaluate their potential (bio)degradability^{55,69–74}. Matos *et al.*⁵¹ designed the poly(ethylene 2,5-furandicarboxylate)-co-poly(lactic acid) (PEF-co-PLA) copolyesters, that modified PEF to a promising (bio)degradable material. The authors copolymerized different molar ratios of bis(hydroxyethyl)-2,5-furandicarboxylate (BHEFDC - PEF precursor) with oligomeric poly(lactic acid) (PLA) (M_n ca. 5000 g. mol⁻¹) using Sb₂O₃ or SnCl₂·2H₂O as a catalyst (**Figure 9**). In general, these copolyesters had a rigid amorphous structure. They have proved, through hydrolytic degradation in phosphate buffer solution, that the PEF-co-PLA copolyesters have improved degradative capacities when compared to the PEF homopolymer. For example, the incorporation of only 8 mol% of PLA in the PEF-co-PLA substantially increased its degradation without drastically altering its thermal properties, since it kept a very high thermal decomposition temperature (T_d) and high T_g values (ca. 324 and 76 °C, respectively), similar to PEF homopolymer⁵¹.

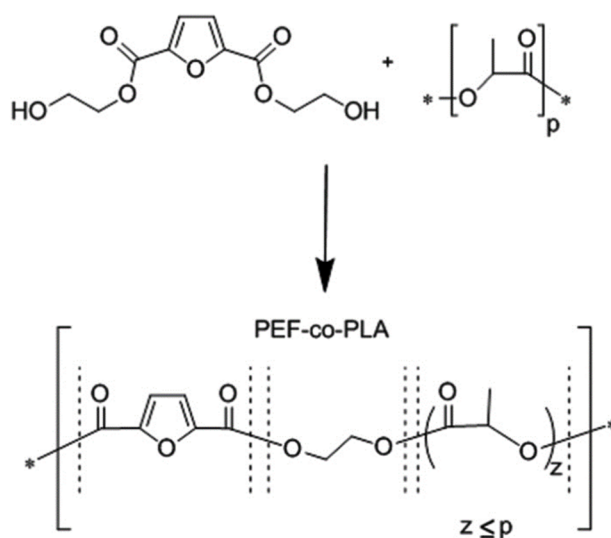


Figure 9- Scheme of PEF-co-PLA synthesis through polycondensation of BHEFDC and PLA. Adapted from Sousa *et al.*²³.

In another study, to overcome the total lack of crystallinity of poly(isosorbide 2,5-furandicarboxylate) homopolymer, Chebbi *et al.*⁶⁷ copolymerized it with PDF giving rise to poly(decamethylene-co-isosorbide 2,5-furandicarboxylate) (PDIsF). These copolyesters were synthesized from DMFDC and diverse feed molar ratios of 1,10-decanediol (flexible) and isosorbide (rigid), via a three-step melt polycondensation method (**Figure 10**). The authors evaluated the thermal and mechanical properties and soil biodegradation of these

copolyesters. All PDIsF studied had a semi-crystalline structure with excellent thermal stability with T_d values above 405 °C. The increase from 5 to 40% of the feed molar ratio of isosorbide substantially increased the T_g from -1.2 to 20.6 °C, also increasing the thermo-oxidative stability. In contrast, as the isosorbide increased, the T_m decreased from ca. 111 to 64 °C. Further, PDIsF copolyesters with low amounts of isosorbide (5 to 15% feed molar ratio) showed a substantial mechanical improvement over the homopolymer PDF. This is important, as it has been observed that these PDIsF copolyesters (containing 5 to 15% feed molar ratio of isosorbide) were clearly sensitive to biodegradation processes in the soil.

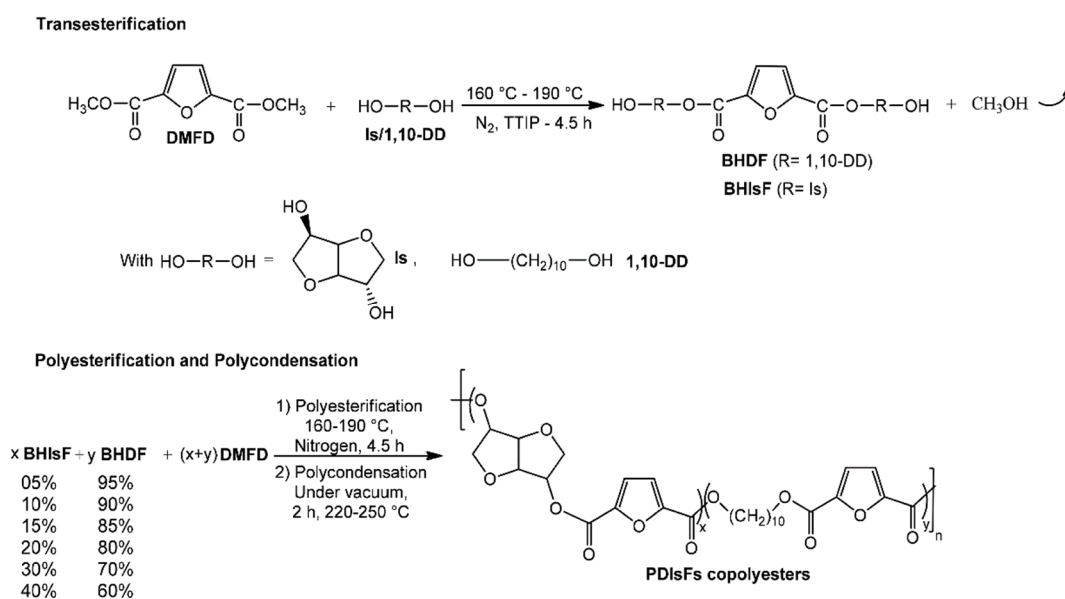


Figure 10- Scheme of synthesis route of copolyesters PDIsFs from Isosorbide, 1,10-Decanediol, and DMFDC. Adapted from Chebbi *et al.*⁶⁷.

Poly(ethylene dodecanedioate-2,5-furandicarboxylate) (PEDF) copolyesters were synthesized by Jia *et al.*⁷⁵. These copolyesters were synthesized from EG and different feed molar ratios of DMFDC and dimethyl dodecanedioate (DMDC) via 2-stage melt polymerization (**Figure 11**). The thermal and mechanical properties and the potential (bio)degradability of these copolyesters were evaluated. All copolyesters showed high thermal stability, with T_d above 350 °C. With the increase in the mol% of DMDC, the PEDF copolyester changed from amorphous elastomers (30 and 40 mol% of DMDC) to a semi-crystalline structure. Enzymatic degradation by a lipase from the porcine pancreas in phosphate buffer solution showed that, in general, there was an increase in degradation with the increase in mol% of DMDC, which evidenced that aromatic ester bonds (formed by DMFDC and EG) are more difficult to degrade than aliphatic ester (formed by DMDC and

EG). In this case, the degradation was more affected by the DMFDC quantity than by the crystallinity. However, the copolyester with 60 mol% DMDC exhibited a curiously improved degradation compared to the other copolyesters, probably because the two factors (crystallinity/amount of DMFDC) played a combinatory role⁷⁵.

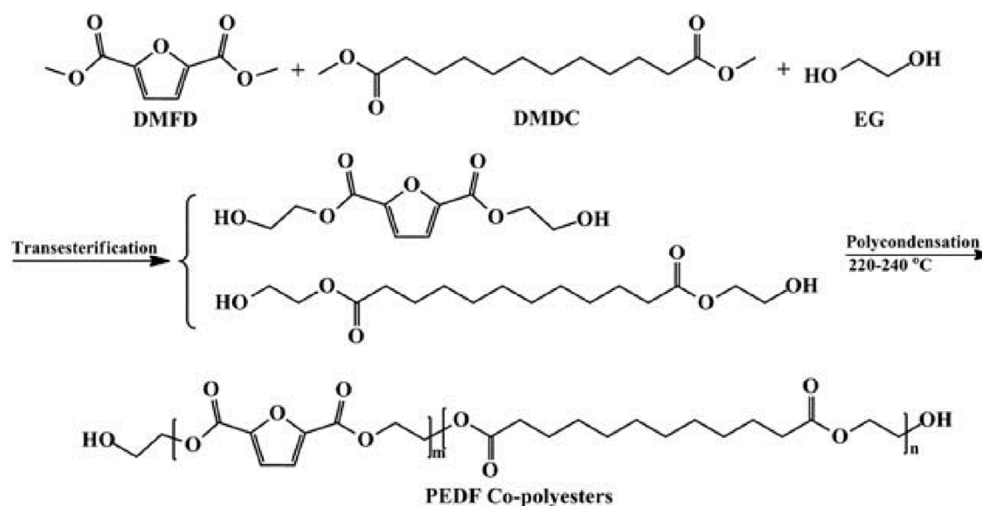


Figure 11- Scheme of co-polyesters PEDFs synthesis from DMFDC (DMFD in the figure), DMDC, and EG. Adapted from Jia *et al.*⁷⁵.

The bio-based furanic–aliphatic homopolyesters have proven to be excellent substitutes for petrochemical polymers, in terms of thermal and mechanical properties. However, as observed for their petrochemical counterparts, they may exhibit reduced (bio)degradability. Copolymerization has been successfully used for enhancing biodegradability, and with the adequate design of the copolyesters, without drastically altering their desired properties.

2. Polymer Degradation

2.1. What is polymer degradation?

Polymer degradation is any physical or chemical change in the polymer as a result of environmental factors (light, heat, moisture, chemical conditions, or biological activity) through chemical, physical or biological reactions, resulting in bond scission and subsequent chemical transformations. Degradation can be observed in the change of material properties such as mechanical, optical, or electrical characteristics, in crazing, cracking, erosion, discoloration, phase separation, or delamination⁷⁶. These processes are commonly termed “abiotic” degradation if they involve parameters like mechanical stress, light or temperature, or “biotic” degradation (biodegradation) if they involve naturally

occurring microorganisms like bacteria, fungi, and algae⁷⁷. In nature, abiotic and biotic factors act synergistically, the abiotic degradation is critical to initiate polymer degradation, as it results in loss of mechanical and structural properties, increasing the available surface area for both microbial colonization and physicochemical interactions.

2.2. Abiotic degradation

Abiotic degradation occurs mainly due to four factors: mechanical, thermal, chemical, and photo-degradation, the last two are considered the most efficient abiotic factors occurring in the environment⁷⁸.

Mechanical degradation can take place due to compression, tension, and/or shear forces. This process is not predominant but can activate or accelerate the degradation, acting synergistically with other factors⁷⁹. In an aquatic environment, this process is facilitated by the action of waves and attrition with sand and other sediments¹⁹.

Chemical degradation can be due to interaction with atmospheric pollutants, agrochemicals, oxygen, or water. Water may lead to polymer hydrolysis if the polymer contains hydrolyzable covalent bonds such as esters, anhydrides, and amides, this process is dependent on parameters as water activity, temperature, pH, and time⁷⁸. This kind of degradation is correlated with the polymers' crystallinity because crystalline domains limit the diffusion of O₂ and H₂O, contrariwise the amorphous domains facilitate this⁷⁸.

Thermal degradation of polymers results from overheating, high temperatures make the polymer chain unstable, which leads to changes in the properties of the polymers, like the reduction of weight and ductility or color changes. Two types of reactions may occur, random molecular scission of the long-chain backbone or chain-end scission of C–C bonds⁸⁰. However, in the environment, this type of degradation is difficult to occur, since the melting point of polymers is considerably higher than the environmental temperatures, but some thermoplastics polymers have a melting temperature near the environmental conditions or composting temperature (for example the PCL, with a $T_m \cong 60 \text{ }^\circ\text{C}$)⁷⁸. Nevertheless, the temperature is a factor that positively affects the degradation, polymers with semicrystalline structure such as poly(lactic acid) (PLA) or poly(butylene terephthalate) (PBT), have structural changes around their glass transition temperatures (50 °C for L-PLA, 25 °C for PBT), resulting in altered chain mobility. Above T_g (rubbery state), the polymer becomes less rigid, facilitating the accessibility to chemical and biological degradations⁸¹.

Under T_g (glassy state), additional crystallite formation (called spherulites) may occur, producing interspherulitic cracks and the brittleness of the thermoplastic polymers⁸².

Photo-degradation is caused due to the absorption of solar radiation by the polymer. Ultraviolet (UV) radiation is responsible for the direct photo-degradation (photolysis, initiated photooxidation), visible light (400–760 nm) accelerates polymeric degradation by heating and, infrared radiation (760–2500 nm) accelerates thermal oxidation. UV absorption by the polymer activates their electrons to excited states and causes oxidation, C-C bond cleavage, and other degradation⁷⁶. Considering that this is one of the most efficient factors in the environment, some polymers were developed with photosensitive molecular structures added to the polymer chain to improve the photo-degradation^{83,84}.

The degradative capacity of abiotic factors is not the same in all-natural environments. In the water column, the polymers can be buoyant, neutrally buoyant or they can sink depending on their composition, density, and shape. For example, microplastics are distributed throughout the water column, low-density microplastics are predominantly found in the sea-surface microlayer and, high-density microplastics are normally found in the benthic zone. It's important to highlight that in the marine environment, the biofouling phenomenon in plastics can increase its density⁸⁵ also, plastic particles can adhere to each other, factors that cause buoyant plastics to sink⁸⁶. The deep-sea has been proposed to act as a global sink for microplastic pollution⁸⁷, in this deep environment both abiotic and biotic degradation is extremely low, temperature and sunlight- or oxidation-mediated processes are minimal, also the diversity and density of microbial communities is reduced, that allows the accumulation and durability of plastic particles on the seabed, constituting a permanent source of environmental exposure^{88,89}. On the other hand, in less deep waters, plastics are more exposed to abiotic degradation⁸⁸, and on the surface of these plastics are present several microbial communities of autotrophs, heterotrophs, and symbionts, with an active role in its biodegradation⁹⁰.

2.3. Biodegradation of polymers

Biotic degradation, or biodegradation, is mediated by microorganisms and it is defined as a ***“process which is capable of decomposition of materials into carbon dioxide, methane, water, inorganic compounds, or biomass in which the predominant mechanism is the enzymatic action of microorganisms, that can be measured by standard tests, in a specified period of time, reflecting available disposal conditions”***^{91,92}. It is considered that biodegradation occurs after or concomitant with

abiotic biodegradation. This previous abiotic degradation weakens the structure of polymers, making them more susceptible to microbial attack^{93,94}, and it allows the beginning of biodegradation processes carried out by physical, chemical, and enzymatic action of microorganisms.

The interaction between plastics and microorganisms has been studied by the scientific community aiming to understand the mechanisms involved in biodegradation. Currently, the biodegradation process is divided into four main steps: (i.) biodeterioration, (ii.) biofragmentation, (iii.) assimilation, (iv.) mineralization⁹⁵ (**Figure 12**).

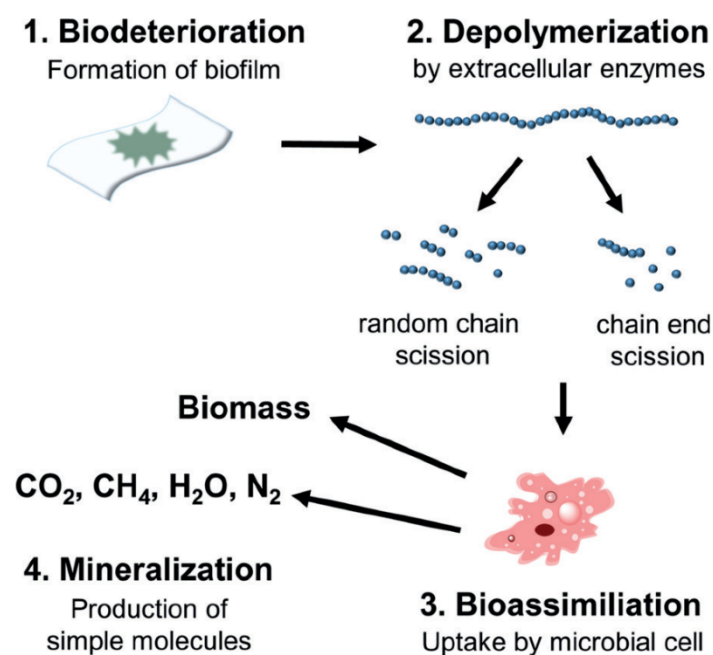


Figure 12- Schematic representation of the different steps involved in biodegradation. Adapted from Haider *et al.*¹¹.

i. Biodeterioration:

Biodeterioration is the deterioration of polymer properties caused by microorganisms. In this first step, microorganisms damage the polymer by physical, chemical, and/or enzymatic action, resulting in macroscopic alterations (such as holes, cracks, and color changes) and the initial breakdown of the polymer material into smaller particles. The biodeterioration results from the activity of microorganisms growing on the surface or inside the polymer material⁷⁸.

The physical biodeterioration occurs because microorganisms secrete a complex matrix made of polymers (e.g., polysaccharides and proteins) that allows them to adhere to plastics. This matrix infiltrates the polymer pores and modifies their size, distribution, moisture degrees, and thermal transfers. The entry of matrix into the pores allows microorganisms to grow inside, consequently, increasing the pore size and promoting cracks, which results in the weakening of the polymeric material⁷⁸. A relevant aspect of the matrix is that it acts as a surfactant, facilitating the exchanges between the hydrophobic and hydrophilic phases. Further, the matrix promotes the accumulation of pollutants, a potential nutrition source for microorganisms, that leads to microorganism development and accelerate the biodeterioration⁹⁶.

The chemical biodeterioration is caused by the chemical compounds released by the metabolism of microorganisms. During growth, microorganisms can use organic and/or inorganic sources to develop, depending on the metabolic processing of the source and the type of microorganisms involved a large variety of acid compounds are released. They induce water to enter the polymer pores, enhancing the hydrolysis process, leading to the formation of oligomers and monomers^{78,97}.

The enzymatic biodeterioration is related to the ability of microorganisms to produce enzymes, such as lipases, ureases, or proteases. These enzymes bind to some type of polymers and catalyze the hydrolysis of specific bonds⁷⁸.

ii. Biofragmentation/ Depolymerization:

This step refers to the catalytic action that cleaves polymers into oligomers, dimers, or monomers (small fragments of low molecular weight). It is critical to allow later assimilation by the microorganisms since, without biofragmentation, high molecular weight macromolecules are unable to cross microbial membranes^{78,97}. Biofragmentation is carried out by the ectoenzyme or free-radicals secreted by the microorganisms. There are a wide variety of enzymes that act in different ways. Enzymes are biological catalysts of a protein nature which exhibit different molecular weight ranging from several thousand to several million g/mol⁹⁷. During growth, microorganisms produce constitutive enzymes that are not dependent on the presence of specific polymers, but they can also adapt cellular machinery to produce inducible enzymes in response to the recognition of a specific polymer⁷⁸. Extracellularly, enzymes may be free or fixed to particles, its enzymatic action may occur inside (endoenzymes) or at the ends (exoenzymes) of the polymeric chain. They may be

specific to a particular polymer or cleave different types of polymers. In biofragmentation processes, the most relevant groups of enzymes are hydrolases (enzymatic hydrolysis), and oxidoreductases (enzymatic oxidation)⁷⁸.

Free radicals may also play an active role in biofragmentation, these molecules may be secreted by microorganisms or produced by enzymes in the extracellular environment, these free radicals attack the polymeric chain causing oxidation reactions that lead to their breakdown^{78,97}.

iii. Assimilation:

After biofragmentation oligomers, dimers and monomers are released. This step is characterized by the uptake of these small molecules by the microorganisms and their use in microbial metabolism. These fragments must pass the microbial membranes to be assimilated. Small oligomers, dimers, and monomers can be transported⁹⁸. Some monomers are easily transported to the cytoplasm via specific membrane carriers⁷⁸. In contrast, the cell membrane can be impermeable to other fragments that prevent them from being assimilated, however, these molecules may undergo biotransformation reactions being converted into products (organic intermediates like acids, alcohols, and ketones) that can be assimilated^{78,99}. Inside the microorganisms, the transported fragments are oxidized by catabolic pathways leading to the production of energy (e.g. adenosine triphosphate), constitutive elements of the cell structure, and new biomass^{78,95}. Microorganisms, depending on their ability to grow under aerobic or anaerobic conditions, essentially use three catabolic pathways to produce the energy to maintain cellular activity, structure, and reproduction: aerobic respiration, anaerobic respiration, and fermentation⁷⁸. After processing these fragments by catabolic pathways, various end products can be formed: in the presence of oxygen there is the formation of CO₂ and H₂O and microbial biomass, in an anoxic environment are formed CO₂, H₂O, microbial biomass and under methanogenic conditions CH₄⁷⁶ or under sulfidogenic condition H₂S¹⁰⁰. If the catabolic pathways have microbial biomass (organic matter) as the end products, degradation may not be complete. These metabolites can be transported out of microorganisms if they do not have the metabolic capacity to transform them, or do not want to metabolize or store them. In the extracellular environment, excreted metabolites may be used by other microorganisms that can continue biodegradation, or maybe non-assimilable compounds⁹⁵. Microbial organic metabolites excreted can represent an ecotoxic hazard at different level⁹⁷.

iv. Mineralization:

The biodegradation process is completed if mineralization occurs. Mineralization is the process where the catabolic pathways have mineral components (completely oxidized metabolites) as their end products, such as CO₂, N₂, CH₄, H₂O⁹⁵. Mineral molecules released by microorganisms do not represent an eco-toxicological risk for the environment, since they follow the biogeochemical cycles⁹⁷.

Biodegradation of polymers is dependent on several factors (**Figure 13**): exposure conditions, characteristics of the polymer, type of microorganism(s) involved, and previous abiotic degradation^{76,101}. Exposure parameters, namely, humidity, temperature, pH, salinity, the presence or absence of oxygen, and the supply of different nutrients influence the polymer biodegradation, as well as on the microbial population and enzymatic activity^{10,101}. Numerous polymer characteristics can influence biodegradation, such as flexibility, crystallinity, molecular weight, functional groups, hydrophobicity, and more^{76,101}. Flexible polymeric chains facilitate the fitting of the active site of enzymes, for example, aliphatic polyesters are easily biodegraded than aromatic polyesters¹⁰¹. The molecular weight determines several physical properties of the polymer, biodegradation becomes difficult with the increase in molecular weight¹⁰². Crystalline structures are more resistant to biodegradation than amorphous ones, their organized structure with strong interchain hydrogen bonds limits the enzymatic access¹⁰¹. Generally, polyesters with a higher melting temperature have less biodegradability⁹⁹. Besides all the above mentioned, other factors, for example, low molecular weight additives (e.g., plasticizers), polymers blends, copolymers, cross-linking, substituents and tacticity may play an important role in biodegradation¹⁰¹.

It is also important to point out that polymer biodegradation studies (even non-biodegradable polymers) are usually successful, but under optimal conditions created in the laboratory, under environmental conditions, they may not occur in the same way. In natural environments the exposure conditions are more inconstant and diverse, most laboratory studies fail to reproduce these conditions, such as mixed microbiological populations, water salinity variation, and natural cycles of temperature and light¹⁹. In addition, homogeneous materials of a given thickness or morphology are normally used for research, which does not consider the changes caused to the polymer when exposed to the environment, not only change in size and morphology but also chemical composition, propensity for aggregation,

hydrodynamic size, and chemical and colloidal stability¹⁹. A good example of this is PET. PET is considered a non-biodegradable plastic and accumulates in the environment, but a study has already reported that under laboratory conditions the bacteria *Ideonella sakaiensis* 201-F6 can degrade and assimilate it. In this study, the bacteria degraded PET films almost completely in just six weeks at 30°C¹⁰³. The environment where the polymer ends is probably the factor that most influences its rate of biodegradation. Exposure conditions vary substantially between composting, soil, and marine environments, and the same polymer may have different rates of biodegradation in each of these environments¹¹.

Factors affecting polymer biodegradation		
<p>Abiotic factors</p> <ul style="list-style-type: none"> ▪ Temperature ▪ pH ▪ Moisture content ▪ UV radiation ▪ Salinity 	<p>Organism</p> <ul style="list-style-type: none"> ▪ Hydrophobicity ▪ Extracellular enzymes ▪ Biosurfactants 	<p>Polymer characteristics</p> <ul style="list-style-type: none"> ▪ Morphology ▪ Flexibility ▪ Crystallinity ▪ Molecular weight ▪ Functional groups ▪ Plasticizers/additives ▪ Blends of polymers ▪ Copolymers ▪ Cross-linking ▪ Hydrophobicity ▪ Tacticity

Figure 13- Parameters that affect the biodegradation of polymers. Adapted from Artham et al.¹⁰¹.

2.4. Polymer degrading microorganisms – *Penicillium brevicompactum*

Polymer degrading microorganisms are widely distributed in the environment, such as marine waters, soil, aerobic and anaerobic sludge, industrial wastes, compost, and also in the human body¹⁰⁴. Bacteria, archaea, fungi, and other eukaryotic beings (e.g. algae) have already been detected by numerous studies in plastics collected from the ocean⁹⁴. Several studies have been proving in laboratory conditions the biodegradative capacity of these microorganisms, a lot of bacteria and fungi with the capacity to degrade plastics have already been described⁹⁴, some reviews list these plastic degraders^{76,94,99,105,106}.

The fungi kingdom consists of a wide variety of eukaryotic organisms, morphologically classified as filamentous fungi, yeasts, or dimorphic fungi. These organisms can be considered saprotrophic (decomposition of dead material) obligated or opportunistic

organisms (decomposers, mutualists, or pathogens)^{107,108}. Filamentous fungi have been the most reported¹⁰⁹. The filamentous network structure gives them the advantage to explore and grow in places that are difficult for other microorganisms to access, as it allows them to extend through substrates in search of nutrients¹⁰⁹. Fungi are mostly aerobic and can inhabit terrestrial and aquatic environments, even in extreme environmental conditions^{110,111}. These organisms are provided with several extraordinary strategies, such as powerful enzymatic systems, the adsorption capacity, and the production of natural biosurfactants (i.e., hydrophobins), which allows them to use polymers as a source of carbon and energy¹⁰⁹. Several studies have reported this ability that some fungi have to biodegrade fossil-based polymers (conventional plastics)^{92,112,113}.

The filamentous fungi belonging to the genus *Penicillium* (phylum Ascomycota, class Eurotiomycetes, order Eurotiales, family Aspergillaceae¹¹⁴) have shown promising capabilities in degrading conventional plastics. The genus *Penicillium* was suggested by Link in 1809 to accommodate asexual fungi that bore penicillum (painter's brush)-like fruiting bodies¹¹⁵. These fungi are usually characterized by forming green colonies, and their conidia are cylindrical to bottle-shaped and aggregated in compact penicilli¹¹⁶. Including more than 400 species, *Penicillium* is widely distributed in all habitats (soil, plants, air, aquatic environments, indoor environments, and food)¹¹⁷. Some *Penicillium* strains are adapted to live in marine environments, this ability to tolerate high concentrations of salts can be an advantage in the application of these microorganisms in the bioremediation field¹¹⁸. *Penicillium brevicompactum* can live in saline environments and is particularly common in Adriatic salterns¹¹⁹. Also, Gonçalves *et al.*¹²⁰ studied the presence of the genus *Penicillium* in coastal marine environments from Portugal and observed that *P. brevicompactum* was one of the most frequently identified¹²⁰. Regarding the biodegradation of polymers by *P. brevicompactum* there is not much information. Lugauskas *et al.*¹²¹ evaluated the colonization of fungi in various types of polymers exposed to different environmental conditions. They observed that in polyethylene (PE) samples the most dominant isolated fungus was *P. brevicompactum*. This fungus was also frequently isolated from other polymers¹²¹. In addition to *P. brevicompactum*, other species of the genus *Penicillium* showed a potential to biodegrade plastics. Namely, *P. simplicissimum* can biodegrade and use polyethylene as a carbon source^{122,123}. Ojha *et al.*¹²⁴ isolated several fungi from PE sheets and demonstrated that the fungi *P. oxalicum* and *P. chrysogenum* have a great capacity to biodegrade this polymer. After 90 days of PE (different densities) incubation with these fungi, they obtained weight loss (%) values between $\approx 34 - 59\%$ ¹²⁴. Sepperumal *et al.*¹²⁵ reported that *Penicillium* species caused chemical changes in

PET flakes and powdered PET, and there was the assimilation of this polymer as a carbon source¹²⁵. Novak *et al.* evaluated the biodegradation of PET films, and after 84 days of incubation in the presence of the fungus *P. funiculosum* they observed that there were important chemical changes in the polymer chains¹²⁶.

Considering all this information, the genus *Penicillium* presents potential to biodegrade fossil-based polymers, specifically to biodegrade PET. The bio-based PEF as mentioned above is structurally and has properties similar to PET polymer. In this context, *P. brevicompactum* emerged to be a good option for assessing the biodegradation of PEF.

II. Synthesis of Poly(ethylene 2,5-furandicarboxylate) (PEF) and evaluation of biodegradation by the fungus *Penicillium brevicompactum*

1. Background

Considering what was previously contextualized, PEF biodegradation has not yet been demonstrated under relevant environmental conditions¹²⁷. It is essential to promote more studies to obtain an environmental perspective on its biodegradation¹²⁷.

The genus *Penicillium* has been distinguished for including several species with a promising ability to degrade fossil-based polymers^{121–126}. *P. brevicompactum* growth has already been reported in several polymeric materials, and in PE samples it was the most frequently isolated fungus¹²¹.

In this context, the objective of the present study was to evaluate the biodegradation of PEF by the fungus *Penicillium brevicompactum*. PEF was synthesized by a 2-stage melt polymerization approach, and the success of its synthesis was confirmed by Attenuated total reflection Fourier transform infrared spectroscopy (ATR-FTIR) and ¹H nuclear magnetic resonance (¹H NMR). A biodegradation test was designed based on gravimetric and ATR-FTIR analysis of the fungus and PEF microparticles.

2. Material and Methods

2.1. Materials:

To synthesize the DMFDC and PEF: 2,5-furandicarboxylic acid (FDCA, 98 %) was acquired from TCI Chemicals. Ethylene glycol (EG, > 99%), trifluoroacetic acid (TFA, 99%), titanium-(IV) isopropoxide (Ti-(OiPr)₄, 99.999% trace metals basis), deuterated trifluoroacetic acid (TFA-d, 99.5 atom % D) and deuterated tetrachloroethane (TCE-d₂, 99.5 atom % D) were purchased from Sigma–Aldrich. Concentrated hydrochloric acid (HCl, 37 %) was purchased from Panreac. Methanol (analytical grade) and chloroform (HPLC grade) were purchased from Fisher Chemical.

Biodegradation test - culture medium: D(+)-glucose (anhydrous, for bacteriology) was acquired from LabKem. Peptone special was purchased from Sigma–Aldrich. Sodium Chloride (NaCl, reagent grade) was acquired from Scharlab, and malt extract from Oxoid. All chemicals were used as received unless otherwise stated.

2.2. Synthesis of dimethyl 2,5-furandicarboxylate (DMFDC):

DMFDC was synthesized by Fischer esterification of the FDCA as already reported in ^{32,57}. Briefly, FDCA reacts with an excess of methanol (0.2/8.9 mol), under acidic conditions (aqueous HCl 37%, 15 mL) at 80 °C for approximately 15 h (**Figure 14**). The mixture was then cooled to room temperature. The ensuing white precipitate formed in the mixture was isolated by filtration and thoroughly washed with cold methanol until reaching pH = 5. The DMFDC retained in the filter was dried in the oven at 40 °C for 3 days.

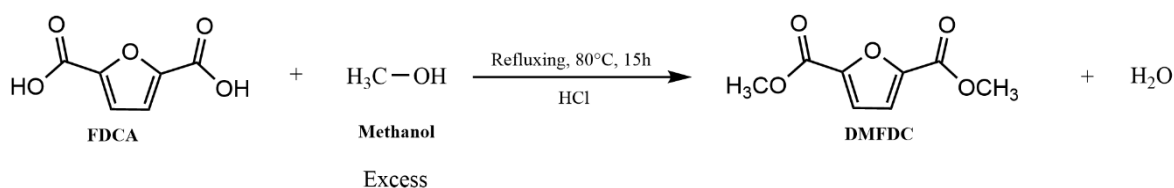
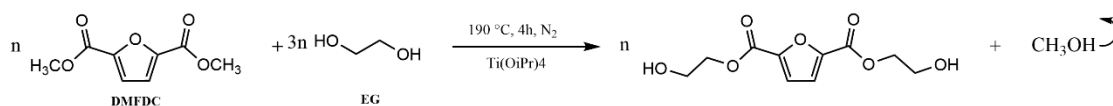


Figure 14- DMFDC synthesis scheme.

2.3. Synthesis of poly(ethylene 2,5-furandicarboxylate) and film preparation:

PEF was synthesized by a 2-stage melt polymerization approach (**Figure 15**). DMFDC and ethylene glycol (EG) were charged with a molar ratio of diester/diol = 1/3 to a reaction apparatus with magnetic stirring and under a nitrogen atmosphere. The mixture was gradually heated until it became homogeneous (≈ 120 °C), at this point the catalyst Ti-(OiPr)₄ (0.14 mol%) was added. The temperature was gradually increased to 190 °C, and the reaction allowed to proceed for 4h. Subsequently, the vacuum was switched on, and a stabilization period of 30 minutes was carried out at 190 °C. Then, the reaction proceeded (polytransesterification stage) under vacuum, and the temperature was gradually increased to 210 °C and kept in these conditions for 3h.

1ST STAGE: TRANSESTERIFICATION



2ND STAGE: POLYTRANSESTERIFICATION

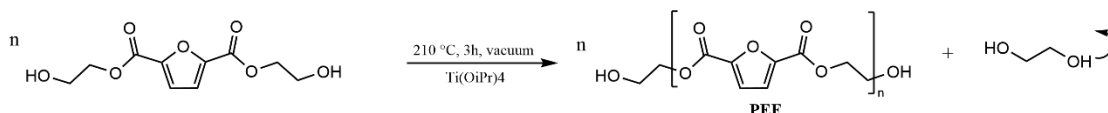


Figure 15- PEF synthesis scheme

When the reaction finished the polymer was purified: the reaction mixture was dissolved in CHCl_3 with a few drops of TFA and precipitated in an excess of cold methanol (ca. 1 L), filtered, and the precipitate was dried in the oven at 40 °C for 3 days.

PEF films were prepared by melting. A rectangular aluminum mold (ca. 10 x 70 x 1 mm; width x length x thickness) was filled with powdered PEF and the temperature was gradually increased until melting was observed (~ 200 °C). When the polymer was completely melted and visually uniform, the mold was allowed to cool to room temperature. Finally, the film was removed from the mold. For the biodegradation test, the films were mechanically cut into fragments with a size ≤ 2 mm.

2.4. Microorganism - *Penicillium brevicompactum*

Penicillium brevicompactum (CMG 72) was isolated in our lab, from a contaminated culture of *Zalerion maritimum*. The identification of the strain was confirmed through phylogenetic analysis of sequences of the rDNA internal transcribed spacer region (ITS), as described by Gonçalves *et al.*¹²⁰.

Before the biodegradation test, this fungus was grown at 25 °C in a growth medium containing 20 g/L of glucose, 20 g/L of malt extract, 1 g/L of peptone, and 35 g/L NaCl, under stirring for 7 days.

2.5. PEF biodegradation test by the fungus *Penicillium brevicompactum*

Results obtained by our working group regarding the biodegradation of PEF by the fungus *P. brevicompactum* during 28 days of incubation were not conclusive, with imperceptible biodegradation being observed. Bearing this in mind and considering that 28 days of incubation may be insufficient time to observe PEF biodegradation, the present assay was designed to maximize the incubation time of the fungus *P. brevicompactum*, to promote a longer contact time between the fungus and the PEF. For this purpose, a procedure with discontinuous feeding of the culture medium was developed, which is an unusual procedure in polymer biodegradation tests.

Three types of Erlenmeyer flasks were used, growth control (GC), PEF control (PC), and PEF + *P. brevicompactum* (PEF+*P.b*) (**Figure 16**). All Erlenmeyer (of 100 mL) consisted of 50 mL of culture medium prepared with the following concentrations: 35 g/L of NaCl, 4.6 g/L of glucose, 16.3 g/L of malt extract, and 0.56 g/L of peptone. Additionally, in the GCs 0.5 g of fungus were inoculated. In PCs, 0.015 g of PEF microparticles were added. The PEF+*P.b*

were prepared with both 0.5 g of inoculated fungus and 0.015 g of PEF microparticles. The Erlenmeyer's were autoclaved with the culture medium and with/without polymer and only after the fungus was inoculated under aseptic conditions. For each incubation time, 3 GC, 3 PC, and 4 replicates of the PEF+*P.b* were prepared. Also, 3 PC replicates were prepared to be analyzed after autoclaving. A total of 60 Erlenmeyer flasks were prepared for six incubation times: 14, 28, 42, 56, 70, and 84 days. The Erlenmeyer's were placed in a shaker at 25 °C with stirring at 120 rpm. At each incubation time, the respective Erlenmeyer flasks were removed, and the fungus and the PEF microparticles were separated from the medium by filtration.

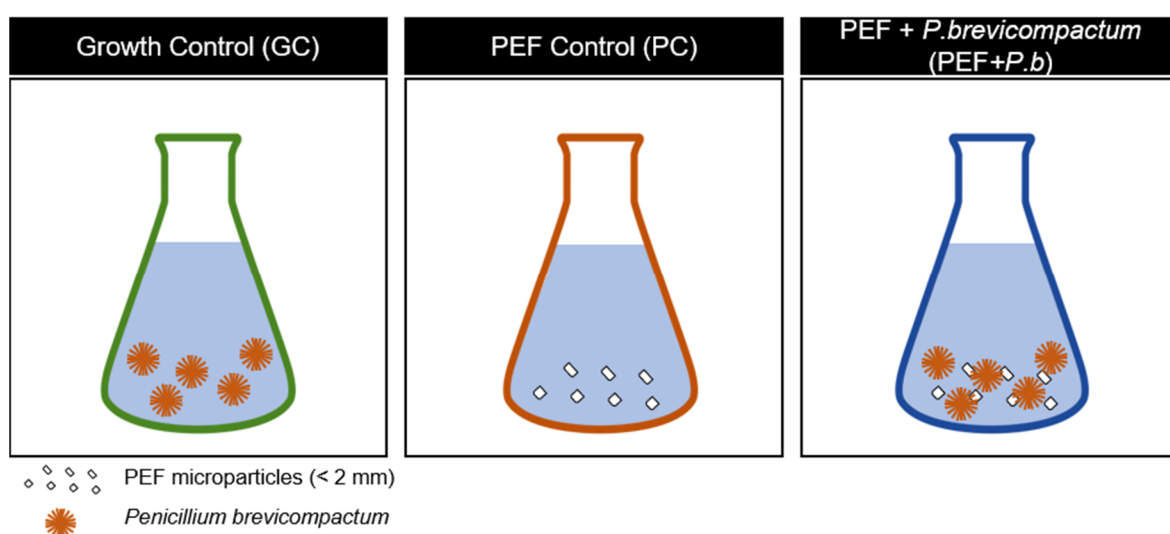


Figure 16- Composition of the Erlenmeyer used in biodegradation test.

The fungus biomass was recovered, frozen, and lyophilized, and later weighed and analyzed by ATR-FTIR spectroscopy. The PEF microparticles were stored, dried in the oven at 40 °C for 2 days, and then weighed and analyzed by ATR-FTIR spectroscopy. The culture medium was collected at 56 days of incubation, frozen and lyophilized, and then analyzed by ATR-FTIR spectroscopy and ¹³C ssNMR.

Discontinuous feeding of the culture medium was performed every 14 days of incubation. Every 14 days, 10 mL of culture medium prepared with 35 g/L of NaCl, 11 g/L of glucose, 40.75 g/L of malt extract, and 1.4 g/L of peptone were added under aseptic conditions to all Erlenmeyer. To design this method of feeding, a PEF biodegradation test was carried out for 28 days in which the growth of *P. brevicompactum* and its consumption of culture medium were evaluated, as well as the biodegradation of PEF, results available in **Supplementary data A**. This 10 mL contained half the amount of initial nutrients in the

50mL, the goal was to try to promote the longevity of the fungus, but without excessively increasing its growth (biomass), a factor that can compromise the survival of the fungus (due to lack of space and nutrients), as well as trying to promote the use of PEF by the fungus. The procedure used in this biodegradation test is schematically summarized in **Figure 17**.

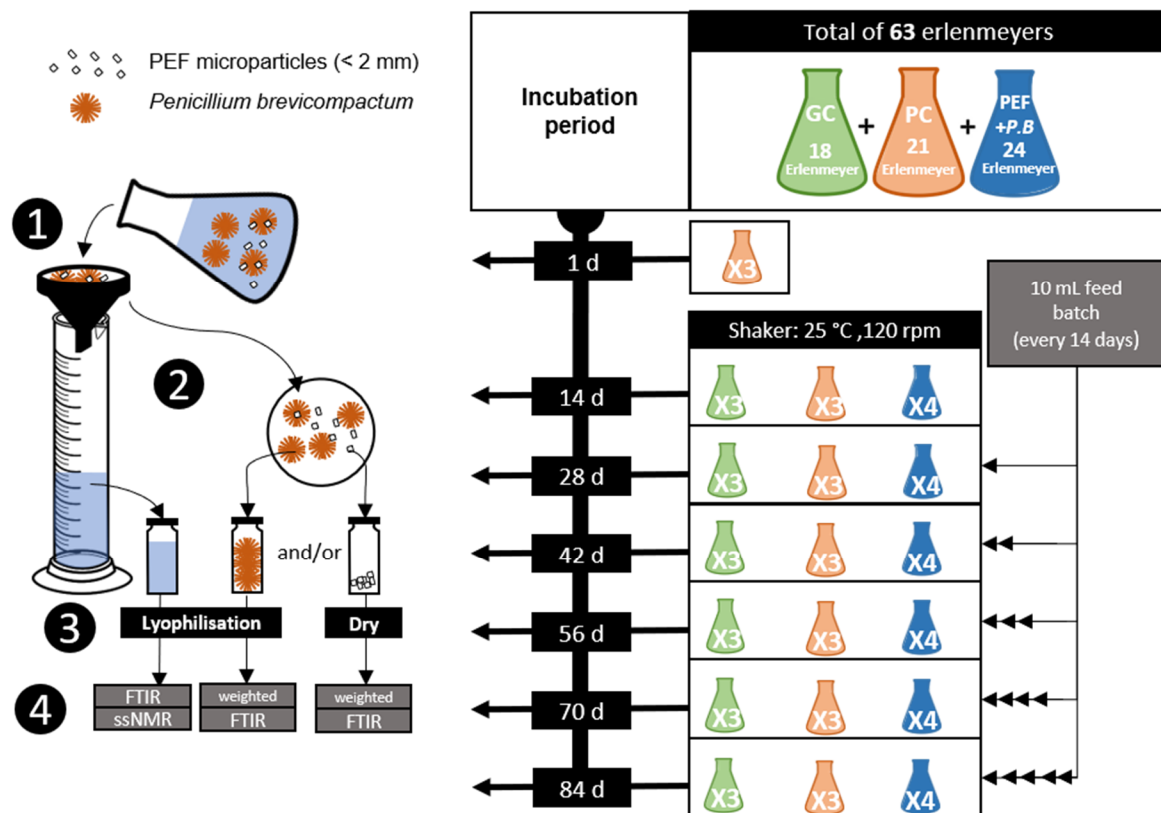


Figure 17- Schematic summary of the PEF biodegradation test by the fungus *Penicillium brevicompactum*. After each incubation time: **1)** Filtration of the fungus and/or PEF microparticles; **2)** Separation of the fungus and/or PEF, and culture medium; **3)** PEF (drying 40°C), fungus and culture medium (lyophilization); **4)** Analysis of results.

2.6. Analysis

Attenuated total reflection Fourier transform infrared spectroscopy (ATR-FTIR) analyses were carried out using a Perkin Elmer (USA) Spectrum BX FTIR instrument. The FDCA and the synthesized DMFDC and PEF were analyzed within the 4000-500 cm^{-1} range, with a resolution of 8.0 cm^{-1} at 128 scans. In the biodegradation test, the PEF and lyophilized culture medium samples were analyzed within the range of 4000-500 cm^{-1} , with a resolution of 4.0 cm^{-1} at 64 and 32 scans, respectively. The lyophilized fungus samples were analyzed within the range of 4000-400 cm^{-1} , with a resolution of 8.0 cm^{-1} at 64 scans. Air was used for the background spectrum.

^1H NMR spectroscopy spectrum of PEF was recorded on a Bruker AMX 300 spectrometer operating at 300.13 MHz. Deuterated tetrachloroethane (TCE-d_2 , 99.5 atom % D) and 3 drops of deuterated trifluoroacetic acid (TFA-d , 99.5 atom % D) were used as solvents. Chemical shifts (δ) were obtained at 60 °C and expressed in parts per million (ppm), reported relative to the main solvent (TCE-d_2).

^{13}C Solid-State Nuclear Magnetic Resonance Spectroscopy (^{13}C ssNMR) spectra were acquired using a Bruker Avance-III 400 MHz spectrometer, operating at 9.4 T, with 4 mm probe and frequency of 12 kHz, in CP MAS.

3. Results and Discussion

3.1. Synthesis of DMFDC and PEF and characterization

DMFDC was synthesized by Fisher's esterification, as described previously, and a white powder was obtained in 34% yield. Low value compared to the literature^{57,128}. The characterization of DMFDC via FTIR spectroscopy (**Figure 18** and **Table 2**) allowed us to verify the success of its synthesis. Comparing the FTIR spectra of the FDCA with DMFDC, it was possible to observe peaks of characteristic bands in common, such as the C=C peak appeared around 1582 and 1526 cm^{-1} , furan ring breathing peak 1026 cm^{-1} and 2,5-disubstituted ring peaks appeared around 972, 828, and 758 cm^{-1} . The main differences between the spectrum of the two compounds allow confirming the formation of DMFDC, namely, the disappearance of the elongation O-H (carboxylic acid) between 3300-2300 cm^{-1} , the displacement to a higher wavenumber of the peak associated with the carbonyl group (C = O; from 1656 to 1708 cm^{-1}) and the appearance of a new peak associated with the C-H bonds of the methyl group (CH_3) at 2970 cm^{-1} . The DMFDC spectrum was in line with those already reported in other studies^{57,128}.

PEF was successfully synthesized, with an isolation yield of *ca.* 58%. The typical FTIR spectrum of PEF (**Figure 18** and **Table 2**) was essentially the same as that of its precursor DMFDC, except for the presence of low-intensity peaks detected at 2964 and 2913 cm^{-1} related to the antisymmetric and symmetric stretching of C-H bond of aliphatic CH_2 groups (instead of the CH_3) and a very weak OH peak around 3494 cm^{-1} , corresponding to end groups, suggested that the PEF reached a reasonably high molecular weight. The FTIR spectrum obtained for PEF is identical to those already reported^{32,38,129}.

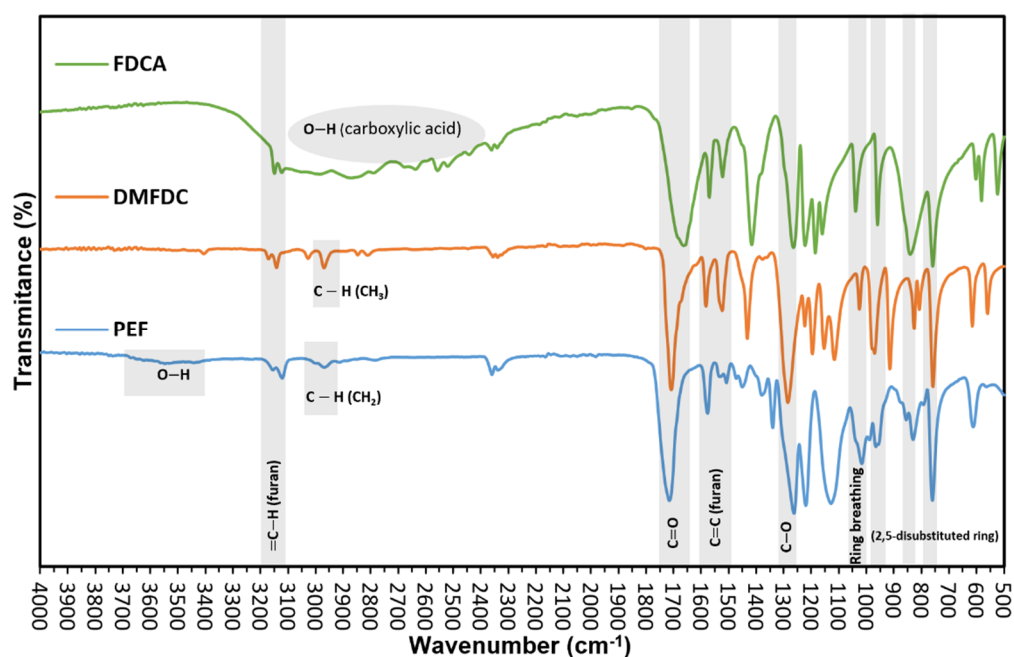


Figure 18- ATR-FTIR spectrums of FDCA, DMFDC, and PEF.

Table 2 - ATR-FTIR Data of FDCA, DMFDC, and PEF.

Assignment (functional group)	Wavenumber (cm ⁻¹)		
	FDCA	DMFDC	PEF
O-H	---	---	3494
O-H (carboxylic acid)	3300-2200	---	---
=C-H (furan)	3150	3174	3156
C-H (CH ₃)	---	2970	---
C-H (C H ₂)	---	---	2964;2913
C=O (COOH)	1656	---	---
C=O (COOCH ₃)	---	1708	---
C=O (COOCH ₂ CH ₂)	---	---	1716
C=C (furan ring)	1570;1524	1582,1526	1576;1508
C-O	1266	1286	1262
Ring breathing	1040	1026	1016
2,5-disubstituted ring	960;844;758	972;828;758	966;832;760

Regarding the ¹H NMR spectra (**Figure 19** and **Table 3**) of PEF, typical chemical shifts and integration areas were observed¹³⁰: ¹H NMR (300 MHz, TCE-d₂) δ 7.32 (s, 2H), 4.72 (s, 4H). The main chemical shifts were observed (a) at 4.72 ppm attributed to the methylene groups and at (b) 7.32 ppm related to furan protons. Resonances (a) and (b) were presented as singlets due to the symmetry of FDCA¹³¹. The proportion of the integral areas of the protons a:b was 2:1, which indicated that the polymer had the correct structure. Additionally, it was possible to observe resonances related to methylene protons in terminal positions (e) at 4.59 and (f) at 4.13 ppm, this made it possible to calculate a DP_n ≈ 44 and number-average molecular weight (M_n) ≈ 8103 g.mol⁻¹. Resonances (c) at 4.59 ppm (overlapped with the peak (e)) and (d) at 4.02 ppm indicate the formation of diethylene glycol (DEG).

The formation of this ether-bridge affects the final properties of PEF, and, as already reported^{130,132}, is promoted when large amounts of diol (EG) are used in relation to DMFDC, such as the conditions used in the present study.

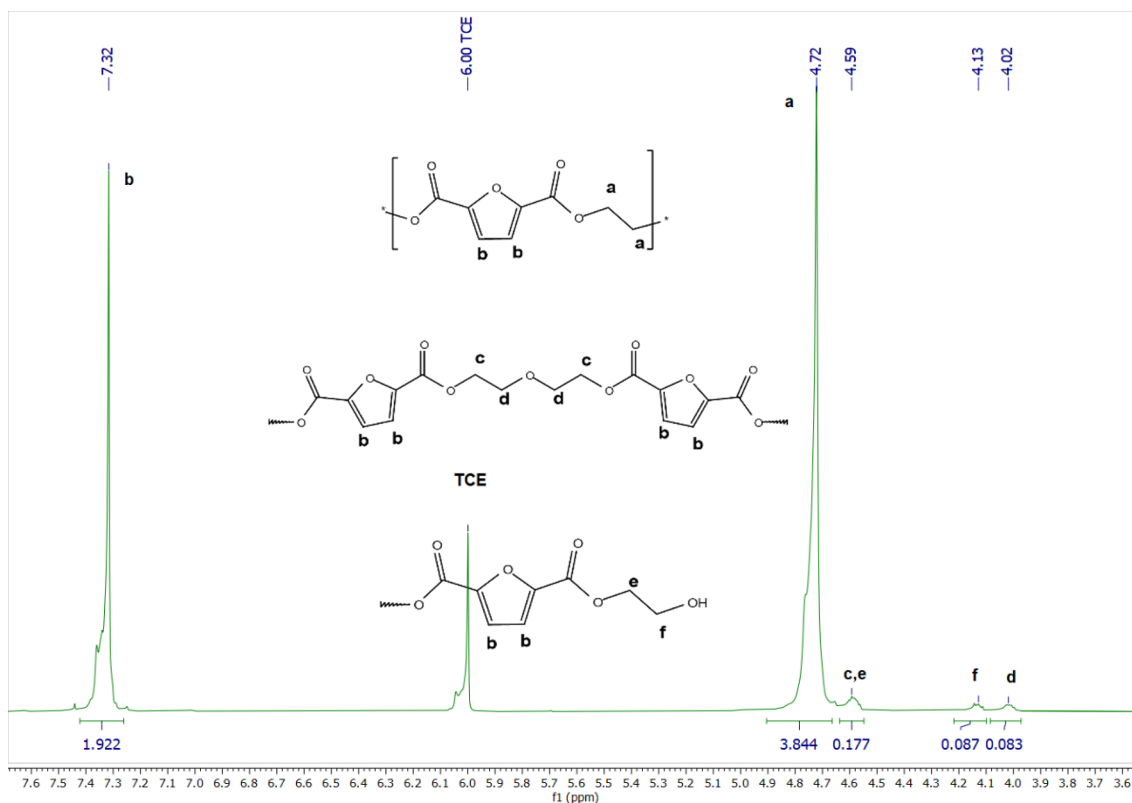


Figure 19- ¹H NMR spectra of PEF [300 MHz, TCE+ 3 drops TFA, reference (TCE) = 6.00 ppm]

Table 3 - ¹H NMR resonances of PEF [300 MHz, TCE-d₂+ 3 drops TFA-d, reference (TCE) = 6.00 ppm]

PEF			
δ /ppm	Integration area	Multiplicity	Assignments
7.32	1.9	s	b
6.00	---	s	TCE solvent
4.72	3.8	s	a
4.59	0.18	m	c+e
4.13	0.09	m	f
4.02	0.08	m	d

3.2. PEF biodegradation by the fungus *Penicillium brevicompactum*

In the present biodegradation assay, the incubation time idealized in the methodology was not reached, and it was only possible to keep the fungus alive in the PEF+*P.b* samples up to approximately 42 days and in the GCs until about 56 days of incubation. Due to this fact, the following sections will be analyzed and discussed the results obtained only up to 56 days of incubation. For better understanding, the results are divided into 2 parts: Weight

and ATR-FTIR analysis of the fungus, and weight and ATR-FTIR analysis of the PEF microparticles. The results obtained from the analysis (ATR-FTIR and ^{13}C ssNMR) of the culture medium at 56 days of incubation are available in **Supplementary data B**.

3.2.1. Weight and ATR-FTIR analysis of *Penicillium brevicompactum*

To be able to observe the influence of the PEF on the growth and behavior of the fungus throughout the incubation times, we used the GCs as a comparison of the PEF+*P.b* Erlenmeyer flasks. Throughout the test, as we can see in **Figure 20** and **Table 4**, higher values of growth of the fungus were always obtained in the GC than in the PEF+*P.b* Erlenmeyer flasks. This difference was obvious in the 42 days of incubation.

These observations indicate that PEF probably had a negative effect on the growth of the fungus. Also, the death of the fungus was observed in all samples of PEF+*P.b* near 42 days of incubation (loss of structure and browning of the medium). In contrast, at 42 days of incubation, the fungus in the GCs was alive, with a healthy structure and color (**Figure 21**). To also study the death of the fungus in the GCs the test was maintained, and the death of the fungus in the GCs was observed at approximately 56 days of incubation. This time interval of approximately 14 days between the death of the fungus in PEF+*P.b* and the death in GC flasks supported the hypothesis that PEF is having a negative effect on the growth of the fungus. This behavior of the fungus suggests that there was no PEF biodegradation.

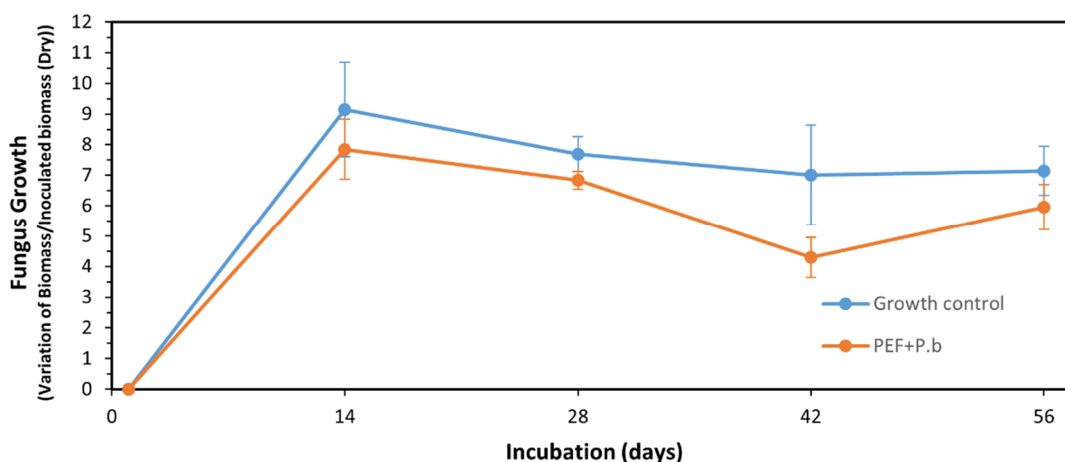


Figure 20- Variation of *Penicillium brevicompactum* biomass throughout the experiment.

Table 4- Variation of *Penicillium brevicompactum* biomass throughout the experiment

Erlenmeyer condition		Inoculated Biomass (Wet) (g)	Inoculated Biomass (Dry) (g)	Final Biomass (Dry) (g)	Variation of Biomass	Growth	Growth mean \pm SD
14 days							
GC	R1	0.517	0.0444	0.419	0.375	8.43	9 \pm 2
	R2	0.523	0.0450	0.535	0.490	10.9	
	R3	0.510	0.0438	0.398	0.354	8.08	
PEF+P.b	R1	0.517	0.0444	0.410	0.366	8.23	8 \pm 1
	R2	0.523	0.0450	0.352	0.307	6.83	
	R3	0.515	0.0443	0.368	0.324	7.31	
	R4	0.512	0.0440	0.441	0.397	9.02	
28 days							
GC	R1	0.533	0.0458	0.427	0.381	8.32	8 \pm 1
	R2	0.515	0.0443	0.363	0.319	7.20	
	R3	0.527	0.0453	0.387	0.342	7.54	
PEF+P.b	R1	0.505	0.0434	0.324	0.281	6.46	7 \pm 0
	R2	0.502	0.0431	0.339	0.296	6.86	
	R3	0.510	0.0438	0.343	0.299	6.83	
	R4	0.518	0.0445	0.364	0.319	7.18	
42 days							
GC	R1	0.505	0.0434	0.415	0.372	8.56	7 \pm 2
	R2	0.524	0.0450	0.367	0.322	7.15	
	R3	0.522	0.0449	0.283	0.238	5.31	
PEF+P.b	R1	0.522	0.0449	0.237	0.192	4.28	4 \pm 1
	R2	0.536	0.0461	0.213	0.167	3.62	
	R3	0.502	0.0431	0.267	0.224	5.19	
	R4	0.517	0.0444	0.226	0.182	4.09	
56 days							
GC	R1	0.506	0.0435	0.363	0.320	7.35	7 \pm 1
	R2	0.515	0.0443	0.390	0.346	7.81	
	R3	0.523	0.0450	0.326	0.281	6.25	
PEF+P.b	R1	0.523	0.0450	0.336	0.291	6.47	6 \pm 1
	R2	0.516	0.0443	0.322	0.278	6.26	
	R3*	0.500	0.0430				
	R4	0.526	0.0452	0.276	0.231	5.11	

* Broken sample

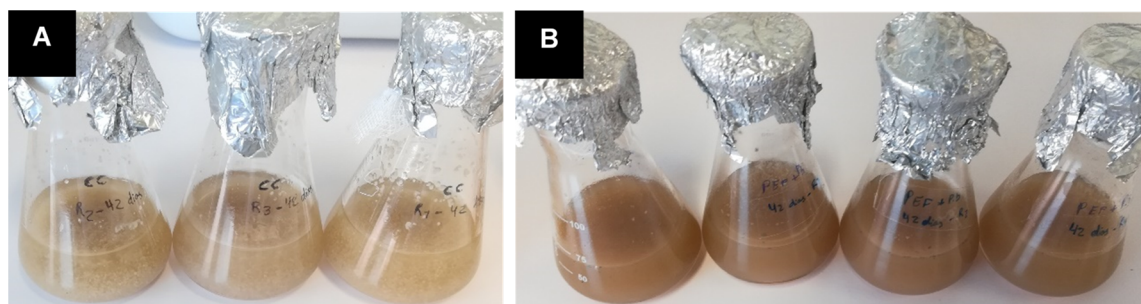


Figure 21- Differences between Erlenmeyer flasks at 42 days of incubation. A) GC flasks (live fungus) B) PEF+P.b flasks (dead fungus).

ATR-FTIR analyses were carried out for the *P. brevicompactum* mycelium to evaluate the differences between the chemical profiles of the fungus grown in the GC and PEF+*P.b* flasks throughout the trial. **Figure 22** shows the ATR-FTIR spectra obtained during the assay for *P. brevicompactum*. To facilitate data visualization, only one GC spectrum and one PEF+*P.b* spectrum were selected for each incubation time. The obtained spectra are similar to those already reported for other fungi^{92,133}. We observed a wide peak between 3700 and 3050 cm^{-1} , attributed to the stretching vibrations of the O-H and N-H bonds (present in several macromolecules). Two peaks in the 2996–2800 cm^{-1} region, caused by stretching of CH_2 and CH_3 functional groups of lipids mainly, but also proteins¹³⁴. Additionally, peak within the 1800–1700 cm^{-1} region, caused by the C=O stretching in esters, typically from lipids. One peak found between 1700-1600 cm^{-1} , caused by C=O stretching, Amide I (proteins, chitin), and one peak between 1600-1500 cm^{-1} , caused by C-N-H deformation, Amide II (proteins, chitin)¹³⁵. Peaks detected between 1500-1300 cm^{-1} arising predominantly from CH_2 and CH_3 bending mode of lipids and proteins. The peaks between 1250-1200 cm^{-1} and around 1080 cm^{-1} were attributed to P=O asymmetric and symmetric stretching vibrations and phospholipids^{134,136}. The peak between 1200-900 cm^{-1} is frequently attributed to C-O and C-O-C stretching (carbohydrates)^{134,135}. Lastly, the region between 900-600 cm^{-1} may contain weakly expressed bands arising from aromatic ring vibrations of phenylalanine, tyrosine, tryptophan, and the various nucleotides¹³⁴. In **Figure 22** we can see that there was a small relief in the 700-600 cm^{-1} region in the ATR-FTIR of the fungi that grew in PEF+*P.b*, this peak was the only one different from the ATR-FTIR of the controls and it may indicate that the presence of PEF has altered the fungus metabolism in some way. Then, throughout the test, increases and decreases in the intensities of some peaks are observed, which may be linked to the presence of PEF, but also the scarcity of nutrients and the respective death of the fungus. Namely, throughout the incubation times, there was a decrease in peak intensity between 1800-1700 cm^{-1} (typical of lipids), a plausible explanation for this reduction was that the fungus performed autolysis due to the lack of nutrients in the medium, the carbon starvation may have led the fungus to use the lipids as an alternative carbon source^{92,137}. An increase in the two peaks between 1700-1500 cm^{-1} (caused by amides in proteins) was also observed. With the death of the fungus, a sharpening of the peak is noted between 3700-3050 cm^{-1} , this sharpening is observed in the samples of PEF+*P.b* at 42 days (dead fungus) while in GC at 42 days (live fungus) do not show this sharpness, at 56 days with both fungi dead, both the GC and PEF+*P.b* showed this sharpening. The formation of this sharpening may be associated with the

decomposition of the fungus after its death. These results support the hypothesis that in the presence of PEF there is a faster death of the fungus.

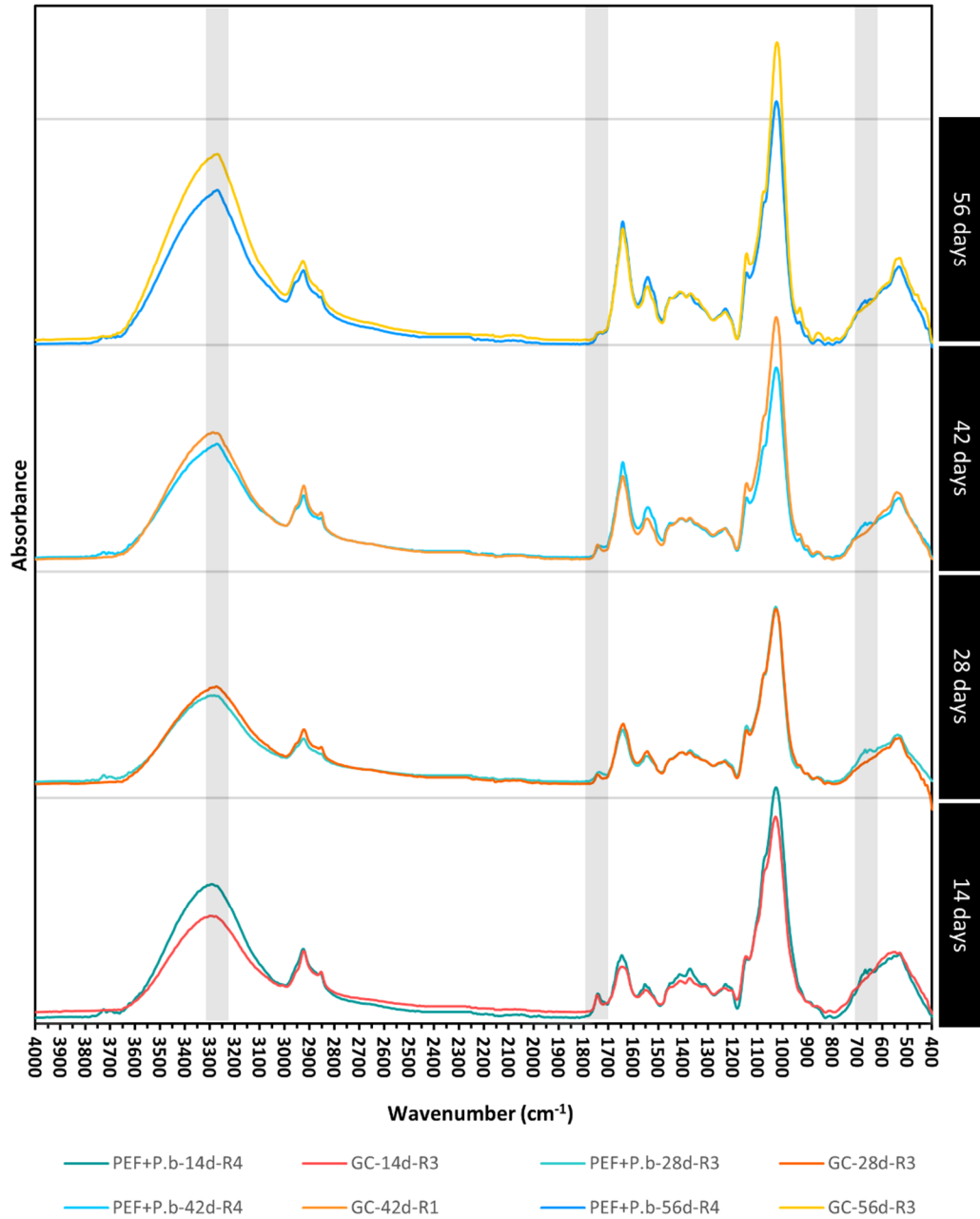


Figure 22- Infrared spectra in the region 400-4000 cm⁻¹ from *Penicillium brevicompactum* throughout the experiment.

3.2.2. Weight and ATR-FTIR analysis of the PEF microparticles

To evaluate the influence of the fungus on the biodegradation of the PEF microparticles, over the incubation times we used PCs in comparison with the PEF+*P.b* flasks. The controls allow us to evaluate if there is a loss of PEF caused by the culture medium or if this eventual loss is attributed to the biodegradation of the fungus. **Table 5** and **Figure 23** show the variation in the weight of the PEF microparticles during the biodegradation test. The values obtained for PEF removal are very close to 0%, which indicated that under these conditions the *P. brevicompactum* could not biodegrade the PEF microparticles. Some values of % PEF Removed Mean up to 9% were observed, but they can be justified by losses of PEF in the filtration and separation process, or even due to degradation caused by the culture medium since these losses are also observed in controls. It is necessary to leave a note, that in the PEF+*P.b* of the 56 days of incubation the fungus had also died a little before the 42 days of incubation, the data being present here only because the bottles were kept in the incubator until the 56 days to compare later with the GC fungus.

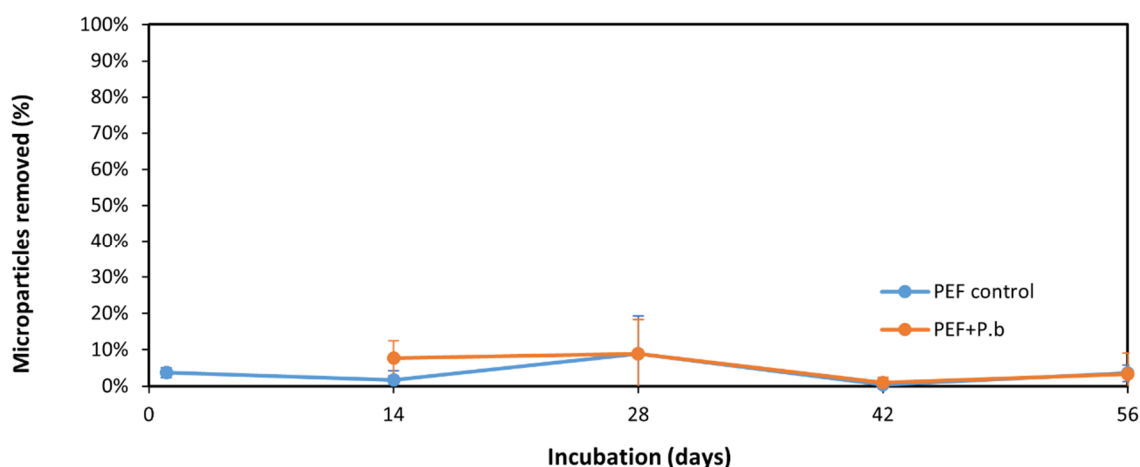


Figure 23- Variation of PEF microparticles before and after their exposure to *Penicillium brevicompactum*.

The PEF microparticles recovered were analyzed by ATR-FTIR and the spectra obtained are presented in **Figure 24**. The results obtained demonstrated that there was no change in the typical PEF ATR-FTIR throughout the trial. No changes that could indicate biodegradation were observed, such as the shift of peaks, or the appearance/disappearance of peaks. These results agree with the lack of PEF removal observed throughout the test and indicate that *P. brevicompactum* in this interval in which it was in contact with PEF did not have the ability to perform biodegradation.

Table 5 - Variation of PEF microparticles before and after their exposure to *Penicillium brevicompactum*

Erlenmeyer condition	PEF beginning (g)	PEF recovered (g)	PEF removed(g)	% PEF Removed	% PEF Removed Mean \pm SD	
1 day						
PEF control	R1	0.0152	0.0148	0.0004	3%	4 \pm 2%
	R2	0.0154	0.0149	0.0005	3%	
	R3	0.0152	0.0144	0.0008	5%	
14 days						
PEF control	R1	0.0155	0.0166	-0.0011	0%	2 \pm 2%
	R2	0.0151	0.0150	0.0001	1%	
	R3	0.0152	0.0145	0.0007	5%	
PEF+<i>P.b</i>	R1	0.0155	0.0153	0.0002	1%	8 \pm 5%
	R2	0.0149	0.0131	0.0018	12%	
	R3	0.0159	0.0148	0.0011	7%	
	R4	0.0154	0.0138	0.0016	10%	
28 days						
PEF control	R1	0.0154	0.0157	-0.0003	0%	9 \pm 10%
	R2	0.0153	0.0143	0.0010	7%	
	R3	0.0158	0.0126	0.0032	20%	
PEF+<i>P.b</i>	R1	0.0152	0.015	0.0002	1%	9 \pm 9%
	R2	0.0156	0.0121	0.0035	22%	
	R3	0.0155	0.0149	0.0006	4%	
	R4	0.0155	0.0143	0.0012	8%	
42 days						
PEF control	R1	0.0154	0.0152	0.0002	1%	0 \pm 1%
	R2	0.0159	0.0166	-0.0007	0%	
	R3	0.0156	0.0158	-0.0002	0%	
PEF+<i>P.b</i>	R1	0.0157	0.0156	0.0001	1%	1 \pm 2%
	R2	0.0162	0.0164	-0.0002	0%	
	R3	0.0156	0.0151	0.0005	3%	
	R4	0.0161	0.0172	-0.0011	0%	
56 days						
PEF control	R1	0.0154	0.0147	0.0007	5%	4 \pm 2%
	R2	0.0156	0.0152	0.0004	3%	
	R3	0.0158*				
PEF+<i>P.b</i>	R1	0.0156	0.0156	0.0000	0%	3 \pm 6%
	R2	0.0152	0.0137	0.0015	10%	
	R3	0.0155*				
	R4	0.0161	0.017	-0.0009	0%	

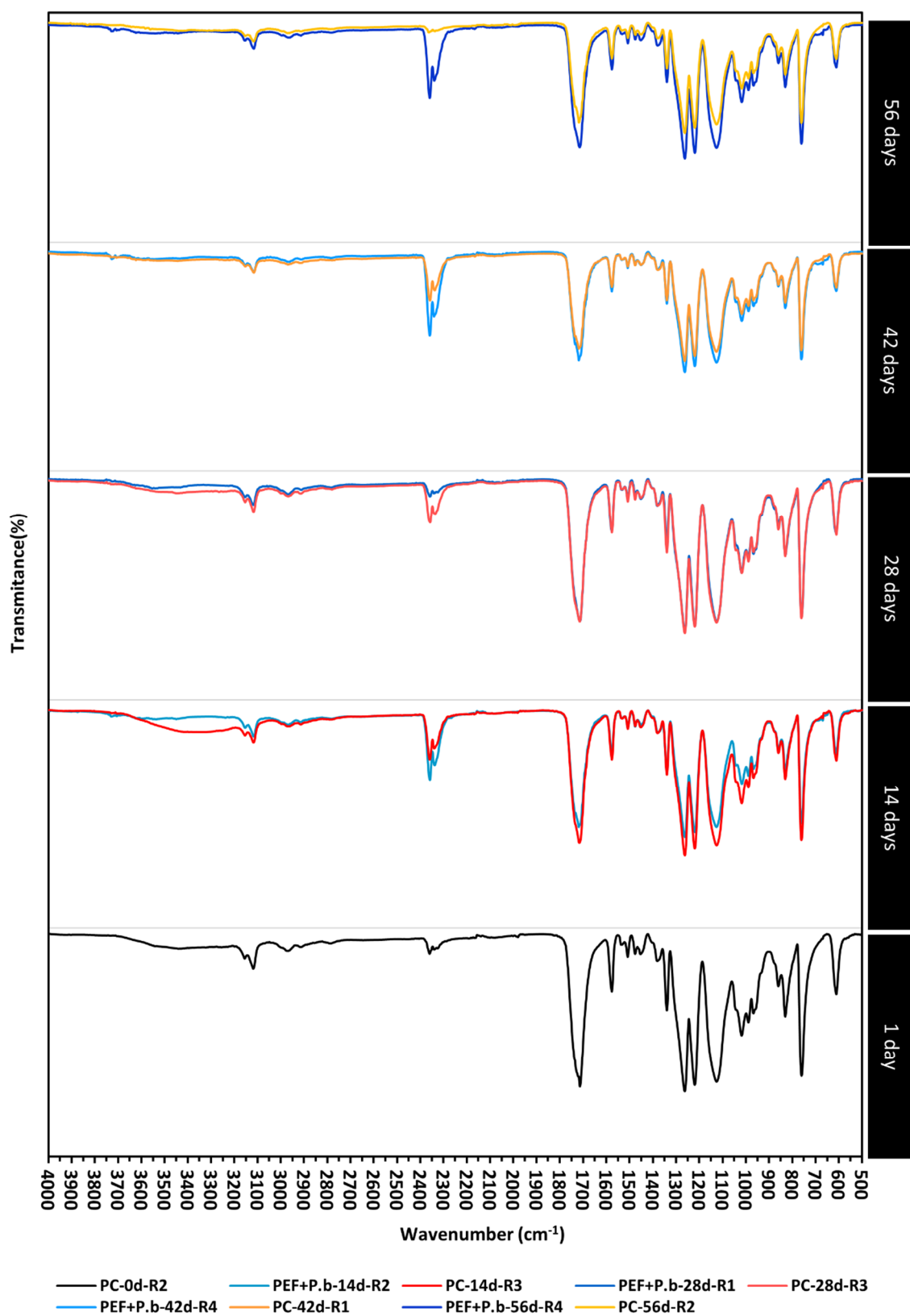


Figure 24- Infrared spectra in the region 500-4000 cm⁻¹ from the PEF microparticles throughout the experiment.

4. Conclusion

In this work, the PEF was successfully synthesized and the fungus *P. brevicompactum* was used to evaluate its biodegradation. The method designed to assess biodegradation allowed only to keep the fungus alive in the presence of PEF microparticles until almost 42 days of incubation. Our results showed that the PEF had a negative effect on the growth of the fungus, and sudden death of the fungus was observed in the presence of PEF microparticles. The chemical changes in the fungus obtained by ATR-FTIR are in accordance with what was observed visually.

There was no considerable removal of PEF promoted by the fungus biodegradation. Also, no chemical changes were observed in the PEF ATR-FTIR. These observations lead us to conclude that *P. brevicompactum* under these conditions was not able to biodegrade PEF. On the contrary, a negative effect was observed on the fungus. These results support the hypothesis that PEF is poorly biodegradable. However, it is important to note that the biodegradation of polymers is dependent on several factors (abiotic, type of microorganism, and characteristics of the polymer) and further biodegradation studies are needed, not only for PEF but also for other furanic-aliphatic polyesters.

III. Synthesis, characterization and degradation of poly(isosorbide 2,5-furandicarboxylate)-copoly(isosorbide 1,12-dodecanedioate) copolyesters (PIsFDDs)

1. Background

As has already been contextualized in the previous sections, the growing concern with the destruction of the environment and sustainability has promoted the remarkable challenge of developing alternative bio-based and biodegradable polymers¹³⁸.

2,5-furandicarboxylic acid (FDCA)-based polyesters have been considered promising sustainable alternatives, and their synthesis conditions have been extensively studied^{23,38,139,140}. However, it is considered that these FDCA-based homopolyesters have low biodegradability⁵¹. Copolymerization through the introduction of aliphatic moieties is one of the most effective methods for tailoring the properties of a polymer and even to improve its (bio)degradability rate^{23,67}. Some furanic-aliphatic copolyesters following this approach were revealed to be very promising^{51,61,67}.

In this regard, in this study, we have copolymerized FDCA (or its dimethyl derivative) with 1,4:3,6-dianhydro-D-glucitol, known as isosorbide (Is), and dodecanedioic acid (DDA), a long-chain dicarboxylic acid, that can be obtained from renewable resources by oxidation of *Vernonia galamensis* oil^{141,142}

Is is one of the most promising eco-friendly monomers available on an industrial scale through hydrogenation followed by dehydration of D-glucose derived from cereal starch¹⁴³ and is considered as an excellent alternative to several petroleum-based chemicals¹⁴⁴. Because of its rigid molecular structure, good thermal stability, and chirality properties, which enhance the glass transition temperature (T_g)¹⁴³, several approaches have been undertaken to utilize isosorbide as a monomer for numerous aliphatic-aromatic polyesters. In this context, isosorbide has been substituted with other partial alkanediol, and consequently, the isosorbide-containing copolyesters have improved properties^{67,145}.

DDA is used in a wide variety of applications including powder coatings, adhesives, paint materials, corrosion inhibitors, and surfactants^{146,147}. The presence of the long aliphatic chain moieties in the copolymers provide them with flexible structures⁷⁵.

In the next sections, the synthesis, characterization, and degradation of poly(isosorbide 2,5-furandicarboxylate)-co-(isosorbide 1,12-dodecanedioate)s are described below.

2. Material and Methods

2.1. Materials

2,5-furandicarboxylic acid (FDCA, 98 %) was purchased from TCI Chemicals. Dibutyltin(IV) oxide (DBTO) was purchased from TEGOKAT 248. 1,12-dodecanedioic acid (DDA 99%), isosorbide (Is, 99 %), trifluoroacetic acid (TFA, 99%), titanium(IV) isopropoxide (Ti(OiPr)₄, 99.999 %), deuterated chloroform (CDCl₃, 99.8 atom % D), deuterated trifluoroacetic acid (TFA-d, 99.5 atom % D), lipase from porcine pancreas (PPL) and sea salts (NutriSelect™ Basic) were purchased from Sigma–Aldrich. Methanol (analytical grade), chloroform (HPLC grade), sodium phosphate monobasic anhydrous (NaH₂PO₄, colorless-to-white crystals) were purchased from Fisher Chemical. Sodium phosphate dibasic (Na₂HPO₄, 99+%) was acquired from ACROS Organics. All chemicals and solvents were used without further purification.

2.2. Synthesis of dimethyl 2,5-furandicarboxylate (DMFDC)

Several DMFDC syntheses were performed. The procedure used for the synthesis of DMFDC was the same as described in the previous **Chapter II**.

2.3. Synthesis of copolyesters poly(isosorbide 2,5-furandicarboxylate)-co-(isosorbide 1,12-dodecanedioate)s (PIsFDD)

PIsFxDDy copolyesters with different molar compositions X/Y % = 100/0, 90/10, 80/20, 70/30, and 60/40, where X and Y stands for furan and DDA moieties relative percentages, respectively) were synthesized by an adjusted melt polycondensation reaction process (**Figure 25**) previously reported⁵⁶. According to this procedure, DMFDC, DDA, and Is were charged into the reaction apparatus with a molar ratio of (diacids) /diol = 1/2.05 with Ti(OiPr)₄ catalyst (0.1 wt % relative to the weight of the total monomers). In the first step, the reaction mixture was heated from 160-170 °C for 4 h under a nitrogen atmosphere. Subsequently, in the second step, an additional amount of diacids were added (DMFDC+DDA) in a molar ratio of 1/1.05 relatively to the macrodiol prepared in the previous step. The reaction proceeded from 160-190 °C, for 4.5 h, under a nitrogen atmosphere. In the third step of polycondensation, the vacuum was applied slowly, for 0.5h. The temperature of the melt was raised to 220 - 250 °C). The obtained (co)polymers were

purified by dissolving them in a mixture of CHCl_3/TFA and then, precipitated in cold methanol, filtered, and dried at $40\text{ }^\circ\text{C}$.

PIsFxDy copolyesters with the other molar compositions $X/Y\% = 0/100, 10/90, 20/80, 30/70,$ and $40/60$) were prepared following another bulk polytransesterification procedure (**Figure 25**) reported elsewhere¹⁴⁸. Briefly, DMFDC and DDA were mixed with Is in a molar ratio of $1/2.05$ ((DMFDC+DDA)/Is); DBTO catalyst ($0.5\text{ mol}\%$ relative to the total of monomers) was added, and in the first stage, esterification reactions could proceed at $180\text{--}190\text{ }^\circ\text{C}$ for 3h, under a nitrogen atmosphere. Subsequently, in the second stage, the polycondensation step was carried out under vacuum by reacting the resulting monomers with an additional amount of (DMFDC+DDA) in a molar ratio of $1/1.05$, at $210\text{--}220\text{ }^\circ\text{C}$, for 6h. After the polymerization was completed, the melt was cooled to room temperature, and the target (co)polymers were purified by dissolving in a mixture of CHCl_3/TFA , and then precipitated in cold methanol, filtered, and dried at $40\text{ }^\circ\text{C}$.

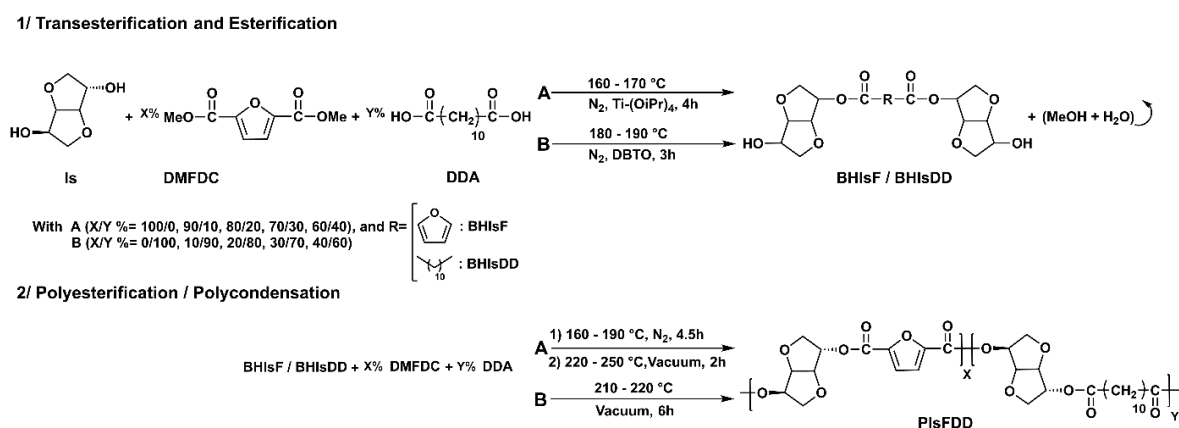


Figure 25- Synthesis of poly(isosorbide 2,5-furandicarboxylate)-co-(isosorbide 1,12-dodecanedioate) copolyesters.

2.4. Film preparation

The PIsF, PIsDD, and PIsFDDs films were prepared by melting. A rectangular aluminum mold (*ca.* $10 \times 30 \times 1\text{ mm}$; width \times length \times thickness) was filled in with the respective polymer powder and the temperature was gradually increased until melting was observed. When the polymer was completely melted and visually uniform, the mold was cooled to room temperature (keeping the mold on the heating plate). Finally, the film was removed from the metal mold. **Figure 26** shows examples of the obtained film specimens.

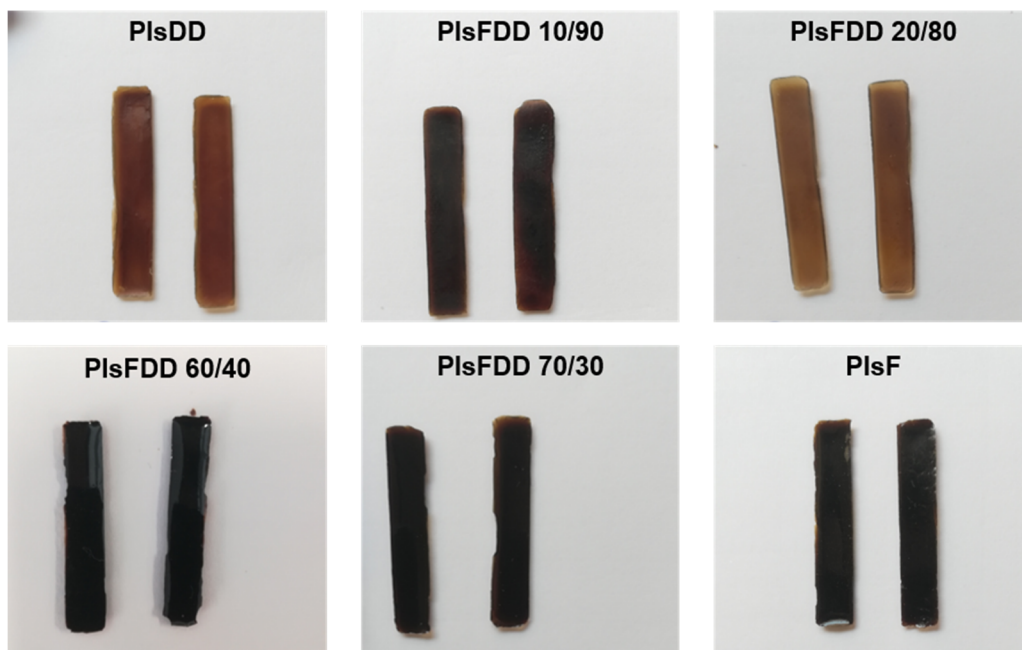


Figure 26- PlsDD, PlsF, and PlsFDD copolymer specimens produced by melting.

2.5. Hydrolytic and enzymatic degradation tests

The degradation tests were carried out under 3 different conditions:

- (a) Hydrolytic degradation in phosphate buffer solution (PBS),
- (b) Enzymatic degradation (in PBS + lipase from the porcine pancreas),
- (c) Hydrolytic degradation in simulated marine conditions.

To perform these tests, the films PlsDD, PlsF, PlsFDD 60/40, and PlsFDD 10/90 were used. These polymer films were cut to achieve dimensions of approximately 0.5 x 0.5 centimeters and a weight of 16–31 milligrams, and 3 replicas of each polymer were used.

In the hydrolytic degradation in PBS, the films were placed in vials with 10 ml of PBS (0.1M, pH 7.4) and incubated at 37 °C.

For enzymatic degradation, the films were placed in 10 mL of PBS with the addition of lipase from the porcine pancreas (1 mg.ml⁻¹) and incubated at 37 °C.

In the hydrolytic degradation in marine conditions, the films were placed in 10 mL of a sea salts solution (35 g/L, pH 8.2) and incubated at room temperature (temperature range of 14 - 22 °C).

For each degradation assay, the same 3 replicates were reused successively at all incubation times (3-7-14-21-28-35 days). After each period, the samples were removed

from the solutions, thoroughly washed with distilled water, dried at 40 °C for 3 days under vacuum, and weighed. Then, the same films were replaced in renewed solutions until the next incubation time, and the same process was repeated. The weight-loss percentage was calculated using the expression: weight loss (%) = $[(W_0 - W_t) / W_0] \times 100$, where W_0 is the initial weight, and W_t is the weight after each incubation period, respectively.

2.5.1. Solutions preparation

PBS (0.1M, pH 7.4) was prepared by dissolving ≈ 8.6 g of sodium phosphate dibasic (Na_2HPO_4) and ≈ 4.7 g of sodium phosphate monobasic (NaH_2PO_4) in 0.8 L of distilled water. Stirred until the salts were completely dissolved. The pH was adjusted to 7.4; and finally, the volume adjusted to 1 L.

Sea salts are a mixture of synthetic salts (e.g., NaCl, MgCl_2 , CaCl_2 , KCl, Na_2SO_4 , NaHCO_3 , NaBr) similar to salts dissolved in seawater. Sea salts solution was prepared by dissolving 35g of this mixture in 1 liter of distilled water. The solution was stirred until the salts were completely dissolved. The pH was adjusted to 8.2.

The solutions were autoclaved after preparation.

2.6. Characterization techniques

Fourier Transform Infrared Spectroscopy (ATR-FTIR) spectra were obtained using a PARAGON 1000 Perkin Elmer FTIR Spectrophotometer equipped with a single horizontal Golden Gate ATR cell. The spectra were recorded at a resolution of 8 cm^{-1} and 128 scans in the spectral region of $500\text{-}4000 \text{ cm}^{-1}$.

^1H , ^{13}C nuclear magnetic resonance spectroscopy (^1H , ^{13}C NMR) analyses of samples dissolved in CDCl_3 were recorded using a Bruker AMX 300 spectrometer operating at 300 and 75 MHz, respectively. All chemical shifts were expressed in parts per million (ppm) using tetramethylsilane (TMS) as the internal reference.

Intrinsic viscosity measurements of copolyesters were performed using an Ubbelohde type viscometer at 25 °C in a mixture of phenol/1,1,2,2-tetrachloroethane (50/50 wt%/wt%). All copolyesters were dissolved in that solvent mixture (0.1 g per 20 mL) and kept at 140 °C for 20 min to achieve complete dissolution. The intrinsic viscosity $[\eta]$ of each sample was determined by the ratio of specific viscosity and solution concentration (η_{sp}/C , where $\eta_{sp} = (t_1 - t_0) / t_0$). C , t_1 , and t_0 present respectively the concentration of the solution, the flow time of solution, and the flow time of the pure solvent.

Differential scanning calorimetry analysis thermograms of polyester were obtained with a Pyris Diamond DSC calorimeter from PerkinElmer, using nitrogen as purging gas (20 mL min⁻¹), and aluminum pans (30 μ L, 3 bar) to encapsulate the samples (ca. 5 mg). The calorimeter was calibrated for heating temperature with approximately 10 mg of each of the following metals: 99.999% pure indium, $T_f = 156.60$ °C, and 99.999% pure lead, $T_f = 327.47$ °C. Scans were conducted with a heating rate of 10 °C min⁻¹ in the temperature range of -40 to 250 °C.

Thermogravimetric analyses (TGA) were carried out with a Shimadzu TGA50 analyzer equipped with a platinum cell, using platinum pans to encapsulate the samples. Thermograms were recorded under a nitrogen flow of 20 mL min⁻¹ and heated at a constant rate of 10 °C min⁻¹ from room temperature up to 800 °C.

Dynamic mechanical thermal analyses (DMTA) of thick samples (10.0 \times 5 \times 1 mm), dispersed in a foldable stainless-steel sheet, acquired from Materials Pocket of Triton technology, were performed with a Tritec 2000 DMTA Triton equipment operating in the bending (single cantilever) mode. Tests were carried out at 1 and 10 Hz and the temperature was varied from -80 to 250 °C, at 2 °C/min. The T_g of the PlsFDD copolyesters were determined from the maximum of $\tan \delta$, at 1 Hz.

X-ray diffraction analyses were carried out using the Philips X'pert MPD instrument operating with CuK α radiation ($\lambda = 1.5405980$ Å) at 40 kV and 50 mA. Samples were scanned in the 2θ range of 5 to 70°, with a step size of 0.026°, and time per step of 67 s.

3. Results and discussion

A novel series of fully biobased poly(isosorbide 2,5-furandicarboxylate)-co-(isosorbide 1,12-dodecanedioate) (PlsFDD) copolyesters derived from Is, DMFDC, and DDA were successfully prepared (**Figure 26** and **Table 6**). The copolyester isolation yields, after purification, were between 36-59 % and their intrinsic viscosities ($[\eta]$) near 0.11–0.2 dL g⁻¹.

3.1. Structural characterization of the PlsFDD copolyesters

The detailed chemical structures of PlsFDD copolyesters and their related homopolymers were extensively studied by ATR-FTIR and ¹H NMR.

The ATR-FTIR spectra of PlsF, PlsDD, and PlsFDD copolyesters (**Figure 27**) display a very intense band near 1723 cm^{-1} , assigned to the C=O stretching vibration, characteristic of ester groups and another typical band at 1271 cm^{-1} , assigned to the C-O-C stretching mode also of ester groups. The presence of these two bands, as well as the absence of relevant OH bond stretching near 3400 cm^{-1} , confirms the success of these polymerizations. It is also observed two bands near 2976 and 2820 cm^{-1} attributed to the anti-symmetrical and symmetrical stretching modes (C-H_{asym} and C-H_{sym}, respectively) of the C-H bond of the (CH₂) groups mainly related to DDA. As expected, these two bands relative intensity increase with the content of DDA in the copolyester backbone. In the case of both PlsF and PlsFDDs copolyesters, the characteristic absorption peaks of the furan ring were also detected, including =C-H at 3130 cm^{-1} and C=C at 1575 cm^{-1} . The ATR-FTIR spectra of all copolyesters are available in the **Supplementary data C** section.

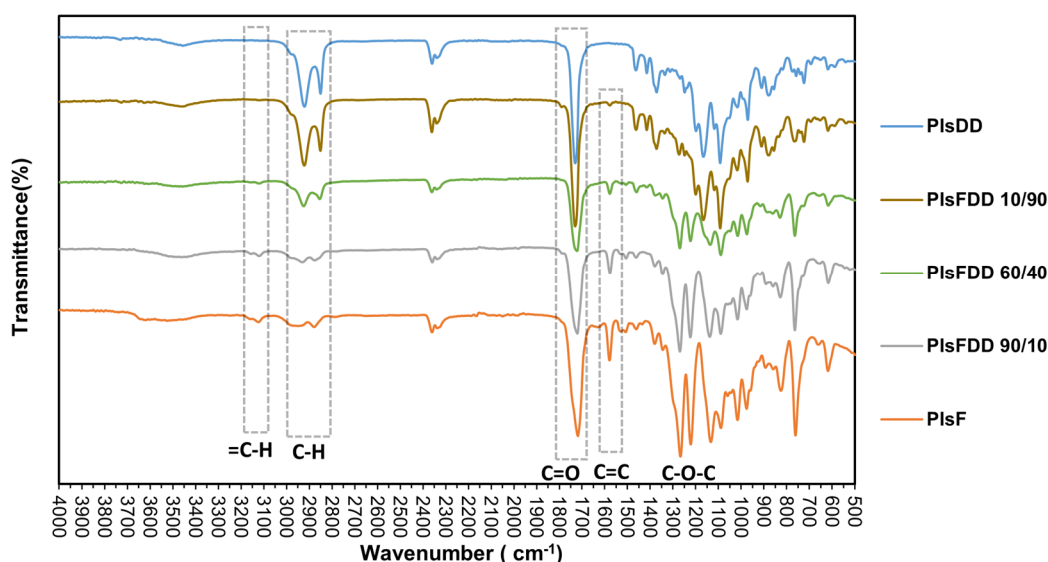


Figure 27- ATR-FTIR spectra of prepared PlsFDD copolyesters, PlsF, and PlsDD homopolymers.

The ¹H NMR analysis (**Figure 28**) confirms the basic PlsF expected structure, displaying two resonances at 7.24 and 7.29 ppm, ascribed to the furan ring protons (a) in different chemical environments. This is most probably due to the non-planar nature of isosorbide moiety and the different spatial orientations of the hydroxyl groups. The isosorbide proton resonances are split into five multiplets at 5.40, 5.07, 4.69, 4.05 ppm ascribed to (b+e), (g), (d), (c+f) respectively⁶⁷.

Also, for PlsDD the ¹H NMR spectrum displays the typical isosorbide moiety signals around 3.5-5.3 ppm. The outer methylene groups (h), middle CH₂ (i), and inner CH₂ (j) in the DD

unit appear at 2.33, 1.63, and 1.27 ppm, respectively¹⁴⁹. For PlsFDDs copolyesters, all the proton resonances from PlsF and PlsDD homopolyesters can be clearly distinguished. The chemical shifts at 7.24 and 7.29 ppm are attributed to the two protons of the furan ring (a).

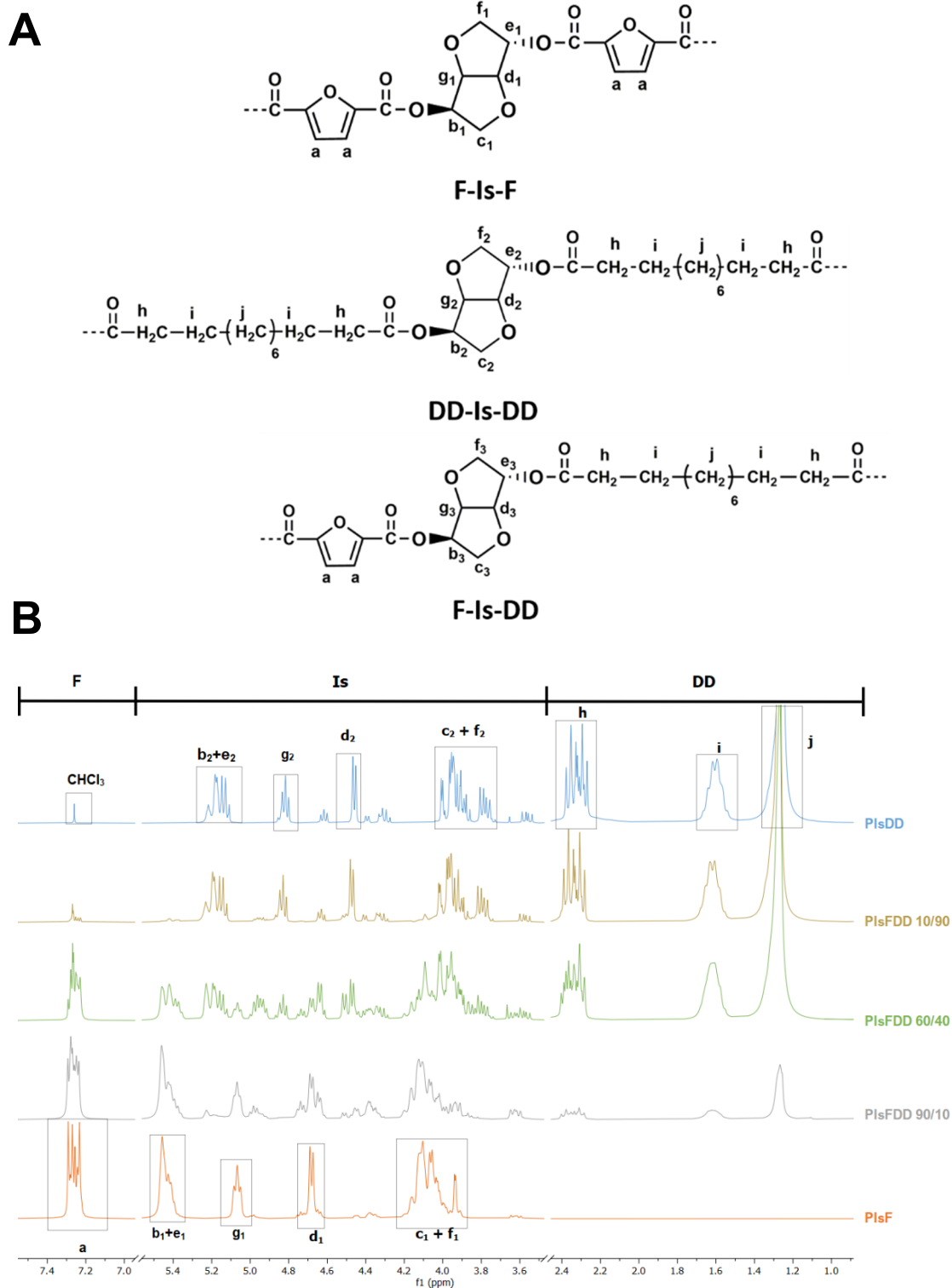


Figure 28- (A) Chemical structure of F-Is-F, DD-Is-DD, and F-Is-DD triads (B) ¹H NMR spectra of PlsF, PlsDD, and PlsFDDs copolyesters in CDCl₃.

The resonances appearing at the 3.5-5.6 ppm range were assigned to the isosorbide protons. The methylene groups signal of 1,12-dodecanoate unit were observed between 1.14-2.5 ppm. The ¹H NMR spectra of all copolyesters are available in the **Supplementary data C** section. The real molar percentages of the furan (F) and dodecanedioate (DD) moieties incorporated into the copolyesters backbone were accessed to correctly interpret the structure-property relationships, such as the thermal and mechanical behavior. Therefore, they were estimated based on ¹H NMR using the relative integration areas of different methylene protons resonances associated with each moiety (I_a and I_h as shown in **Figure 28**) according to:

$$\%F = [(I_a/2) / (I_a/2 + I_h/4)] \times 100, \text{ and } \%DDA = [(I_h/4) / (I_h/4 + I_a/2)] \times 100$$

Data of **Table 6** clearly shows that the real molar fraction of PIsF and PIsDD units, assessed by ¹H NMR data, are in acceptable agreement with the initial molar feed ratios, despite some tendency to incorporate more DDA units than F ones. This is possibly due to the higher reactivity of DDA under the applied reaction conditions.

Table 6 - Molar composition obtained by ¹H NMR, yields, and intrinsic viscosities of purified PIsFDD samples.

	(DMFDC / DDA) initial feed	(DMFDC / DDA) real ^a	Yields (%)	$[\eta]^b$ (dL/g)
PIsDD	0/100	-	45	0.20
PIsFDD 10/90	10/90	6/94	59	0.18
PIsFDD 20/80	20/80	12/88	37	0.17
PIsFDD 30/70	30/70	27/73	43	*
PIsFDD 40/60	40/60	30/70	39	*
PIsFDD 60/40	60/40	47/63	50	0.17
PIsFDD 70/30	70/30	62/36	36	0.12
PIsFDD 80/20	80/20	76/24	49	0.13
PIsFDD 90/10	90/10	88/12	40	0.11
PIsF	100/0	-	43	0.20

^a Feed molar ratio assessed by ¹H NMR data. ^b Intrinsic viscosities of the copolyester's solution in a mixture of phenol/TCE at 25 °C. * data not acquired.

3.2. X-ray diffraction analysis (XRD)

The XRD patterns of these novel copolyesters and their PIsDD and PIsF homopolymers counterparts are shown in **Figure 29**. PIsDD is a semi-crystalline homopolymer showing five main diffraction peaks at $2\theta = 5.1^\circ$, 17.9° , 19.5° , 21.2° , and 24.8° , similar to previously reported¹⁴⁹. Oppositely, PIsF homopolymer is amorphous and displays according to a halo centered at $\approx 18^\circ$, as previously reported⁵⁶. This amorphous character of PIsF is promoted by the asymmetric isosorbide hydroxyl groups (*endo* and *exo*) and by Is random incorporation inhibiting crystallization, forming instead an amorphous mess⁵⁶. PIsFDD 20/80 displayed a semi-crystalline structure, with diffraction patterns like PIsDD. PIsFDD 10/90 also displayed some crystallinity ($2\theta = 18.1^\circ$). On the other hand, PIsFDD 30/70 and PIsFDD 40/60 were in an amorphous state. For higher incorporation of F moiety, their pattern also displayed some crystalline character, with a peak centered at $\approx 18.4^\circ$.

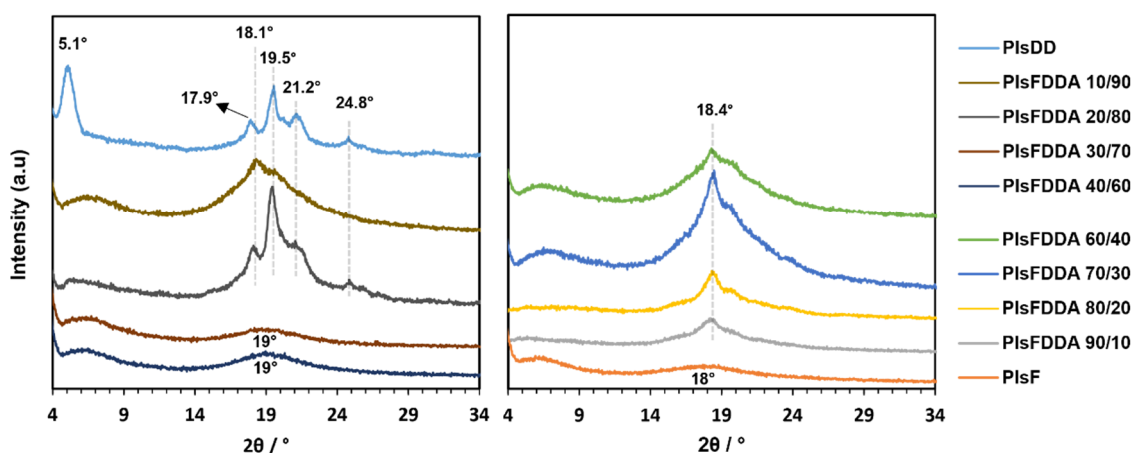


Figure 29- XRD patterns of PIsFDD copolyesters, PIsF, and PIsDD homopolymers.

3.3. Thermal behavior

From this point on, due to the Covid-19 pandemic, we had to reduce the number of samples analyzed. Six polymers were chosen, both homopolymers and PIsFDD 10/90, 20/80, 60/40, and 70/30 copolyesters.

PIsFDD copolyesters have been characterized mainly in terms of their thermal behavior by DSC (**Figure 30**), DMTA (**Figure 31**), and TGA (**Figure 32**) analyses. The thermal properties of the PIsFDD copolyesters are shown in **Table 7**.

DSC curves clearly show melting transitions for PlsDD, PlsFDD 10/90, and PlsFDD 20/80 ($T_m \sim 73.2, 71.9$ °C, and 70.6 °C, respectively) according to their semicrystalline character (as XRD results highlighted). The T_m obtained for PlsDD is in accordance with the data reported by Okada *et al.*¹⁵⁰ ($T_m = 70$ °C). The DSC traces of the PlsFDD 60/40 and 70/30 copolyesters showed no melting transitions. Additionally, PlsFDD 10/90, 20/80, 60/40, and 70/30 traces also showed a glass transition (T_g) at ca. -9.1 °C, -8.6 °C, 32 and 59.6 °C, respectively. We observed that an increase in the incorporation of furan moieties (F relative to DD moieties) induced an increase in T_g values. This was probably due to the fact that F moiety is much stiffer than DD moiety. The DSC trace of the PlsF homopolymer was not successfully acquired, so this result is not shown here. However, in the literature, PlsF presented a DSC curve with a T_g at 157 °C⁵⁶.

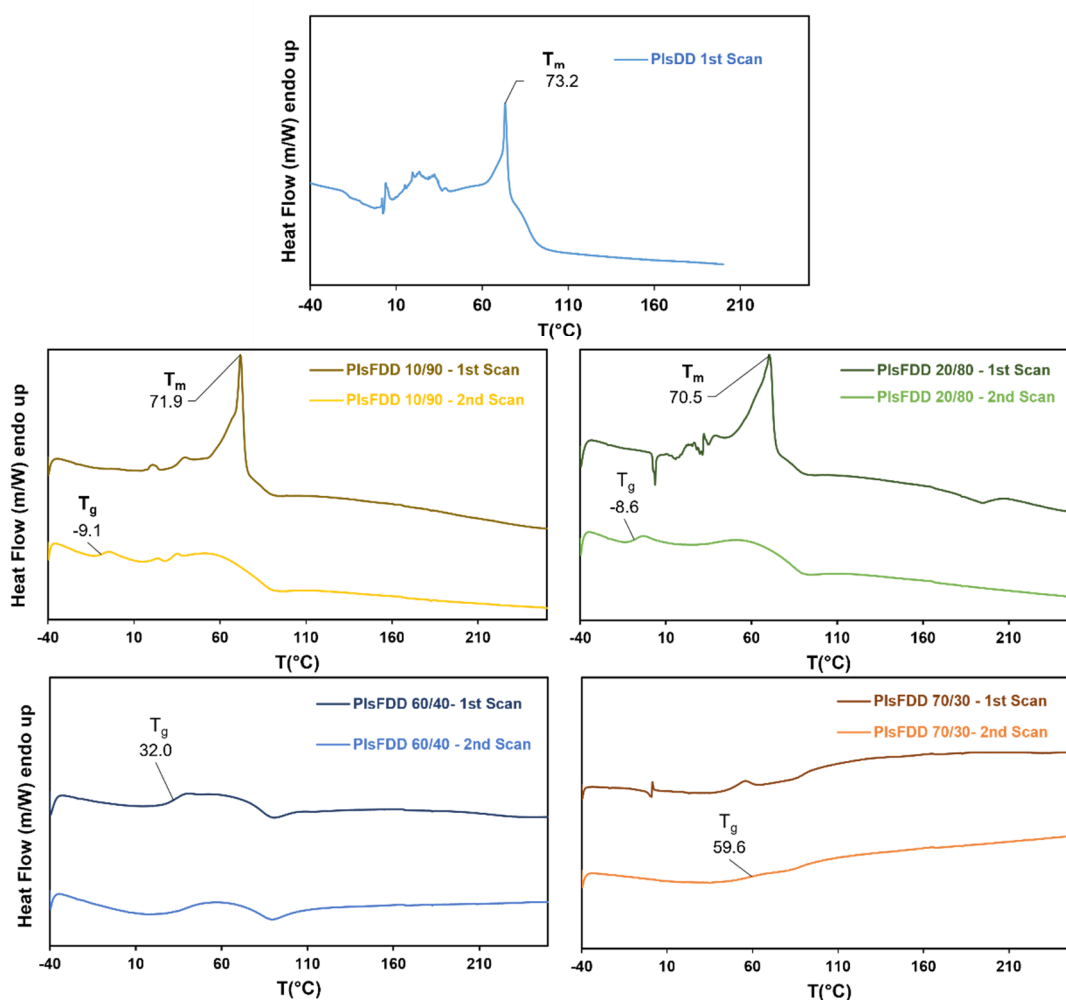


Figure 30- DSC 1st/2nd scan curves of copolyesters, and 1st scan curve of PlsDD homopolymer.

DMTA analysis (**Figure 31**) was used to further characterize these novel polymers. $\tan \delta$ traces showed T_g values of -6.3, 1.7, 0.2, 54.2, and 73.8 °C, for PlsDD, PlsFDD 10/90, 20/80, 60/40, 70/30 copolyesters, respectively. In general, it was found that the T_g increased with the increasing amount of F moiety. This is in accordance with DSC results reported earlier. However, it is important to note that the T_g values of PlsFDD 20/80 was slightly higher than that of 10/90. In some of the $\tan \delta$ traces of the copolyesters it was also possible to observe β transitions and the onset of melting.

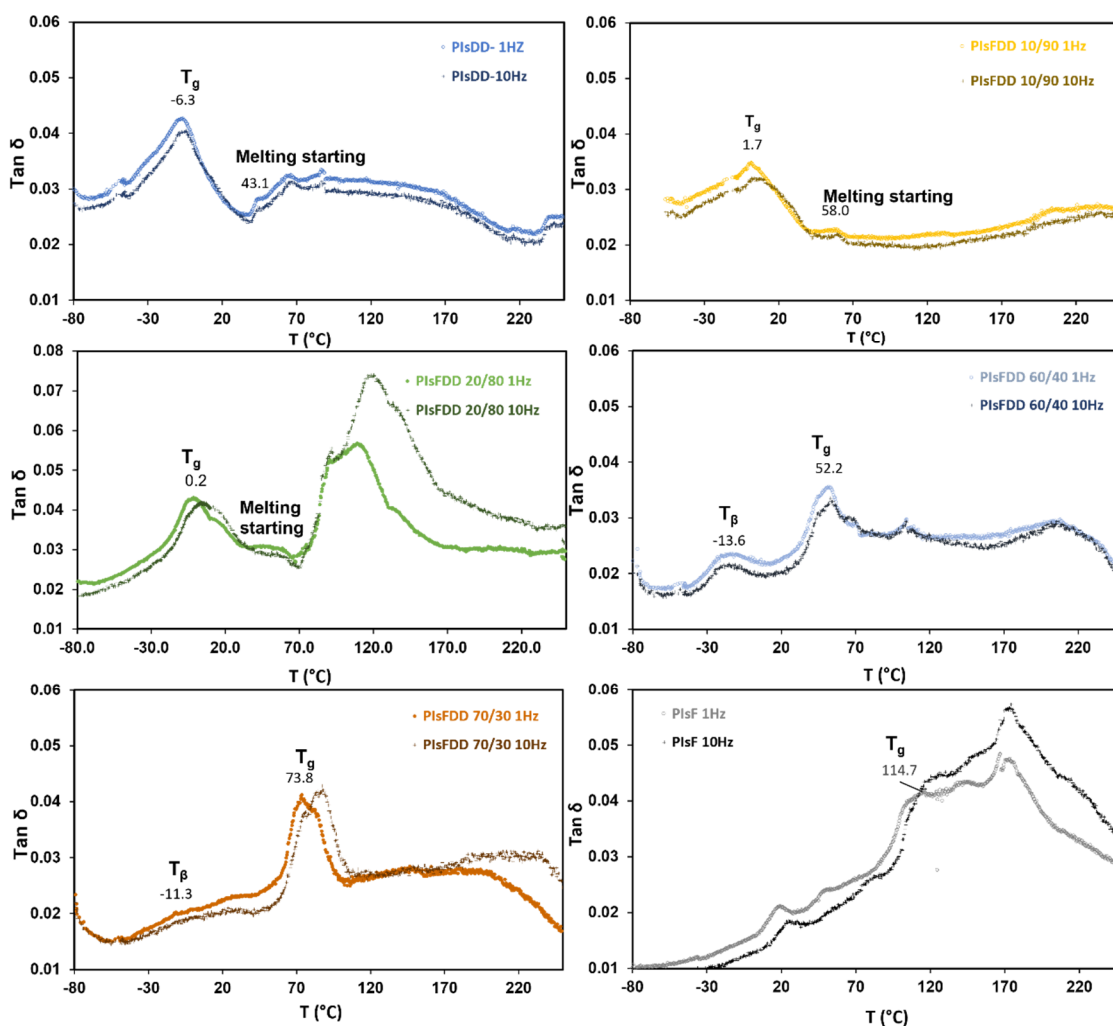


Figure 31- $\tan \delta$ of PlsDD, PlsF, and PlsFDD copolyesters, at 1 and 10 Hz.

Thermal degradation and stability of polymers are important parameters to determine their applicability. To evaluate the thermal stability of copolyesters, we perform thermogravimetric analysis (TGA) from room temperature up to 800 °C under a nitrogen atmosphere. TG and DTG (1st derivate TG) curves are represented in **Figure 32**. The

decomposition temperatures at 5% and 10% weight loss ($T_{d,5\%}$ and $T_{d,10\%}$), and the maximum degradation temperature ($T_{d,max}$) are listed in **Table 7**. All copolyesters were thermally stable up to approximately 287 °C. They presented a single weight loss step with $T_{d,5\%}$, values between 286.7 - 330.4 °C. Regarding the values of $T_{d,max}$, we obtained values between 398.7- 423.5 °C. Our $T_{d,max}$ value of PlsDD homopolymer is fully consistent with what was reported in the literature ($T_{d,max} = 425$ °C)¹⁵⁰. Further, we observed that with the increase in the amount of the DD moiety there was an increase in $T_{d,max}$. Similar trend was also reported by Jia *et al.*⁷⁵ for poly(ethylene dodecanedioate 2,5-furandicarboxylate) copolyesters. Typically the PlsFDD copolyesters, except that of PlsFDD 20/80, showed superior thermal stability compared to PEF ($T_{d,5\%} = 300$ °C; $T_{d,max} = 398$)^{32,55}.

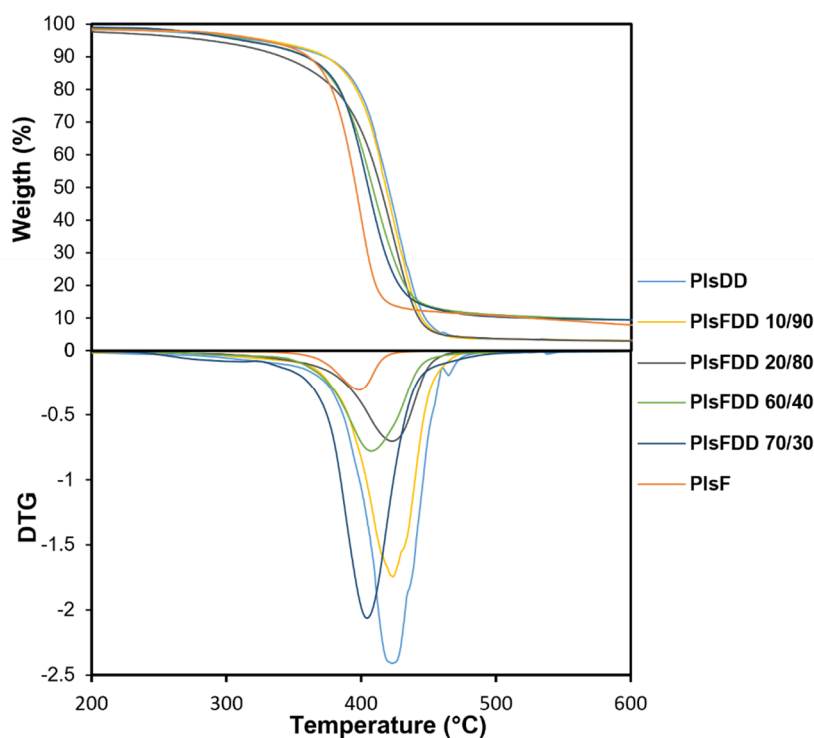


Figure 32- TGA and DTG thermograms of PlsFDD and corresponding homopolyesters.

Table 7- Thermal Properties of copolyesters PlsFDD with Different Compositions

Copolyester	TGA			DSC			DMTA ^c	
	$T_{d,5\%}$ (°C)	$T_{d,10\%}$ (°C)	$T_{d,max}$ (°C)	T_g (°C)	T_{cc} (°C)	T_m (°C)	T_β (°C)	T_g (°C)
PlsDD	323.9	373.1	423.0	-	-	73.2 ^a	-	-6.3
PlsFDD 10/90	330.4	373.7	423.5	-9.1	-	71.9 ^a	-	1.7
PlsFDD 20/80	286.7	341.1	422.7	-8.6	-	70.6 ^a	-	0.2
PlsFDD 60/40	314.9	359.2	407.7	32.0 ^a	-	-	-13.6	52.2
PlsFDD 70/30	312.1	359.2	404.0	59.6	-	-	-11.3	73.8
PlsF	327.3	360.9	398.7	-	-	-	-	114.7

^a 1st DSC Heating Scan

^c Tan δ values at 1 Hz

3.4. Degradation studies of PIsFDDs and their homopolymers counterparts

In the present study, to assess the potential of these PIsFDD copolyesters as novel (bio)degradable products we have evaluated their degradability under different conditions during 35 days, namely **a)** hydrolytic degradation, at pH 7.4, using a phosphate buffer solution (PBS) and, **b)** enzymatic degradation in the presence of porcine pancreas lipase, at pH 7.4. We have also studied the **c)** degradation under salt conditions (sea salt solution, pH 8.2) to evaluate the copolymer's behavior under simulated marine conditions. This latter experiment is quite relevant having into consideration that today a high percentage of polymers ends up in the ocean or seas. The weight loss percentage results through time are shown in **Figure 33**.

For hydrolytic degradation in PBS, PIsF homopolymer did not lose weight during the 35 days of the experiment, indicating that this high- T_g polymer did not degrade. Oppositely, PIsFDD 10/90 had the highest weight loss (ca. 5%). This value is quite similar to those previously reported by Sousa *et al.* for the degradation studies under similar conditions, such as the work with PEF-co-PLA⁵¹, and with poly(1,20-eicosanediyl 2,5-furandicarboxylate) (PE20F)⁵⁷. For both studies, the weight loss, after 35 days, was \approx 5–6%.

The enzymatic degradation studies prompted higher weight loss percentages degradation, with values between 2.1–17.0 %. In this set of experiments, PIsDD homopolymer showed the highest weight loss (%) value (around 17%), followed by PIsFDD 10/90 with \approx 11%. This result is comparable with the result obtained for the (bio)degradable polyester PE20F, where similar conditions of enzymatic degradation were used⁵⁷. A general trend observed is the fact that the weight loss (%) increases with the decreasing molar incorporation of FDCA units, which is likely attributable to the fact that the aromatic ester bonds formed are more difficult to degrade than aliphatic ester bonds involving DDA and Is⁷⁵.

Regarding the results of hydrolytic degradation in marine conditions, we obtained very modest weight loss (%) values, with a maximum at 2.6% for PIsDD and 2.4% for PIsFDD 10/90. Compared to enzymatic and even hydrolytic degradation in PBS, PIsFDD 10/90 and 60/40 copolyesters and PIsDD homopolymer had lower weight losses (%). The PIsF homopolymer as in PBS-media also did not show weight loss (%) in salt condition.

In general, we observed that the increase of F moiety in copolyesters led to a decrease in enzymatic and hydrolytic degradation. In the case of **(a)** hydrolytic degradation in PBS,

PIsFDD 10/90 degraded more than PIsDD (without F moiety), oppositely to what was observed for enzymatic mediated degradation. This can be justified by the fact that PIsFDD 10/90, was less crystalline than PIsDD, this may have facilitated the entry of water in the polymeric chain, promoting greater hydrolytic degradation. The same was not observed, however, with the enzymatic studies probably because in this case the specificity of the enzymes also played a role.

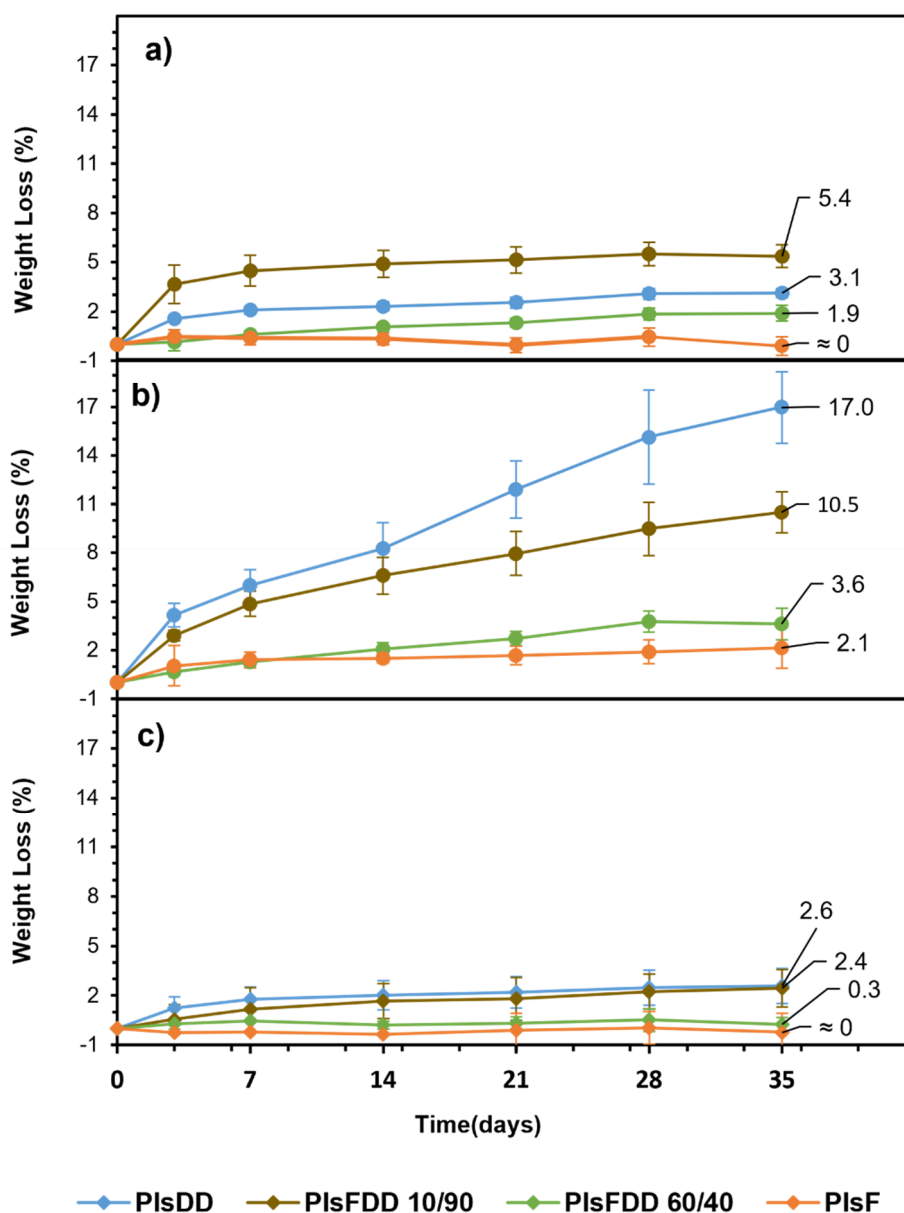


Figure 33- a) hydrolytic degradation in PBS (37°C); b) enzymatic degradation in PBS using lipase from porcine pancreas (37°C) c) hydrolytic degradation under marine conditions.

4. Conclusion

In this work, and aiming to obtain furan-based copolyesters with improved (bio)degradability, a series of poly(isosorbide 2,5-furandicarboxylate)-co-(isosorbide 1,12-dodecanedioate) copolyesters were successfully synthesized entirely from renewable sources.

PIsFDD copolyesters structures were proven by ATR-FTIR and ^1H NMR, and their compositions were clearly controlled by the feed molar ratio. Depending on the F/DD moiety ratio, they acquired amorphous or semi-crystalline structures.

About thermal behavior, T_m values of 72 °C and 71 °C were observed for PIsFDD 10/90 and 20/80 copolyesters, respectively. Both DSC and DMTA analysis showed that T_g values increased with the increasing of the rigid F moiety in the polymer backbone chain: T_g values between $\approx -6 - 60$ °C (DSC) and from $\approx 0 - 74$ °C (DMTA). PIsFDD copolyesters revealed good thermal stability, with $T_{d,5\%}$ values of above 287 °C and $T_{d,max}$ values above 404 °C.

Regarding their (bio)degradation, the increasing of F moiety in the structure of the PIsFDDs copolyesters contributed to a decrease in their weight loss percentage degradation. PIsFDD copolyesters could potentially be used as biodegradable materials. In fact, these results point out, for example, that PIsFDD 10/90 only after 35 days loss $\approx 5\%$ to $\approx 11\%$ of its weight depending on using hydrolytic (in PBS) or enzymatic degradation conditions, respectively. Probably in the future, using further analysis (e.g., SEM micrographs); more time-experiments deeper insights could be inferred.

IV. Conclusion and future perspectives

The environmental impacts related to non-sustainable polymers from fossil sources have been imposing immense research on more sustainable and biodegradable alternative polymers. The polymers studied in the present thesis produced from the FDCA, namely FDCA-based polyesters, have been showing as excellent sustainable alternatives to fossil-based polymers^{23,151,152}. Of this vast family, PEF is the most promising polymer that is expected to hit the market in 2023. However, they are expected to be poorly (bio)degradable. One of the great needs in this scientific field is, thus, to study the (bio)degradation of these new polyesters and to prepare new ones that can be (bio)degradable.

The present thesis focused essentially on the synthesis, characterization, and evaluation of the (bio)degradation of FDCA-based polyesters.

In the first study, we tried to evaluate the biodegradation of PEF by the fungus *Penicillium brevicompactum*. A discontinuous minimal fed-batch culture biodegradation assay was used to try to increase the fungus incubation time with PEF. After 42 days of incubation, no substantial removal of the polymer was observed, nor a change in the chemical structure of the PEF that indicated biodegradation. In addition, a negative effect of PEF on the growth of the fungus was observed. We concluded that *P. brevicompactum* with the methodology used and incubation time could not biodegrade the PEF. These results support the hypothesis that, at an environmental level, the PEF may be poorly biodegradable, presenting identical hazards to current fossil-based polymers. However, it is important to promote further studies regarding PEF biodegradation to have a more assertive view of its environmental impact. It will be relevant to use different culture conditions, different microorganisms, and try to achieve longer incubation periods, as well as analyzing the compounds derived from that biodegradation. It will be interesting to promote studies that evaluate the environmental biodegradation of PEF, isolate these microorganisms, and subsequently testing the biodegradation in optimal conditions.

In the second study, we successfully synthesized for the first time fully bio-based PIsFDD copolyesters by melt polycondensation. PIsFDDs were synthesized with different proportions of a rigid unit (F moiety) and a flexible unit (DD moiety) in an attempt to develop

polymers with appreciable thermo-mechanical properties and good (bio)degradability. They acquired amorphous or semi-crystalline structures. Their thermal behavior changed according to the different feed molar ratios used, T_g values increased with an increase of F moiety in the polymeric structure. They also showed an adjusted degradation rate, with the increase in the DD moiety there was an increase in their degradation. In the future, PIsFDDs could be able to play a competitive alternative in the production of biodegradable products. However, further work should be performed to complement these results. Currently, the degradation tests are being continued and scanning electron microscope (SEM) images will be obtained from PIsFDD films. It will also be relevant to characterize their mechanical properties, barrier properties (water, CO_2 , and O_2), as well as to test their biodegradation.

In conclusion, this thesis dealt with an unexplored theme, the (bio)degradation of FDCA-based polyesters. This is an extremely important issue, not only to assess the associated risks of the use/end of life of these polyesters but also crucial for the future development of eco-friendlier end of life management strategies (recycling, degradation/biodegradation). To date, PEF biodegradation has not yet been demonstrated under environmentally relevant conditions, the present thesis also failed to demonstrate its biodegradation, emphasizing the fact that it is necessary to promote more research on this topic. On the other hand, the present thesis demonstrated that the copolymerization of FDCA with other aliphatic unities can be an effective strategy to synthesize new potentially biodegradable FDCA-based polyesters.

V. References

1. United Nations Department of Economic and Social Affairs/Population Division. *World Population Prospects 2019, Volume I: Comprehensive Tables (ST/ESA/SER.A/426)*. (2019).
2. Uniyal, S., Paliwal, R., Kaphaliya, B. & Sharma, R. K. Human Overpopulation: Impact on Environment. in *Environmental Issues Surrounding Human Overpopulation* 1–11 (IGI Global, 2017). doi:10.4018/978-1-5225-1683-5.ch001.
3. Pimentel, D. World overpopulation. *Environ. Dev. Sustain.* **14**, 151–152 (2012) doi:10.1007/s10668-011-9336-2.
4. Brundtland, G. *Report of the World Commission on Environment and Development: Our Common Future*. <http://www.un-documents.net/our-common-future.pdf> (1987).
5. Nations, U. *Transforming our world: The 2030 agenda for sustainable development (A/RES/70/1)*. sustainabledevelopment.un.org.
6. Thompson, R. C., Swan, S. H., Moore, C. J. & vom Saal, F. S. Our plastic age. *Philos. Trans. R. Soc. B Biol. Sci.* **364**, 1973–1976 (2009) doi:10.1098/rstb.2009.0054.
7. Andrady, A. L. & Neal, M. A. Applications and societal benefits of plastics. *Philos. Trans. R. Soc. B Biol. Sci.* **364**, 1977–1984 (2009) doi:10.1098/rstb.2008.0304.
8. Plastics europe. *Plastics-the Facts 2019 An analysis of European plastics production, demand and waste data*. https://www.plasticseurope.org/application/files/9715/7129/9584/FINAL_web_version_Plastics_the_facts2019_14102019.pdf (2019).
9. Emadian, S. M., Onay, T. T. & Demirel, B. Biodegradation of bioplastics in natural environments. *Waste Manag.* **59**, 526–536 (2017) doi:10.1016/j.wasman.2016.10.006.
10. Ahmed, T., Shahid, M., Azeem, F., Rasul, I., Shah, A. A., Noman, M., Hameed, A., Manzoor, N., Manzoor, I. & Muhammad, S. Biodegradation of plastics: current scenario and future prospects for environmental safety. *Environ. Sci. Pollut. Res.* **25**, 7287–7298 (2018) doi:10.1007/s11356-018-1234-9.
11. Haider, T. P., Völker, C., Kramm, J., Landfester, K. & Wurm, F. R. Plastics of the Future? The Impact of Biodegradable Polymers on the Environment and on Society. *Angew. Chemie Int. Ed.* **58**, 50–62 (2019) doi:10.1002/anie.201805766.
12. Geyer, R., Jambeck, J. R. & Law, K. L. Production, use, and fate of all plastics ever made. *Sci. Adv.* **3**, e1700782 (2017) doi:10.1126/sciadv.1700782.
13. Gregory, M. R. Environmental implications of plastic debris in marine settings—entanglement, ingestion, smothering, hangers-on, hitch-hiking and alien invasions. *Philos. Trans. R. Soc. B Biol. Sci.* **364**, 2013–2025 (2009) doi:10.1098/rstb.2008.0265.
14. Jambeck, J. R., Geyer, R., Wilcox, C., Siegler, T. R., Perryman, M., Andrady, A., Narayan, R. & Law, K. L. Plastic waste inputs from land into the ocean. *Science (80-)*. **347**, 768–771 (2015) doi:10.1126/science.1260352.
15. Koelmans, A. A., Besseling, E. & Shim, W. J. Nanoplastics in the Aquatic Environment. Critical Review. in *Marine Anthropogenic Litter* 325–340 (Springer International Publishing, 2015). doi:10.1007/978-3-319-16510-3_12.
16. Rochman, C. M., Browne, M. A., Underwood, A. J., Van Franeker, J. A., Thompson, R. C. & Amaral-Zettler, L. A. The ecological impacts of marine debris: Unraveling the demonstrated evidence from what is perceived. *Ecology* **97**, 302–312 (2016) doi:10.1890/14-2070.1.
17. Browne, M. A., Galloway, T. & Thompson, R. Microplastic—an emerging contaminant of potential concern? *Integr. Environ. Assess. Manag.* **3**, 559–561 (2007)

- doi:10.1897/1551-3793(2007)3[559:LD]2.0.CO;2.
18. Carbery, M., O'Connor, W. & Palanisami, T. Trophic transfer of microplastics and mixed contaminants in the marine food web and implications for human health. *Environ. Int.* **115**, 400–409 (2018) doi:10.1016/j.envint.2018.03.007.
 19. da Costa, J. P., Santos, P. S. M., Duarte, A. C. & Rocha-Santos, T. (Nano)plastics in the environment - Sources, fates and effects. *Sci. Total Environ.* **566–567**, 15–26 (2016) doi:10.1016/j.scitotenv.2016.05.041.
 20. Kamm, B. & Kamm, M. Principles of biorefineries. *Appl. Microbiol. Biotechnol.* **64**, 137–145 (2004) doi:10.1007/s00253-003-1537-7.
 21. Jong, E. de, Higson, A., Walsh, P. & Wellisch, M. *Task 42 Biobased Chemicals - Value Added Products from Biorefineries. A report prepared for IEA Bioenergy-Task* <https://www.ieabioenergy.com/wp-content/uploads/2013/10/Task-42-Biobased-Chemicals-value-added-products-from-biorefineries.pdf> (2012).
 22. Werpy, T. & Petersen, G. *Top Value Added Chemicals from Biomass: Volume I -- Results of Screening for Potential Candidates from Sugars and Synthesis Gas.* <http://www.osti.gov/bridge> (2004) doi:10.2172/15008859.
 23. Sousa, A. F., Vilela, C., Fonseca, A. C., Matos, M., Freire, C. S. R., Gruter, G.-J. M., Coelho, J. F. J. & Silvestre, A. J. D. Biobased polyesters and other polymers from 2,5-furandicarboxylic acid: a tribute to furan excellency. *Polym. Chem.* **6**, 5961–5983 (2015) doi:10.1039/C5PY00686D.
 24. Bioplastics – European Bioplastics e.V. <https://www.european-bioplastics.org/bioplastics/>.
 25. Bioplastics, E. *Global production capacities of bioplastics 2018-2023 Bioplastics market data 2018.* www.european-bioplastics.org (2018).
 26. Jia, Z., Wang, J., Sun, L., Liu, F., Zhu, J. & Liu, X. Copolyesters developed from bio-based 2,5-furandicarboxylic acid: Synthesis, sequence distribution, mechanical, and barrier properties of poly(propylene- co -1,4-cyclohexanedimethylene 2,5-furandicarboxylate)s. *J. Appl. Polym. Sci.* **136**, 47291 (2019) doi:10.1002/app.47291.
 27. de Vries, J. G. Green Syntheses of Heterocycles of Industrial Importance. 5-Hydroxymethylfurfural as a Platform Chemical. *Adv. Heterocycl. Chem.* **121**, 247–293 (2017) doi:10.1016/bs.aihch.2016.09.001.
 28. de Jong, E., Dam, M. A., Sipos, L. & Gruter, G.-J. M. Furandicarboxylic Acid (FDCA), A Versatile Building Block for a Very Interesting Class of Polyesters. in *ACS Symposium Series* vol. 1105 1–13 (2012). doi:10.1021/bk-2012-1105.ch001.
 29. Triebel, C., Nikolakis, V. & Ierapetritou, M. Simulation and economic analysis of 5-hydroxymethylfurfural conversion to 2,5-furandicarboxylic acid. *Comput. Chem. Eng.* **52**, 26–34 (2013) doi:10.1016/j.compchemeng.2012.12.005.
 30. Rathod, P. V. & Jadhav, V. H. Efficient Method for Synthesis of 2,5-Furandicarboxylic Acid from 5-Hydroxymethylfurfural and Fructose Using Pd/CC Catalyst under Aqueous Conditions. *ACS Sustain. Chem. Eng.* **6**, 5766–5771 (2018) doi:10.1021/acssuschemeng.7b03124.
 31. Pouloupoulou, N., Smyrnioti, D., Nikolaidis, G. N., Tsitsimaka, I., Christodoulou, E., Bikiaris, D. N., Charitopoulou, M. A., Achilias, D. S., Kapnisti, M. & Papageorgiou, G. Z. Sustainable Plastics from Biomass: Blends of Polyesters Based on 2,5-Furandicarboxylic Acid. *Polymers (Basel)*. **12**, 225 (2020) doi:10.3390/polym12010225.
 32. Gandini, A., Silvestre, A. J. D., Neto, C. P., Sousa, A. F. & Gomes, M. The furan counterpart of poly(ethylene terephthalate): An alternative material based on renewable resources. *J. Polym. Sci. Part A Polym. Chem.* **47**, 295–298 (2009) doi:10.1002/pola.23130.
 33. Qu, X., Jiang, M., Wang, B., Deng, J., Wang, R., Zhang, Q., Zhou, G. & Tang, J. A Brønsted Acidic Ionic Liquid as an Efficient and Selective Catalyst System for Bioderived High Molecular Weight Poly(ethylene 2,5-furandicarboxylate).

- ChemSusChem* **12**, 4927–4935 (2019) doi:10.1002/cssc.201902020.
34. Eerhart, A. J. J. E., Faaij, A. P. C. & Patel, M. K. Replacing fossil based PET with biobased PEF; Process analysis, energy and GHG balance. *Energy Environ. Sci.* **5**, 6407–6422 (2012) doi:10.1039/c2ee02480b.
 35. Nguyen, H. T. H., Qi, P., Rostagno, M., Feteha, A. & Miller, S. A. The quest for high glass transition temperature bioplastics. *J. Mater. Chem. A* **6**, 9298–9331 (2018) doi:10.1039/c8ta00377g.
 36. Avantium Technology & Markets Day: “Entering the Commercialization Phase for PEF” - Avantium (Press Release). <https://www.avantium.com/investor-relations/avantium-technology-markets-day-entering-the-commercialization-phase-for-pef/> (2019).
 37. Burgess, S. K., Leisen, J. E., Kraftschik, B. E., Mubarak, C. R., Kriegel, R. M. & Koros, W. J. Chain mobility, thermal, and mechanical properties of poly(ethylene furanoate) compared to poly(ethylene terephthalate). *Macromolecules* **47**, 1383–1391 (2014) doi:10.1021/ma5000199.
 38. Jiang, M., Liu, Q., Zhang, Q., Ye, C. & Zhou, G. A series of furan-aromatic polyesters synthesized via direct esterification method based on renewable resources. *J. Polym. Sci. Part A Polym. Chem.* **50**, 1026–1036 (2012) doi:10.1002/pola.25859.
 39. Knoop, R. J. I., Vogelzang, W., Van Haveren, J. & Van Es, D. S. High molecular weight poly(ethylene-2,5-furanoate); Critical aspects in synthesis and mechanical property determination. *J. Polym. Sci. Part A Polym. Chem.* **51**, 4191–4199 (2013) doi:10.1002/pola.26833.
 40. Burgess, S. K., Karvan, O., Johnson, J. R., Kriegel, R. M. & Koros, W. J. Oxygen sorption and transport in amorphous poly(ethylene furanoate). *Polymer (Guildf)*. **55**, 4748–4756 (2014) doi:10.1016/j.polymer.2014.07.041.
 41. Burgess, S. K., Kriegel, R. M. & Koros, W. J. Carbon dioxide sorption and transport in amorphous poly(ethylene furanoate). *Macromolecules* **48**, 2184–2193 (2015) doi:10.1021/acs.macromol.5b00333.
 42. Burgess, S. K., Mikkilineni, D. S., Yu, D. B., Kim, D. J., Mubarak, C. R., Kriegel, R. M. & Koros, W. J. Water sorption in poly(ethylene furanoate) compared to poly(ethylene terephthalate). Part 1: Equilibrium sorption. *Polymer (Guildf)*. **55**, 6861–6869 (2014) doi:10.1016/j.polymer.2014.10.047.
 43. Sipos, L. A Process for preparing a polymer having a 2,5-furandicarboxylate moiety within the polymer backbone and such (co)polymers. WO 2010/077133 A1 (2010).
 44. Zhang, D. & Dumont, M. J. Advances in polymer precursors and bio-based polymers synthesized from 5-hydroxymethylfurfural. *J. Polym. Sci. Part A Polym. Chem.* **55**, 1478–1492 (2017) doi:10.1002/pola.28527.
 45. Weinberger, S., Canadell, J., Quartinello, F., Yeniad, B., Arias, A., Pellis, A. & Guebitz, G. Enzymatic Degradation of Poly(ethylene 2,5-furanoate) Powders and Amorphous Films. *Catalysts* **7**, 318 (2017) doi:10.3390/catal7110318.
 46. Austin, H. P., Allen, M. D., Donohoe, B. S., Rorrer, N. A., Kearns, F. L., Silveira, R. L., Pollard, B. C., Dominick, G., Duman, R., El Omari, K., *et al.* Characterization and engineering of a plastic-degrading aromatic polyesterase. *Proc. Natl. Acad. Sci.* **115**, E4350–E4357 (2018) doi:10.1073/pnas.1718804115.
 47. Gruter, G.-J. *Technology & markets day path to the future*. https://www.avantium.com/wp-content/uploads/2019/06/20190606-Technology-Day_CTO_Gert-Jan_Gruter_breakout_final_.pdf (2019).
 48. Avantium. *Sustainability Manifesto*. <https://www.avantium.com/wp-content/uploads/2020/03/20200325-Avantium-Sustainability-Manifesto-2019.pdf> (2020).
 49. Zhu, J., Cai, J., Xie, W., Chen, P. H., Gazzano, M., Scandola, M. & Gross, R. A. Poly(butylene 2,5-furan dicarboxylate), a biobased alternative to PBT: Synthesis, physical properties, and crystal structure. *Macromolecules* **46**, 796–804 (2013)

- doi:10.1021/ma3023298.
50. Zhou, W., Wang, X., Yang, B., Xu, Y., Zhang, W., Zhang, Y. & Ji, J. Synthesis, physical properties and enzymatic degradation of bio-based poly(butylene adipate-co-butylene furandicarboxylate) copolyesters. *Polym. Degrad. Stab.* **98**, 2177–2183 (2013) doi:10.1016/j.polymdegradstab.2013.08.025.
 51. Matos, M., Sousa, A. F., Fonseca, A. C., Freire, C. S. R., Coelho, J. F. J. & Silvestre, A. J. D. A New Generation of Furanic Copolyesters with Enhanced Degradability: Poly(ethylene 2,5-furandicarboxylate)-co-poly(lactic acid) Copolyesters. *Macromol. Chem. Phys.* **215**, 2175–2184 (2014) doi:10.1002/macp.201400175.
 52. Tsanaktis, V., Papageorgiou, G. Z. & Bikiaris, D. N. A facile method to synthesize high-molecular-weight biobased polyesters from 2,5-furandicarboxylic acid and long-chain diols. *J. Polym. Sci. Part A Polym. Chem.* **53**, 2617–2632 (2015) doi:10.1002/pola.27730.
 53. Ma, J., Yu, X., Xu, J. & Pang, Y. Synthesis and crystallinity of poly(butylene 2,5-furandicarboxylate). *Polymer (Guildf)*. **53**, 4145–4151 (2012) doi:10.1016/j.polymer.2012.07.022.
 54. Fenouillot, F., Rousseau, A., Colomines, G., Saint-Loup, R. & Pascault, J.-P. Polymers from renewable 1,4:3,6-dianhydrohexitols (isosorbide, isomannide and isoidide): A review. *Prog. Polym. Sci.* **35**, 578–622 (2010) doi:10.1016/j.progpolymsci.2009.10.001.
 55. Gomes, M., Gandini, A., Silvestre, A. J. D. & Reis, B. Synthesis and characterization of poly(2,5-furan dicarboxylate)s based on a variety of diols. *J. Polym. Sci. Part A Polym. Chem.* **49**, 3759–3768 (2011) doi:10.1002/pola.24812.
 56. Terzopoulou, Z., Kasmi, N., Tsanaktis, V., Doulikas, N., Bikiaris, D. N., Achilias, D. S. & Papageorgiou, G. Z. Synthesis and Characterization of Bio-Based Polyesters: Poly(2-methyl-1,3-propylene-2,5-furanoate), Poly(isosorbide-2,5-furanoate), Poly(1,4-cyclohexanedimethylene-2,5-furanoate). *Materials (Basel)*. **10**, 801 (2017) doi:10.3390/ma10070801.
 57. Soares, M. J., Dannecker, P. K., Vilela, C., Bastos, J., Meier, M. A. R. & Sousa, A. F. Poly(1,20-eicosanediyl 2,5-furandicarboxylate), a biodegradable polyester from renewable resources. *Eur. Polym. J.* **90**, 301–311 (2017) doi:10.1016/j.eurpolymj.2017.03.023.
 58. Weinberger, S., Haernvall, K., Scaini, D., Ghazaryan, G., Zumstein, M. T., Sander, M., Pellis, A. & Guebitz, G. M. Enzymatic surface hydrolysis of poly(ethylene furanoate) thin films of various crystallinities. *Green Chem.* **19**, 5381 (2017) doi:10.1039/c7gc02905e.
 59. Pellis, A., Haernvall, K., Pichler, C. M., Ghazaryan, G., Breinbauer, R. & Guebitz, G. M. Enzymatic hydrolysis of poly(ethylene furanoate). *J. Biotechnol.* **235**, 47–53 (2016) doi:10.1016/j.jbiotec.2016.02.006.
 60. Haernvall, K., Zitzenbacher, S., Amer, H., Zumstein, M. T., Sander, M., McNeill, K., Yamamoto, M., Schick, M. B., Ribitsch, D. & Guebitz, G. M. Polyol Structure Influences Enzymatic Hydrolysis of Bio-Based 2,5-Furandicarboxylic Acid (FDCA) Polyesters. *Biotechnol. J.* **12**, 1600741 (2017) doi:10.1002/biot.201600741.
 61. Hu, H., Zhang, R., Jiang, Y., Shi, L., Wang, J., Ying, W. Bin & Zhu, J. Toward Biobased, Biodegradable, and Smart Barrier Packaging Material: Modification of Poly(Neopentyl Glycol 2,5-Furandicarboxylate) with Succinic Acid. *ACS Sustain. Chem. Eng.* **7**, 4255–4265 (2019) doi:10.1021/acssuschemeng.8b05990.
 62. Hu, H., Zhang, R., Wang, J., Ying, W. Bin, Shi, L., Yao, C., Kong, Z., Wang, K. & Zhu, J. A mild method to prepare high molecular weight poly(butylene furandicarboxylate-co-glycolate) copolyesters: Effects of the glycolate content on thermal, mechanical, and barrier properties and biodegradability. *Green Chem.* **21**, 3013–3022 (2019) doi:10.1039/c9gc00668k.
 63. Kasmi, N., Wahbi, M., Papadopoulos, L., Terzopoulou, Z., Guigo, N., Sbirrazzuoli,

- N., Papageorgiou, G. Z. & Bikiaris, D. N. Synthesis and characterization of two new biobased poly(pentylene 2,5-furandicarboxylate-co-caprolactone) and poly(hexamethylene 2,5-furandicarboxylate-co-caprolactone) copolyesters with enhanced enzymatic hydrolysis properties. *Polym. Degrad. Stab.* **160**, 242–263 (2019) doi:10.1016/j.polymdegradstab.2019.01.004.
64. Morales-Huerta, J. C., Martínez de Ilarduya, A. & Muñoz-Guerra, S. Blocky poly(ϵ -caprolactone-co-butylene 2,5-furandicarboxylate) copolyesters via enzymatic ring opening polymerization. *J. Polym. Sci. Part A Polym. Chem.* **56**, 290–299 (2018) doi:10.1002/pola.28895.
 65. Soccio, M., Costa, M., Lotti, N., Gazzano, M., Siracusa, V., Salatelli, E., Manaresi, P. & Munari, A. Novel fully biobased poly(butylene 2,5-furanoate/diglycolate) copolymers containing ether linkages: Structure-property relationships. *Eur. Polym. J.* **81**, 397–412 (2016) doi:10.1016/j.eurpolymj.2016.06.022.
 66. Morales-Huerta, J. C., Ciulik, C. B., De Ilarduya, A. M. & Muñoz-Guerra, S. Fully biobased aromatic-aliphatic copolyesters: Poly(butylene furandicarboxylate-co-succinate)s obtained by ring opening polymerization. *Polym. Chem.* **8**, 748–760 (2017) doi:10.1039/c6py01879c.
 67. Chebbi, Y., Kasmi, N., Majdoub, M., Cerruti, P., Scarinzi, G., Malinconico, M., Dal Poggetto, G., Papageorgiou, G. Z. & Bikiaris, D. N. Synthesis, Characterization, and Biodegradability of Novel Fully Biobased Poly(decamethylene-co-isosorbide 2,5-furandicarboxylate) Copolyesters with Enhanced Mechanical Properties. *ACS Sustain. Chem. Eng.* **7**, 5501–5514 (2019) doi:10.1021/acssuschemeng.8b06796.
 68. Hu, H., Zhang, R., Wang, J., Ying, W. Bin & Zhu, J. Fully bio-based poly(propylene succinate-co-propylene furandicarboxylate) copolyesters with proper mechanical, degradation and barrier properties for green packaging applications. *Eur. Polym. J.* **102**, 101–110 (2018) doi:10.1016/j.eurpolymj.2018.03.009.
 69. Yu, Z., Zhou, J., Cao, F., Wen, B., Zhu, X. & Wei, P. Chemosynthesis and characterization of fully biomass-based copolymers of ethylene glycol, 2,5-furandicarboxylic acid, and succinic acid. *J. Appl. Polym. Sci.* **130**, 1415–1420 (2013) doi:10.1002/app.39344.
 70. Thiagarajan, S., Meijlink, M. A., Bourdet, A., Vogelzang, W., Knoop, R. J. I., Esposito, A., Dargent, E., van Es, D. S. & van Haveren, J. Synthesis and Thermal Properties of Bio-Based Copolyesters from the Mixtures of 2,5- and 2,4-Furandicarboxylic Acid with Different Diols. *ACS Sustain. Chem. Eng.* **7**, 18505–18516 (2019) doi:10.1021/acssuschemeng.9b04463.
 71. Kasmi, N., Ainali, N. M., Agapiou, E., Papadopoulos, L., Papageorgiou, G. Z. & Bikiaris, D. N. Novel high Tg fully biobased poly(hexamethylene-co-isosorbide-2,5-furan dicarboxylate) copolyesters: Synergistic effect of isosorbide insertion on thermal performance enhancement. *Polym. Degrad. Stab.* **169**, (2019) doi:10.1016/j.polymdegradstab.2019.108983.
 72. Lomelí-Rodríguez, M., Corpas-Martínez, J., Willis, S., Mulholland, R. & Lopez-Sanchez, J. Synthesis and Characterization of Renewable Polyester Coil Coatings from Biomass-Derived Isosorbide, FDCA, 1,5-Pentanediol, Succinic Acid, and 1,3-Propanediol. *Polymers (Basel)*. **10**, 600 (2018) doi:10.3390/polym10060600.
 73. Xie, H., Wu, L., Li, B.-G. & Dubois, P. Modification of Poly(ethylene 2,5-furandicarboxylate) with Biobased 1,5-Pentanediol: Significantly Toughened Copolyesters Retaining High Tensile Strength and O₂ Barrier Property. *Biomacromolecules* **20**, 353–364 (2019) doi:10.1021/acs.biomac.8b01495.
 74. Sousa, A. F., Coelho, J. F. J. & Silvestre, A. J. D. Renewable-based poly((ether)ester)s from 2,5-furandicarboxylic acid. *Polymer (Guildf)*. **98**, 129–135 (2016) doi:10.1016/j.polymer.2016.06.015.
 75. Jia, Z., Wang, J., Sun, L., Zhu, J. & Liu, X. Fully bio-based polyesters derived from 2,5-furandicarboxylic acid (2,5-FDCA) and dodecanedioic acid (DDCA): From

- semicrystalline thermoplastic to amorphous elastomer. *J. Appl. Polym. Sci.* **135**, 46076 (2018) doi:10.1002/app.46076.
76. Shah, A. A., Hasan, F., Hameed, A. & Ahmed, S. Biological degradation of plastics: A comprehensive review. *Biotechnol. Adv.* **26**, 246–265 (2008) doi:10.1016/j.biotechadv.2007.12.005.
 77. Kyrikou, I. & Briassoulis, D. Biodegradation of Agricultural Plastic Films: A Critical Review. *J. Polym. Environ.* **15**, 125–150 (2007) doi:10.1007/s10924-007-0053-8.
 78. Lucas, N., Bienaime, C., Belloy, C., Queneudec, M., Silvestre, F. & Nava-Saucedo, J.-E. Polymer biodegradation: Mechanisms and estimation techniques – A review. *Chemosphere* **73**, 429–442 (2008) doi:10.1016/j.chemosphere.2008.06.064.
 79. Briassoulis, D. The effects of tensile stress and the agrochemical Vapam on the ageing of low density polyethylene (LDPE) agricultural films. Part I. Mechanical behaviour. *Polym. Degrad. Stab.* **88**, 489–503 (2005) doi:10.1016/j.polymdegradstab.2004.11.021.
 80. Singh, B. & Sharma, N. Mechanistic implications of plastic degradation. *Polym. Degrad. Stab.* **93**, 561–584 (2008) doi:10.1016/j.polymdegradstab.2007.11.008.
 81. Iovino, R., Zullo, R., Rao, M. A., Cassar, L. & Gianfreda, L. Biodegradation of poly(lactic acid)/starch/coir biocomposites under controlled composting conditions. *Polym. Degrad. Stab.* **93**, 147–157 (2008) doi:10.1016/j.polymdegradstab.2007.10.011.
 82. El-Hadi, A., Schnabel, R., Straube, E., Müller, G. & Henning, S. Correlation between degree of crystallinity, morphology, glass temperature, mechanical properties and biodegradation of poly (3-hydroxyalkanoate) PHAs and their blends. *Polym. Test.* **21**, 665–674 (2002) doi:10.1016/S0142-9418(01)00142-8.
 83. Koutny, M., Lemaire, J. & Delort, A.-M. Biodegradation of polyethylene films with prooxidant additives. *Chemosphere* **64**, 1243–1252 (2006) doi:10.1016/j.chemosphere.2005.12.060.
 84. Wiles, D. M. & Scott, G. Polyolefins with controlled environmental degradability. *Polym. Degrad. Stab.* **91**, 1581–1592 (2006) doi:10.1016/j.polymdegradstab.2005.09.010.
 85. Cole, M., Lindeque, P., Halsband, C. & Galloway, T. S. Microplastics as contaminants in the marine environment: A review. *Mar. Pollut. Bull.* **62**, 2588–2597 (2011) doi:10.1016/j.marpolbul.2011.09.025.
 86. Lobelle, D. & Cunliffe, M. Early microbial biofilm formation on marine plastic debris. *Mar. Pollut. Bull.* **62**, 197–200 (2011) doi:10.1016/j.marpolbul.2010.10.013.
 87. Woodall, L. C., Sanchez-Vidal, A., Canals, M., Paterson, G. L. J., Coppock, R., Sleight, V., Calafat, A., Rogers, A. D., Narayanaswamy, B. E. & Thompson, R. C. The deep sea is a major sink for microplastic debris. *R. Soc. Open Sci.* **1**, (2014) doi:10.1098/rsos.140317.
 88. Lambert, S., Sinclair, C. & Boxall, A. Occurrence, degradation, and effect of polymer-based materials in the environment. *Rev. Environ. Contam. Toxicol.* **227**, 1–53 (2014) doi:10.1007/978-3-319-01327-5_1.
 89. Watters, D. L., Yoklavich, M. M., Love, M. S. & Schroeder, D. M. Assessing marine debris in deep seafloor habitats off California. *Mar. Pollut. Bull.* **60**, 131–138 (2010) doi:10.1016/j.marpolbul.2009.08.019.
 90. Zettler, E. R., Mincer, T. J. & Amaral-Zettler, L. A. Life in the “Plastisphere”: Microbial Communities on Plastic Marine Debris. *Environ. Sci. Technol.* **47**, 7137–7146 (2013) doi:10.1021/es401288x.
 91. ASTM International. *ASTM D996-16*. <http://www.astm.org/cgi-bin/resolver.cgi?D996> (2016) doi:10.1520/D0996-16.
 92. Paço, A., Duarte, K., da Costa, J. P., Santos, P. S. M., Pereira, R., Pereira, M. E., Freitas, A. C., Duarte, A. C. & Rocha-Santos, T. A. P. Biodegradation of polyethylene microplastics by the marine fungus *Zalerion maritimum*. *Sci. Total Environ.* **586**, 10–

- 15 (2017) doi:10.1016/j.scitotenv.2017.02.017.
93. Sheth, M. U., Kwartler, S. K., Schmaltz, E. R., Hoskinson, S. M., Martz, E. J., Dunphy-Daly, M. M., Schultz, T. F., Read, A. J., Eward, W. C. & Somarelli, J. A. Bioengineering a Future Free of Marine Plastic Waste. *Front. Mar. Sci.* **6**, 1–10 (2019) doi:10.3389/fmars.2019.00624.
 94. Jacquin, J., Cheng, J., Odobel, C., Pandin, C., Conan, P., Pujo-Pay, M., Barbe, V., Meistertzheim, A.-L. & Ghiglione, J.-F. Microbial Ecotoxicology of Marine Plastic Debris: A Review on Colonization and Biodegradation by the “Plastisphere”. *Front. Microbiol.* **10**, 1–16 (2019) doi:10.3389/fmicb.2019.00865.
 95. Dussud, C. & Ghiglione, J. F. Bacterial degradation of synthetic plastics. *CIESM Work. Monogr.* **2014** **46**, 49–54 (2014).
 96. Zanardini, E., Abbruscato, P., Ghedini, N., Realini, M. & Sorlini, C. Influence of atmospheric pollutants on the biodeterioration of stone. *Int. Biodeterior. Biodegrad.* **45**, 35–42 (2000) doi:10.1016/S0964-8305(00)00043-3.
 97. Siracusa, V. Microbial degradation of synthetic biopolymers waste. *Polymers (Basel)*. **11**, (2019) doi:10.3390/polym11061066.
 98. Alshehrei, F. Biodegradation of Synthetic and Natural Plastic by Microorganisms. *J. Appl. Environ. Microbiol.* **5**, 8–19 (2017) doi:10.12691/jaem-5-1-2.
 99. Kale, S. K., Deshmukh, A. G., Dudhare, M. S. & Patil, V. B. Microbial degradation of plastic: a review. *J. Biochem. Technol.* **6**, 952–961 (2015).
 100. Mohan, S. K. & Srivastava, T. Microbial deterioration and degradation of polymeric materials. *J. Biochem. Technol.* **2(4)**, 210–215 (2011).
 101. Artham, T. & Doble, M. Biodegradation of Aliphatic and Aromatic Polycarbonates. *Macromol. Biosci.* **8**, 14–24 (2008) doi:10.1002/mabi.200700106.
 102. Tokiwa, Y., Calabria, B. P., Ugwu, C. U. & Aiba, S. Biodegradability of Plastics. *Int. J. Mol. Sci.* **10**, 3722–3742 (2009) doi:10.3390/ijms10093722.
 103. Yoshida, S., Hiraga, K., Takehana, T., Taniguchi, I., Yamaji, H., Maeda, Y., Toyohara, K., Miyamoto, K., Kimura, Y. & Oda, K. A bacterium that degrades and assimilates poly(ethylene terephthalate). *Science (80-.)*. **351**, 1196–1199 (2016) doi:10.1126/science.aad6359.
 104. Roohi, Bano, K., Kuddus, M., Zaheer, M. R., Zia, Q., Khan, M. F., Ashraf, G. M., Gupta, A. & Aliev, G. Microbial Enzymatic Degradation of Biodegradable Plastics. *Curr. Pharm. Biotechnol.* **18**, (2017) doi:10.2174/1389201018666170523165742.
 105. Pathak, V. M. & Navneet. Review on the current status of polymer degradation: a microbial approach. *Bioresour. Bioprocess.* **4**, 15 (2017) doi:10.1186/s40643-017-0145-9.
 106. Bhardwaj, H., Gupta, R. & Tiwari, A. Communities of Microbial Enzymes Associated with Biodegradation of Plastics. *J. Polym. Environ.* **21**, 575–579 (2013) doi:10.1007/s10924-012-0456-z.
 107. Črešnar, B. & Petrič, Š. Cytochrome P450 enzymes in the fungal kingdom. *Biochim. Biophys. Acta - Proteins Proteomics* **1814**, 29–35 (2011) doi:10.1016/j.bbapap.2010.06.020.
 108. Schmit, J. P. & Mueller, G. M. An estimate of the lower limit of global fungal diversity. *Biodivers. Conserv.* **16**, 99–111 (2007) doi:10.1007/s10531-006-9129-3.
 109. Sánchez, C. Fungal potential for the degradation of petroleum-based polymers: An overview of macro- and microplastics biodegradation. *Biotechnol. Adv.* **40**, 107501 (2020) doi:10.1016/j.biotechadv.2019.107501.
 110. Ivarsson, M., Schnürer, A., Bengtson, S. & Neubeck, A. Anaerobic Fungi: A Potential Source of Biological H₂ in the Oceanic Crust. *Front. Microbiol.* **7**, 12 (2016) doi:10.3389/fmicb.2016.00674.
 111. Raghukumar, S. *Fungi in Coastal and Oceanic Marine Ecosystems. Fungi in Coastal and Oceanic Marine Ecosystems: Marine Fungi* (Springer International Publishing, 2017). doi:10.1007/978-3-319-54304-8.

112. Khan, S., Nadir, S., Shah, Z. U., Shah, A. A., Karunarathna, S. C., Xu, J., Khan, A., Munir, S. & Hasan, F. Biodegradation of polyester polyurethane by *Aspergillus tubingensis*. *Environ. Pollut.* **225**, 469–480 (2017) doi:10.1016/j.envpol.2017.03.012.
113. Balasubramanian, V., Natarajan, K., Rajeshkannan, V. & Perumal, P. Enhancement of in vitro high-density polyethylene (HDPE) degradation by physical, chemical, and biological treatments. *Environ. Sci. Pollut. Res.* **21**, 12549–12562 (2014) doi:10.1007/s11356-014-3191-2.
114. Taxonomy browser (Penicillium). <https://www.ncbi.nlm.nih.gov/Taxonomy/Browser/wwwtax.cgi>.
115. Tsang, C.-C., Tang, J. Y. M., Lau, S. K. P. & Woo, P. C. Y. Taxonomy and evolution of *Aspergillus*, *Penicillium* and *Talaromyces* in the omics era – Past, present and future. *Comput. Struct. Biotechnol. J.* **16**, 197–210 (2018) doi:10.1016/j.csbj.2018.05.003.
116. Guarro, J., Gené, J. & Stchigel, A. M. Developments in Fungal Taxonomy. *Clin. Microbiol. Rev.* **12**, 454–500 (1999).
117. Yadav, A. N., Verma, P., Kumar, V., Sangwan, P., Mishra, S., Panjiar, N., Gupta, V. K. & Saxena, A. K. Biodiversity of the Genus *Penicillium* in Different Habitats. in *New and Future Developments in Microbial Biotechnology and Bioengineering* 3–18 (Elsevier, 2018). doi:10.1016/B978-0-444-63501-3.00001-6.
118. Leitão, A. L. Potential of penicillium species in the bioremediation field. *Int. J. Environ. Res. Public Health* **6**, 1393–1417 (2009) doi:10.3390/ijerph6041393.
119. Butinar, L., Frisvad, J. C. & Gunde-Cimerman, N. Hypersaline waters – a potential source of foodborne toxigenic aspergilli and penicillia. *FEMS Microbiol. Ecol.* **77**, 186–199 (2011) doi:10.1111/j.1574-6941.2011.01108.x.
120. Gonçalves, M. F. M., Santos, L., Silva, B. M. V., Abreu, A. C., Vicente, T. F. L., Esteves, A. C. & Alves, A. Biodiversity of *Penicillium* species from marine environments in Portugal and description of *Penicillium lusitanum* sp. nov., a novel species isolated from sea water. *Int. J. Syst. Evol. Microbiol.* **69**, 3014–3021 (2019) doi:10.1099/ijsem.0.003535.
121. Lugauskas, A., Levinskaite, L. & Pečiulyte, D. Micromycetes as deterioration agents of polymeric materials. *Int. Biodeterior. Biodegrad.* **52**, 233–242 (2003) doi:10.1016/S0964-8305(03)00110-0.
122. Yamada-Onodera, K., Mukumoto, H., Katsuyaya, Y., Saiganji, A. & Tani, Y. Degradation of polyethylene by a fungus, *Penicillium simplicissimum* YK. *Polym. Degrad. Stab.* **72**, 323–327 (2001) doi:10.1016/S0141-3910(01)00027-1.
123. Sowmya, H. V., Ramalingappa, Krishnappa, M. & Thippeswamy, B. Degradation of polyethylene by *Penicillium simplicissimum* isolated from local dumpsite of Shivamogga district. *Environ. Dev. Sustain.* **17**, 731–745 (2015) doi:10.1007/s10668-014-9571-4.
124. Ojha, N., Pradhan, N., Singh, S., Barla, A., Shrivastava, A., Khatua, P., Rai, V. & Bose, S. Evaluation of HDPE and LDPE degradation by fungus, implemented by statistical optimization. *Sci. Rep.* **7**, 1–13 (2017) doi:10.1038/srep39515.
125. Umamaheswari, S., Sepperumal, U., Markandan, M. & Palraja, I. Micromorphological and chemical changes during biodegradation of Polyethylene terephthalate (PET) by *Penicillium* sp. *J. Microbiol. Biotechnol. Res.* **3**, 47–53 (2013).
126. Nowak, B., Pajak, J., Labuzek, S., Rymarz, G. & Talik, E. Biodegradation of poly(ethylene terephthalate) modified with polyester "Bionolle" by *Penicillium funiculosum*. *Polimery* **56**, 35–44 (2011) doi:10.14314/polimery.2011.035.
127. Loos, K., Zhang, R., Pereira, I., Agostinho, B., Hu, H., Maniar, D., Sbirrazzuoli, N., Silvestre, A. J. D., Guigo, N. & Sousa, A. F. A Perspective on PEF Synthesis, Properties, and End-Life. *Front. Chem.* **8**, 585 (2020) doi:10.3389/fchem.2020.00585.
128. Matos, M., Sousa, A. F., Mendonça, P. V. & Silvestre, A. J. D. Co-polymers based

- on Poly(1,4-butylene 2,5-furandicarboxylate) and Poly(propylene oxide) with tuneable thermal properties: Synthesis and characterization. *Materials (Basel)*. **12**, (2019) doi:10.3390/ma12020328.
129. Yu, Z., Zhou, J., Cao, F., Zhang, Q., Huang, K. & Wei, P. Synthesis, Characterization and Thermal Properties of Bio-Based Poly(Ethylene 2,5-Furan Dicarboxylate). *J. Macromol. Sci. Part B Phys.* **55**, 1135–1145 (2016) doi:10.1080/00222348.2016.1238335.
 130. Banella, M. B., Bonucci, J., Vannini, M., Marchese, P., Lorenzetti, C. & Celli, A. Insights into the Synthesis of Poly(ethylene 2,5-Furandicarboxylate) from 2,5-Furandicarboxylic Acid: Steps toward Environmental and Food Safety Excellence in Packaging Applications. *Ind. Eng. Chem. Res.* **58**, 8955–8962 (2019) doi:10.1021/acs.iecr.9b00661.
 131. Thiagarajan, S., Vogelzang, W., J. I. Knoop, R., Frissen, A. E., Van Haveren, J. & Van Es, D. S. Biobased furandicarboxylic acids (FDCAs): Effects of isomeric substitution on polyester synthesis and properties. *Green Chem.* **16**, 1957–1966 (2014) doi:10.1039/c3gc42184h.
 132. Wu, J., Xie, H., Wu, L., Li, B. G. & Dubois, P. DBU-catalyzed biobased poly(ethylene 2,5-furandicarboxylate) polyester with rapid melt crystallization: Synthesis, crystallization kinetics and melting behavior. *RSC Adv.* **6**, 101578–101586 (2016) doi:10.1039/c6ra21135f.
 133. Salman, A., Tsrer, L., Pomerantz, A., Moreh, R., Mordechai, S. & Huleihel, M. FTIR spectroscopy for detection and identification of fungal phytopathogenes. *Spectroscopy* **24**, 261–267 (2010) doi:10.3233/SPE-2010-0448.
 134. Naumann, D. Infrared Spectroscopy in Microbiology. in *Encyclopedia of Analytical Chemistry* (John Wiley & Sons, Ltd, 2006). doi:10.1002/9780470027318.a0117.
 135. Dzurendova, S., Zimmermann, B., Kohler, A., Tafintseva, V., Slany, O., Certik, M. & Shapaval, V. Microcultivation and FTIR spectroscopy-based screening revealed a nutrient-induced co-production of high-value metabolites in oleaginous *Mucoromycota* fungi. *PLoS One* **15**, (2020) doi:10.1371/journal.pone.0234870.
 136. Erukhimovitch, V., Tsrer, L., Hazanovsky, M., Talyshinsky, M., Mukmanov, I., Souprun, Y. & Huleihel, M. Identification of fungal phyto-pathogens by Fourier-transform infrared (FTIR) microscopy. *J. Agric. Technol.* **1(1)**, 145–52 (2005).
 137. Nitsche, B. M., Jørgensen, T. R., Akeroyd, M., Meyer, V. & Ram, A. F. J. The carbon starvation response of *Aspergillus niger* during submerged cultivation: Insights from the transcriptome and secretome. *BMC Genomics* **13**, 380 (2012) doi:10.1186/1471-2164-13-380.
 138. Schneiderman, D. K. & Hillmyer, M. A. 50th Anniversary Perspective: There Is a Great Future in Sustainable Polymers. *Macromolecules* **50**, 3733–3749 (2017) doi:10.1021/acs.macromol.7b00293.
 139. Guidotti, G., Soccio, M., García-Gutiérrez, M. C., Ezquerra, T., Siracusa, V., Gutiérrez-Fernández, E., Munari, A. & Lotti, N. Fully Biobased Superpolymers of 2,5-Furandicarboxylic Acid with Different Functional Properties: From Rigid to Flexible, High Performant Packaging Materials. *ACS Sustain. Chem. Eng.* **8**, 9558–9568 (2020) doi:10.1021/acssuschemeng.0c02840.
 140. Papageorgiou, D. G., Guigo, N., Tsanaktis, V., Exarhopoulos, S., Bikiaris, D. N., Sbirrazzuoli, N. & Papageorgiou, G. Z. Fast Crystallization and Melting Behavior of a Long-Spaced Aliphatic Furandicarboxylate Biobased Polyester, Poly(dodecylene 2,5-furanoate). *Ind. Eng. Chem. Res.* **55**, 5315–5326 (2016) doi:10.1021/acs.iecr.6b00811.
 141. Song, J. W., Lee, J. H., Bornscheuer, U. T. & Park, J. B. Microbial synthesis of medium-chain α,ω -dicarboxylic acids and ω -aminocarboxylic acids from renewable long-chain fatty acids. *Adv. Synth. Catal.* **356**, 1782–1788 (2014) doi:10.1002/adsc.201300784.

142. Ayorinde, F. O., Powers, F. T., Streete, L. D., Shepard, R. L. & Tabi, D. N. Synthesis of dodecanedioic acid from vernonia galamensis oil. *J. Am. Oil Chem. Soc.* **66**, 690–692 (1989) doi:10.1007/BF02669953.
143. Fenouillot, F., Rousseau, A., Colomines, G., Saint-Loup, R. & Pascault, J.-P. Polymers from renewable 1,4:3,6-dianhydrohexitols (isosorbide, isomannide and isoidide): A review. *Prog. Polym. Sci.* **35**, 578–622 (2010) doi:10.1016/j.progpolymsci.2009.10.001.
144. Dussenne, C., Delaunay, T., Wiatz, V., Wyart, H., Suisse, I. & Sauthier, M. Synthesis of isosorbide: An overview of challenging reactions. *Green Chem.* **19**, 5332–5344 (2017) doi:10.1039/c7gc01912b.
145. Kasmi, N., Majdoub, M., Papageorgiou, G. Z. & Bikiaris, D. N. Synthesis and crystallization of new fully renewable resources-based copolyesters: Poly(1,4-cyclohexanedimethanol-co-isosorbide 2,5-furandicarboxylate). *Polym. Degrad. Stab.* **152**, 177–190 (2018) doi:10.1016/j.polymdegradstab.2018.04.009.
146. Takasu, A., Takemoto, A. & Hirabayashi, T. Polycondensation of dicarboxylic acids and diols in water catalyzed by surfactant-combined catalysts and successive chain extension. *Biomacromolecules* **7**, 6–9 (2006) doi:10.1021/bm050485p.
147. Jannesari, A., Ghaffarian, S. R., Mohammadi, N., Taromi, F. A. & Molaei, A. Liquid crystalline thermosets as binder for powder coatings - Thermoanalytical study of the cure characteristics of a carboxylated main chain liquid crystalline oligoester. *Prog. Org. Coatings* **50**, 213–223 (2004) doi:10.1016/j.porgcoat.2004.02.006.
148. Zakharova, E., De Ilarduya, A. M., León, S. & Muñoz-Guerra, S. Sugar-based bicyclic monomers for aliphatic polyesters: A comparative appraisal of acetalized alditols and isosorbide. *Des. Monomers Polym.* **20**, 157–166 (2017) doi:10.1080/15685551.2016.1231038.
149. Marubayashi, H., Ushio, T. & Nojima, S. Crystallization of polyesters composed of isohexides and aliphatic dicarboxylic acids: Effects of isohexide stereoisomerism and dicarboxylic acid chain length. *Polym. Degrad. Stab.* **146**, 174–183 (2017) doi:10.1016/j.polymdegradstab.2017.10.005.
150. Okada, M., Tsunoda, K., Tachikawa, K. & Aoi, K. Biodegradable polymers based on renewable resources. IV. Enzymatic degradation of polyesters composed of 1,4:3,6-dianhydro-D-glucitol and aliphatic dicarboxylic acid moieties. *J. Appl. Polym. Sci.* **77**, 338–346 (2000) doi:10.1002/(SICI)1097-4628(20000711)77:2<338::AID-APP9>3.0.CO;2-C.
151. Terzopoulou, Z., Papadopoulos, L., Zamboulis, A., Papageorgiou, D. G., Papageorgiou, G. Z. & Bikiaris, D. N. Tuning the Properties of Furandicarboxylic Acid-Based Polyesters with Copolymerization: A Review. *Polymers (Basel)*. **12**, 1209 (2020) doi:10.3390/polym12061209.
152. Zhang, J., Liu, Y., Qi, Z., He, L. & Peng, L. Progress in the Synthesis and Properties of 2, 5-Furan Dicarboxylate based Polyesters. *BioResources* **15**, 4502–4527 (2020).

VI. Supplementary data

1. **Supplementary data A-** Preliminary test to evaluate the growth and consumption of culture medium by the fungus *Penicillium brevicompactum* during the biodegradation of PEF.

1.1. Context

This test was carried out to evaluate the growth and consumption of the culture medium by the fungus *Penicillium brevicompactum*, with the subsequent objective of designing a procedure with discontinuous feeding of the culture medium (the method used in **Chapter II**) that would allow increasing the longevity time of the fungus in the PEF biodegradation test. In this sense, a PEF biodegradation test was developed with only two incubation times 14 and 28 days. The objective was to find out at which incubation time the fungus stopped growing and to know approximately the volume of the culture medium that was lost.

1.2. Materials and methods:

All the materials mentioned below are the same as those used in **Chapter II**. The PEF used in this test was also synthesized and characterized as referred to in **Chapter II**.

Briefly, for the PEF biodegradation test, 3 types of Erlenmeyer flasks were used:

- **Growth control (GC):** 50mL of culture medium + 0.5g of fungus (3 replicates / incubation time)
- **PEF Control (PC):** 50mL of culture medium + 0.015g PEF microparticles (3 replicates / incubation time)
- **PEF+ *P. brevicompactum* (PEF+P.b):** 50mL of culture medium + 0.015g PEF microparticles + 0.5g fungus (4 replicates / incubation time)

All Erlenmeyer (of 100 mL) consisted of 50 mL of culture medium prepared with the following concentrations: 35 g/L of NaCl, 4.6 g/L of glucose, 16.3 g/L of malt extract, and 0.56 g/L of peptone. At each incubation time (14 or 28 days), the respective Erlenmeyer flasks were removed, and the fungus and the PEF microparticles were separated from the medium by filtration, the final volume of the filtered culture medium was measured for each flask. The fungus biomass was recovered, frozen, and lyophilized, and later weighed. The PEF

microparticles were stored, dried in the oven at 40 °C for 2 days, and then weighed and analyzed by ATR-FTIR spectroscopy.

1.3. Results and Discussion

According to the data in **Supplementary data table 1**, we observed that during the first 14 days of incubation the fungus grew 8 times more, both in the GCs and in the PEF+*P.b* flasks. Between 14 and 28 days of incubation, there is a decrease in the growth of the fungus, which indicates that after the 14 days there is a decrease in the nutrients in the medium that leads the fungus to start dying. It is also noteworthy that at 28 days the growth of the fungus in the PEF+*P.b* condition was much lower compared with GC.

Supplementary data table 1 - Variation of *Penicillium brevicompactum* biomass throughout the experiment.

Erlenmeyer condition		Inoculated Biomass (Wet) (g)	Inoculated Biomass (Dry) (g)	Final Biomass (Dry) (g)	Variation of biomass	Growth	Growth mean \pm SD
14 days							
GC	R1	0.527	0.0453	0.256	0.211	4.65	8 \pm 3
	R2	0.511	0.0439	0.467	0.423	9.63	
	R3	0.514	0.0442	0.473	0.429	9.71	
PEF+ <i>P.b</i>	R1	0.527	0.0453	0.402	0.357	7.88	8 \pm 1
	R2	0.507	0.0436	0.373	0.329	7.56	
	R3	0.532	0.0457	0.424	0.378	8.27	
	R4	0.566	0.0486	0.481	0.432	8.89	
28 days							
GC	R1	0.507	0.0436	0.251	0.207	4.76	6 \pm 1
	R2	0.520	0.0447	0.320	0.275	6.16	
	R3	0.521	0.0448	0.300	0.255	5.70	
PEF+ <i>P.b</i>	R1	0.516	0.0443	0.175	0.131	2.95	3 \pm 1
	R2	0.512	0.0440	0.258	0.214	4.86	
	R3	0.504	0.0433	0.205	0.162	3.73	
	R4	0.533	0.0458	0.123	0.077	1.69	

Regarding the consumption of culture medium during the growth of the fungus, the results are shown in **Supplementary data table 2**. Probably in all Erlenmeyer flasks after autoclaving there was a loss of about 5 mL in volume. At 14 days of incubation, under GC and PEF+*P.b* conditions there was a culture medium loss mean of about 16 and 18 mL, respectively. At 28 days of incubation, the GC and PEF+*P.b* conditions showed a culture medium loss mean of 16 and 15 mL, respectively. If we then consider the loss of 5 ml in autoclaving, the growth of the fungus up to 14 days was responsible for a loss of approximately 10 ml of the volume of culture medium. From 14 to 28 days of incubation, the fungus does not seem to have caused a loss of volume of culture medium, which agrees with the reduction in the growth of the fungus also in this time interval.

Briefly, through **Supplementary data table 1** and **table 2**, we observed that after 14 days of incubation the fungus decays probably due to the lack of nutrients and that its growth caused a loss of about 10 mL of culture medium.

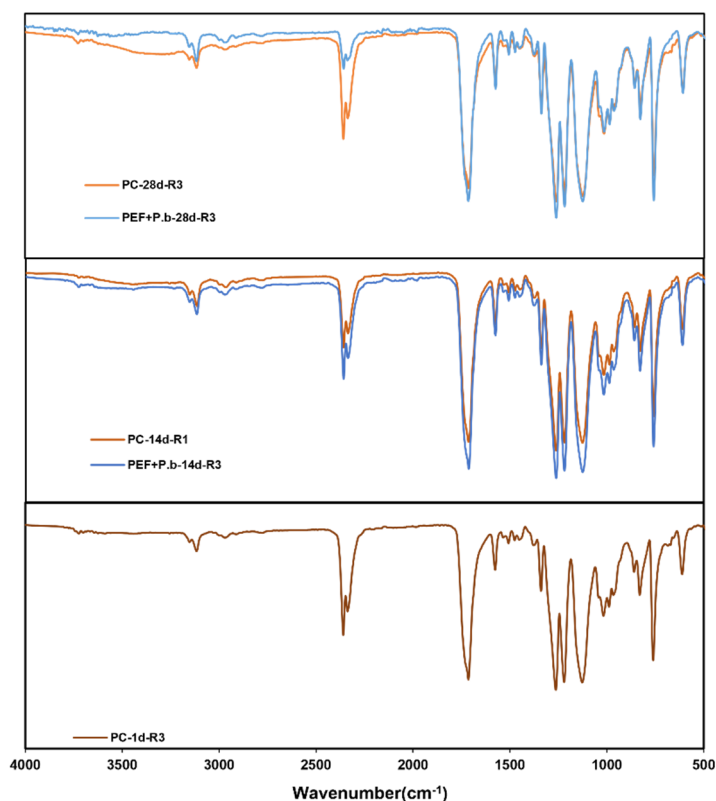
Supplementary data table 2- Culture medium loss during the test

Erlenmeyer condition		Initial culture medium (mL)	Final culture medium (mL)	Culture medium loss (mL)	Culture medium loss Mean \pm SD
1 day – after autoclave					
PC	R1	50	45	5	5 \pm 1
	R2	50	44	6	
	R3	50	46	4	
14 days					
GC	R1	50	37	13	16 \pm 3
	R2	50	33	17	
	R3	50	32	18	
PC	R1	50	43	7	6 \pm 1
	R2	50	44	6	
	R3	50	45	5	
PEF+ <i>P.b</i>	R1	50	32	18	18 \pm 1
	R2	50	32	18	
	R3	50	34	16	
	R4	50	31	19	
28 days					
GC	R1	50	34	16	16 \pm 1
	R2	50	33	17	
	R3	50	34	16	
PC	R1	50	41	9	8 \pm 1
	R2	50	42	8	
	R3	50	43	7	
PEF+ <i>P.b</i>	R1	50	37	13	15 \pm 2
	R2	50	33	17	
	R3	50	36	14	
	R4	50	36	14	

The focus of this 28-day incubation trial was to assess the growth and behavior of the fungus. However, PEF biodegradation was also evaluated, and the results of its gravimetry and ATR-FTIR analysis were also acquired. We can see in **Supplementary data table 3** that there was no considerable PEF removal during the 28-day incubation period with *P. brevicompactum*. There were also no chemical changes in the typical PEF ATR-FTIR spectrum after the 28 days of incubation with the *P. brevicompactum* (**Supplementary data-figure 1**).

Supplementary data table 3- Variation of PEF microplastics before and after their exposure to *Penicillium brevicompactum*

Erlenmeyer condition		PEF beginning (g)	PEF recovered (g)	PEF removed (g)	% PEF removed	% PEF removed mean \pm SD
1 day - after autoclave						
PC	R1	0.0151	0.0120	0.0031	21	7 \pm 12
	R2	0.0152	0.0163	-0.0011	0	
	R3	0.0153	0.0156	-0.0003	0	
14 days						
PC	R1	0.0151	0.016	-0.0009	0	0 \pm 0
	R2	0.0152	0.0167	-0.0015	0	
	R3	0.0152	0.0165	-0.0013	0	
PEF + <i>P.b</i>	R1	0.0154	0.0161	-0.0007	0	1 \pm 2
	R2	0.0152	0.0147	0.0005	3	
	R3	0.0153	0.0158	-0.0005	0	
	R4	0.015	0.0151	-0.0001	0	
28 days						
PC	R1	0.0151	0.0162	-0.0011	0	3 \pm 5
	R2	0.0151	0.0151	0.0000	0	
	R3	0.0151	0.0139	0.0012	7.9	
PEF + <i>P.b</i>	R1	0.0152	0.0140	0.0012	7.9	7 \pm 4
	R2	0.0151	0.0143	0.0008	5	
	R3	0.015	0.0153	-0.0003	0	
	R4	0.015	0.0159	-0.0009	0	



Supplementary data-figure 1- Infrared spectra in the region 500-4000 cm^{-1} from the PEF microparticles throughout the experiment

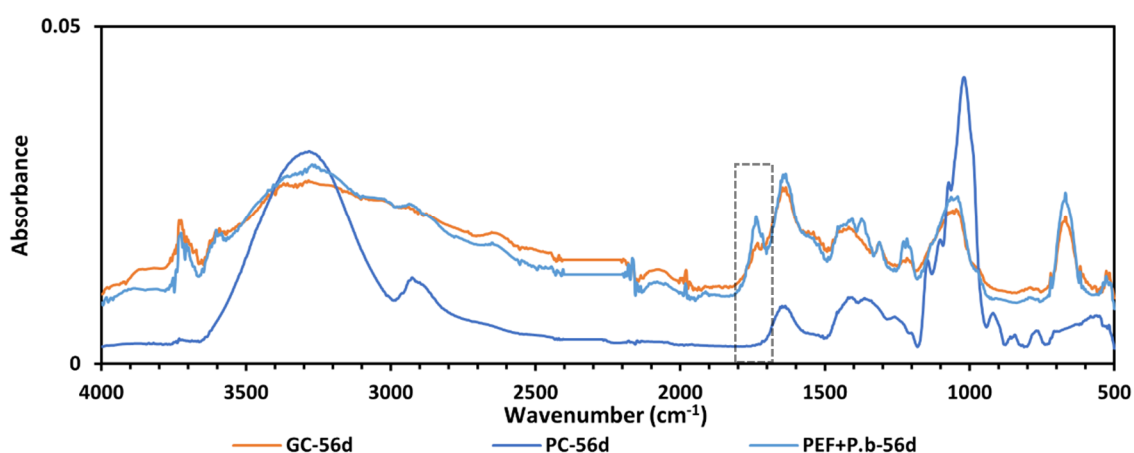
1.4. Conclusion

Based on this data, we concluded that after 14 days of incubation the fungus decays, probably due to a lack of nutrients. We also concluded that at 14 days of incubation the growth of the fungus is responsible for the loss of ≈ 10 mL of the initial 50 mL of culture medium. Based on these results, we designed a discontinuous minimal fed-batch culture method used in the PEF biodegradation test applied in **Chapter II**.

2. Supplementary data B- Chapter II

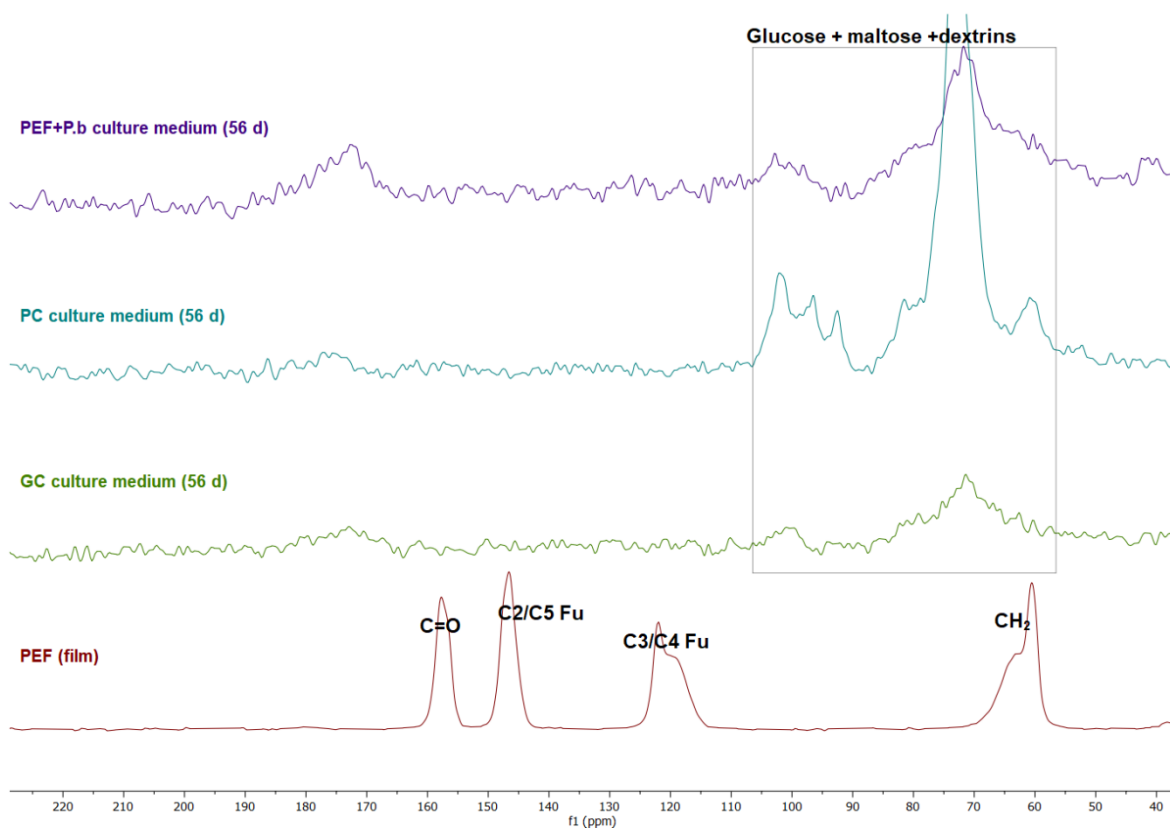
2.1. ATR-FTIR and ^{13}C ssNMR of the culture media at 56 days of incubation

Since the negative effect of PEF on the growth of the fungus was remarkable, we went to evaluate the difference in the chemical composition of the culture medium in GC, PC, and PEF+*P.b*. For this, we used the culture medium of the flasks of the 56 days of incubation. The **Supplementary data-figure 2** shows the FTIR spectra of the culture media. We observed that the PC spectrum showed peak intensities much higher than the Erlenmeyer flasks where the fungus grew (GC and PEF+*P.b*), this indicated that there was the assimilation of nutrients from the medium by the fungus throughout the trial. The PC spectrum has been reduced 5 times to be compared. A peak in 1738 cm^{-1} was observed in the spectrum of the PEF+*P.b* culture medium, this peak is associated with the C=O stretching and may indicate the release of PEF into the culture medium. In the PC spectra, this release is probably not detected due to the intensity of the other peaks.



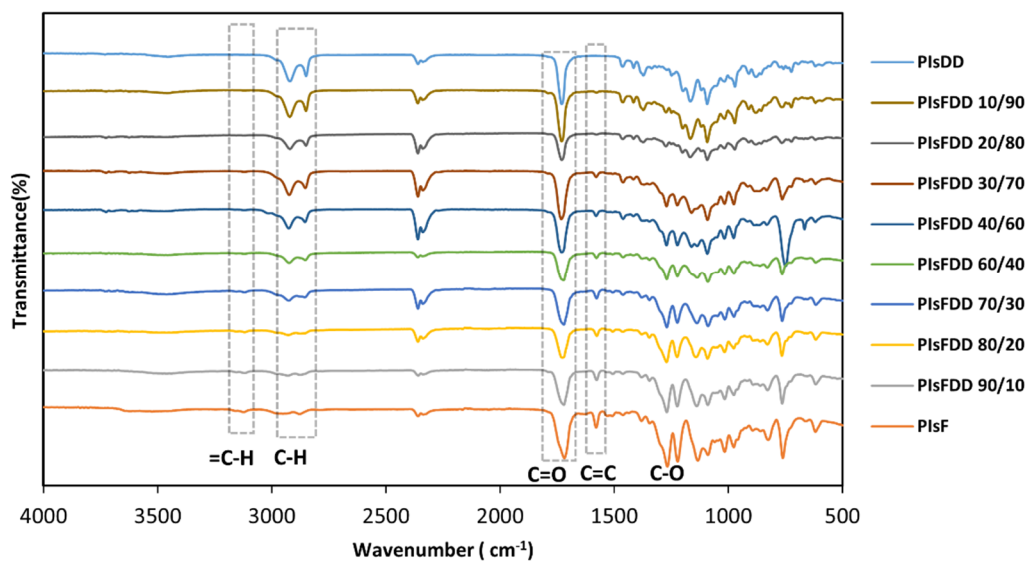
Supplementary data-figure 2- Infrared spectra in the region $500\text{-}4000\text{ cm}^{-1}$ from the culture medium.

^{13}C solid-state NMR of culture media (56 days) was also performed. **Supplementary data-figure 3** shows the acquired spectra. The PEF spectrum was also obtained to try to observe the release of PEF into the culture medium. There were no considerable differences between the culture medium of the GC and PEF+*P.b*. The peaks observed between 56 - 88 ppm and the peaks between 88 - 106 ppm are due to nutrients in the culture medium, namely glucose, maltose, and dextrin. These peaks are more visible in the PC spectrum because they are not consumed by the fungus. Between 165-180 ppm, a peak is detected in both GC and PEF+*P.b* attributed to C=O of carboxylic acid, ester, and amide groups, which may be compounds released into the culture medium from cell death of the fungus. PEF peaks were not observed in culture media. It should be noted that the PEF ^{13}C ssNMR spectrum was also in accordance with the literature³⁷.

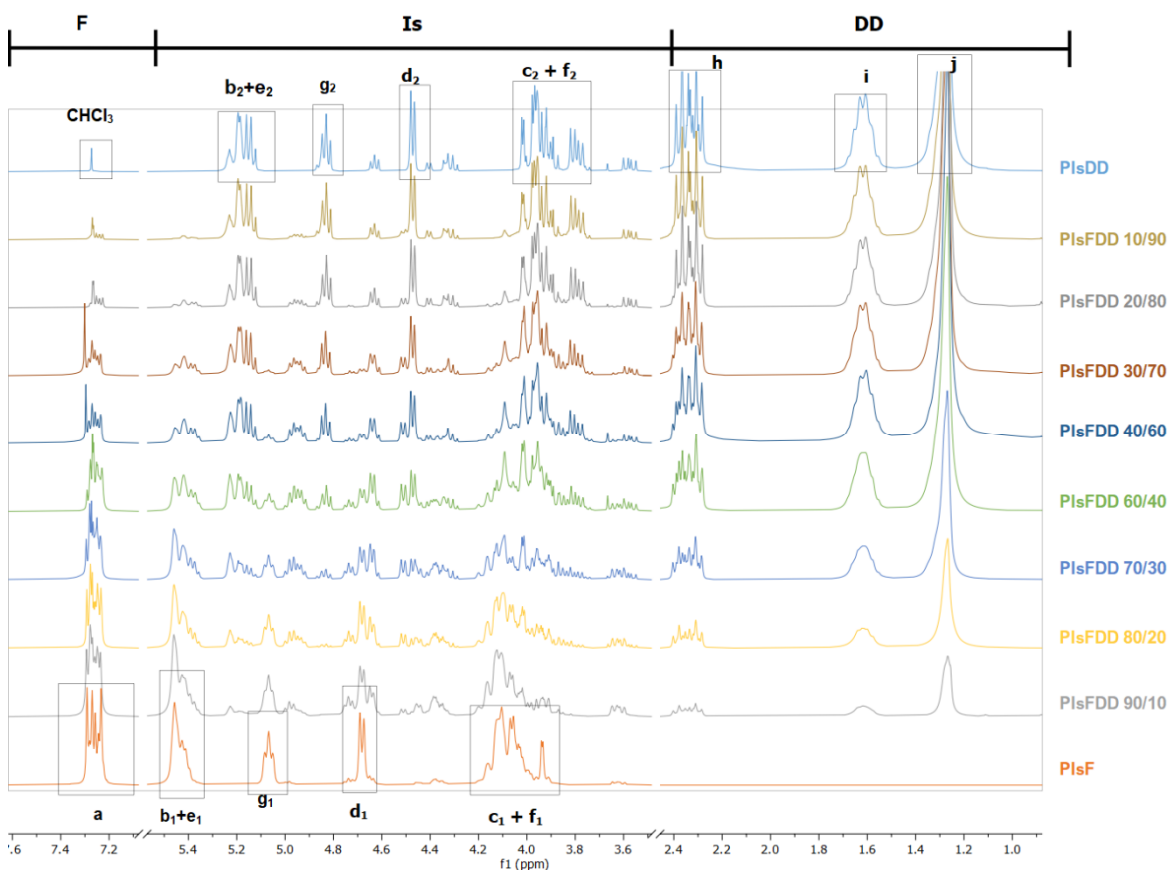


Supplementary data-figure 3- ^{13}C ssNMR of culture medium from 56 days of incubation and PEF (film)

3. Supplementary data C- Chapter III



Supplementary data-figure 4- ATR-FTIR spectra of all prepared PIIFDD copolyesters, PIIF, and PIIsDD homopolyesters.



Supplementary data-figure 5- ^1H NMR spectra of PIIsF, PIIsDD, and all PIIFDDs copolyesters in CDCl_3 .

Supplementary data table 4- ^1H NMR resonances [300 MHz, CDCl_3 , reference (CDCl_3) = 7.26 ppm] of PIsFDD copolyesters, PIsF, and PIsDD homopolyesters.

$\approx \delta$ /ppm	Multiplicity	Assignment	Integration area									
			PIsF	PIsFDDs								PIsDD
			100/0	90/10	80/20	70/30	60/40	40/60	30/70	20/80	10/90	0/100
7.26	m	a	0.75	0.87	0.85	0.82	0.88	0.75	0.92	0.15	0.07	-
5.40	m	b_1, e_1	1	1	1	1	1	1	1	0.17	0.10	-
5.07	t	g_1	0.42	0.37	0.33	0.27	0.24	0.20	0.17	0.03	0.03	-
4.68	m	d_1	0.54	0.70	0.67	0.71	0.75	0.78	0.87	0.21	-	-
4.06	m	c_1+f_1	2.17	-	-	-	-	-	-	-	-	-
5.17	m	b_2, e_2	-	0.16	0.28	0.48	0.96	1.73	2.45	1	1	1
4.84	m	g_2	-	0.04	0.06	0.11	0.27	0.56	0.88	0.41	0.43	0.45
4.47	d	d_2	-	0.08	0.13	0.17	0.34	0.58	0.90	0.44	0.44	0.49
4.02	m	c_2+f_2	-	-	-	-	-	-	-	-	-	2.21
5.31	m	b_3, e_3	-	0.03	0.02	0.02	0.02	0.05	0.04	0.01	0.02	-
4.95	m	g_3	-	0.17	0.26	0.34	0.51	0.63	0.70	0.16	0.10	-
4.51	m	d_3	-	0.05	0.08	0.14	0.18	0.32	0.36	0.08	0.06	-
3.75- 4.21	m	c_3, f_3	-	-	-	-	-	-	-	-	-	-
2.33	m	h	-	0.25	0.54	1.02	2.00	3.47	4.87	2.15	2.04	2.20
1.63	m	i	-	0.24	0.54	0.95	2.04	3.74	5.11	2.15	2.12	2.17
1.27	s	j	-	0.78	1.52	2.88	6.11	11.06	15.84	6.88	6.46	6.37